

Dedicated to my patient and loving
husband, John.

ANALYSIS OF THE EFFECT OF HYSTERETIC RELATIONSHIPS IN
BEAM-COLUMN CONNECTIONS ON THE EARTHQUAKE
RESPONSE OF PRECAST REINFORCED
CONCRETE FRAME SYSTEMS

by

Lori Wilson Brewer, B.S.

THESIS

Presented to the Faculty of the Graduate School of

The University of Texas at Austin

in Partial Fulfillment of the Requirements

for the Degree of

MASTER OF SCIENCE IN ENGINEERING

UNIVERSITY OF TEXAS AT AUSTIN

December 1993

TABLE OF CONTENTS

	Page
1. INTRODUCTION	1
1.1 Overview	1
1.2 Objectives	1
1.3 Scope	2
2. BACKGROUND	3
2.1 Precast Concrete Structural Systems	3
2.2 PRESSS	3
2.3 DRAIN-2DX	5
2.4 15-Story Prototype Structure	7
2.5 5-Story Structure	13
3. ANALYTICAL MODEL	16
3.1 Nonlinear Structural Analysis	16
3.2 DRAIN-2DX Computer Program	17
3.3 Direct Stiffness Method	18
3.4 Equations of Equilibrium	18
3.5 Equilibrium Corrections	20
3.6 Viscous Damping	21
3.7 The P- Δ Effect	23
3.8 State Determination	24
3.9 Beam and Column Elements	24
3.10 Simple Connection Element	29
3.11 Assumptions Used in Analyses	30
4. RESULTS OF DYNAMIC ANALYSIS	32
4.1 Earthquake Ground Motions	32
4.2 15-Story Prototype Frame	35
4.2.1 Structural Displacement Results	35

	Page
4.2.2 Strength Discontinuities	40
4.2.3 Interstory Drifts	40
4.2.4 Inelastic Action	45
4.2.5 Higher Mode Vibrations	65
4.3 5-Story Frame	69
4.3.1 Structural Displacement Results for the 5-Story Frame ..	70
4.3.2 Inelastic Action in the 5-Story Frame	74
5. SUMMARY AND CONCLUSIONS	93
5.1 Overview	93
5.2 Summary of Results	94
5.2.1 Nonlinear Hysteresis	94
5.2.2 Nonlinear-Elastic Hysteresis	96
5.2.3 Gap-Opening Hysteresis	97
5.3 Conclusions	97
REFERENCES	100
VITA	103

LIST OF TABLES

Table		Page
2.1	Properties of Beam and Column Elements for 15-Story Frame ..	9
2.2	Yield Moments of Connection Elements for 15-Story Frame ...	9
2.3	Properties of Beam and Column Elements for 5-Story Frame ..	14
2.4	Yield Moments of Connection Elements for 5-Story Frame	14
4.1	Earthquake Ground Motions	32
4.2	Maximum Displacements of 15th Story and Maximum Building Drifts	39
4.3	Maximum Plastic Rotations and Maximum Accumulated Plastic Rotations for Connection Elements	45
4.4	Maximum Displacements of 5th Story and Maximum Building Drifts	74
4.5	Maximum Plastic Rotations and Maximum Accumulated Plastic Rotations for Connection Elements, 5-Story Frame	85

LIST OF FIGURES

Figure		Page
2.1	Hysteretic Behaviors of Connection Elements [9, 18]	6
2.2	Elevation of 15-Story Prototype Structure	7
2.3	Plan of 15-Story Prototype Structure	8
2.4	Typical Beam and Column Cross-Sections for 15-Story Prototype Structure	10
2.5	Typical Beam-Column Connection	13
2.6	Elevation of 5-Story Structure	14
3.1	Ground Motion Acceleration Response Spectra Compared to 1991 UBC Design Values	16
3.2	Typical Frames Input for Analyses	17
3.3	Corrections for Moment Unbalances	20
3.4	Rayleigh Damping	22
3.5	Two-Component Element Model	25
3.6	Beam or Column Element [9, 18]	25
3.7	M- θ and M- Ψ Relationships for Beam and Column Elements [9,18]	26
3.8	P-M Interaction Surfaces for Beam or Column Element [9, 18] .	27
3.9	Beam or Column Equilibrium Correction for Inelastic Behavior .	28
3.10	Simple Rotational Connection Element [9, 18]	30
4.1	Acceleration Time Histories	33
4.2	Ground Motion Acceleration Response Spectra	34
4.3	Ground Motion Displacement Response Spectra	34
4.4	Displacement Histories of 15th Story	36
4.5	Floor Displacement Envelopes	37
4.6	Interstory Drift Envelopes	41
4.7	Rotation Envelopes of Column Line A Nodes	42
4.8	Accumulated Plastic Rotations, El Centro	46
4.9	Accumulated Plastic Rotations, Scaled El Centro	48
4.10	Accumulated Plastic Rotations, Viña del Mar	50

Figure	Page
4.11 Accumulated Plastic Rotations in Columns, Scaled El Centro . .	54
4.12 Locations of Plastic Hinges, El Centro	55
4.13 Locations of Plastic Hinges, Scaled El Centro	58
4.14 Locations of Plastic Hinges, Viña del Mar	61
4.15 Story Shear Envelopes	64
4.16 Floor Displacements when the 15th Story is at its Maximum Displacement	66
4.17 Floor Displacements when the 1st Story is at its Maximum Displacement	67
4.18 Floor Displacements, Higher Mode Response for Gap-Opening Behavior	69
4.19 Displacement Histories of 5th Story	71
4.20 Floor Displacement Envelopes, 5-Story Frame	72
4.21 Interstory Drift Envelopes, 5-Story Frame	75
4.22 Rotation Envelopes of Column Line A Nodes, 5-Story Frame . .	76
4.23 Accumulated Plastic Rotations, El Centro, 5-Story Frame	78
4.24 Accumulated Plastic Rotations, Scaled El Centro, 5-Story Frame	80
4.25 Accumulated Plastic Rotations, Viña del Mar, 5-Story Frame . . .	82
4.26 Accumulated Plastic Rotations in Columns, 5-Story Frame	84
4.27 Locations of Plastic Hinges, El Centro, 5-Story Frame	86
4.28 Locations of Plastic Hinges, Scaled El Centro, 5-Story Frame . .	87
4.29 Locations of Plastic Hinges, Viña del Mar, 5-Story Frame	89
4.30 Story Shear Envelopes, 5-Story Frame	91

1. INTRODUCTION

1.1 Overview

Precast reinforced concrete structures and their components, depending on the design, construction method, and other factors, exhibit diverse hysteretic behaviors when subjected to strong lateral forces. This study examines the effect that different hysteretic models for beam-column connections have on the behavior of a 5-story and a 15-story precast reinforced concrete frame building subjected to strong earthquake motions.

Three extremely different hysteretic models are utilized to represent beam-column connection behavior. These models include a nonlinear-inelastic model (representative of very good inelastic behavior in monolithic reinforced concrete connections), a nonlinear-elastic model (representative of post-tensioned connection behavior), and a hysteretic model displaying extreme pinching, referred to as the gap-opening model, (associated with opening and closing of joints or cracks and slippage of reinforcement in the concrete).

This study is part of a joint United States-Japan program, "Precast Seismic Structural Systems" (PRESSSS), currently underway in the two countries. The purpose of the U.S. program is to develop new and innovative precast building systems, study the behavior of these systems, and eventually deliver seismic design recommendations or update current codes for precast reinforced concrete construction in seismic zones.

A nonlinear dynamic analysis program, DRAIN-2DX, was updated at the University of California, for the PRESSSS program and is used in this study to model the precast reinforced concrete buildings and subject them to earthquake acceleration records.

1.2 Objectives

The fundamental objectives of this study are:

- To examine the responses of a 15-story and a 5-story precast reinforced concrete frame building with three very different hysteretic models used

to represent the behavior of beam-column connections during strong earthquake motions.

- To study the distribution of inelastic or nonlinear activity in the moment-resisting frames and the effects of this inelastic/nonlinear activity on the overall response of the buildings.

1.3 Scope

Chapter 2 presents background information on the PRESSS program, and describes the 15-story and 5-story buildings and the three hysteretic models selected to represent beam-column behavior. The dynamic analysis program, DRAIN-2DX, is also discussed briefly in Chapter 2 and in more detail in Chapter 3. Chapter 3 also lists parameter values input for the analyses and assumptions made in this study. Chapter 4 presents and examines the results of the dynamic analyses. Comparisons are made between the responses of the frames with different beam-column connection behavior, and the influence of these connections on the inelastic response of the entire building is examined. The conclusions of this study and a summary are included in Chapter 5.

2. BACKGROUND

2.1 Precast Concrete Structural Systems

Structural systems composed of traditional precast concrete elements are considered inferior to other reinforced concrete structural systems used in seismic zones because they are an assembled product and typically do not behave monolithically. It is assumed by most building officials that a precast frame system will fall like a house of cards when subjected to strong lateral forces unless beams and columns are connected "correctly" (different from current practice).

To date, very little is known about the seismic performance of precast concrete frame systems. Since little experimental data exists, present building codes lack seismic design procedures. Designers who wish to work with innovative precast systems are required to verify their designs by performing expensive structural tests. As a result, designers tend to avoid using precast construction in seismic regions. However, with sound experimental and analytical studies on the seismic behavior of precast concrete structures, it is likely that acceptable design codes can be established.

Precast construction techniques are well suited for the future of the construction industry. Manufacturing of members at the factory and later assembling them on site leads to short in situ construction time and reduced labor costs. The economic benefits of the industry have yet to be fully discovered in seismic regions. With robotics and better manufacturing techniques, construction costs could be held to a minimum. A portion of the precast concrete industry in the United States wishes to promote the use of precast concrete in seismic regions and develop better technological methods for its use [22, 23].

2.2 PRESSS

A coordinated research program to study the behavior of precast concrete building systems, develop seismic design recommendations, and promote the use of such systems, was initiated in 1989. The program entitled, "Precast Seismic Structural Systems" (PRESSS) is being conducted as a joint United States and Japanese study under the sponsorship of the UJNR Panel on Wind and Seismic

Effects and the National Science Foundation. Analytical and experimental work are being conducted by both countries on precast components and sub-assemblages, frame systems, and precast wall panels.

The United States program was divided into three phases. The first phase was concept development. It entailed developing the most suitable precast structural system for areas of strong seismicity, updating analytical programs and outlining design recommendations. The second phase, which is currently underway, involves a more thorough investigation of components and sub-assemblages. Following more extensive investigations of multistory super-assemblages, phase three is anticipated to develop final recommendations for seismic design codes [22, 23].

An important part of the PRESSS program is the coordination between the American and Japanese research teams. Their philosophies differ on certain design and construction techniques, including the best method to connect precast frame members. The Japanese are concentrating on the "strong connection" approach. This accepted approach is intended to make the system behave as a monolithic structure by detailing the beam-column connection so that most inelastic behavior is concentrated at beam ends.

American researchers are examining what has been referred to as the "ductile connection" approach. Connections, which are typically located adjacent to columns, are designed to be weaker than the precast members, and connecting elements in each beam-column connection are designed to absorb all inelastic action while the precast members remain elastic. Although the inelastic action is concentrated at the ends of beam elements for each approach, the "ductile connection" method concentrates inelastic action in the actual beam-column connecting elements, while the "strong connection" approach allows yielding in beam reinforcement.

Because ductile connections are intended to yield in connecting elements while beams and columns remain elastic, it is likely that only the connecting elements will require repair following a strong earthquake. In order for building elements to remain elastic, they must be designed with an adequate margin of strength over the connections. This margin of safety along with different types

of connecting elements and material properties are being investigated in the second phase of the PRESS program. Because different connection designs between building elements are likely to lead to very different hysteretic responses for beam-column connections, this investigation examines the influence of three very different hysteretic models on the behavior of two precast buildings.

2.3 DRAIN-2DX

To determine structural responses to ground motions typical of the West Coast region in the United States, substantial analytical studies are paralleling experimental investigations. As part of the PRESS analytical platform, the University of California at Berkeley has developed and updated the computer program DRAIN-2DX. The program is capable of nonlinear-inelastic modeling of structures subjected to earthquake acceleration records.

Elements were developed to model the characteristics of precast concrete members, including a simple connection element with the ability to display various hysteretic responses. The importance of this variable is studied by modeling two buildings using each hysteretic relationship to model the inelastic behavior in the connections and comparing overall responses to earthquake records.

The simple connection element in DRAIN-2DX that was used in this study can behave as any of the three hysteresis loops shown in Fig 2.1. The element can be specified to behave inelastically with large, energy-absorbing hysteresis loops ("nonlinear hysteretic behavior") (Fig 2.1a); it can behave similar to a prestressed element with nonlinear-elastic behavior ("nonlinear-elastic hysteretic behavior") (Fig 2.1b); or it can exhibit extreme pinching such as that shown in Fig. 2.1c ("gap-opening hysteretic behavior"). For ductile precast connections, pinching might be associated with slip in connectiong elements and opening and closing of joints or cracks. The connection element is described further in Section 3.10.

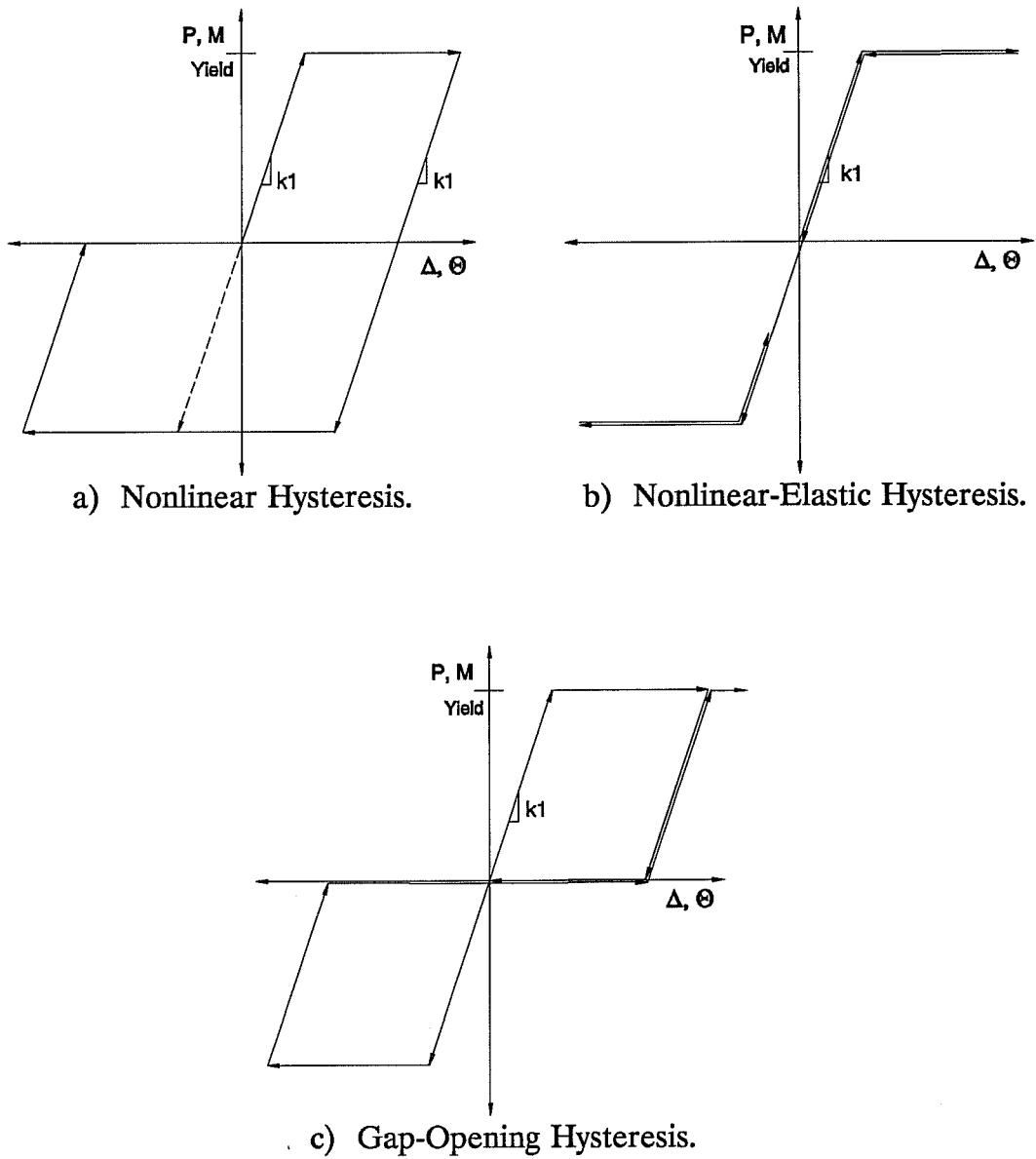


Figure 2.1 Hysteretic Behaviors of Connection Elements [9, 18].

2.4 15-Story Prototype Structure

Prototype structures were developed by both the United States and Japanese research teams. A typical precast moment resisting frame and plan are illustrated in Figs. 2.2 and 2.3 for a 15-story building designed for the U.S. PRESSS program by engineers at Robert Englekirk Consulting Structural Engineers, Inc. The structure measures 105 feet by 205 feet in plan and 200 feet in height. The first story has a height of 18 feet and remaining floor heights measure 13 feet. It was presumed to be located on firm soil, comparable to California soil conditions. The structural dead load was approximated as 80 psf.

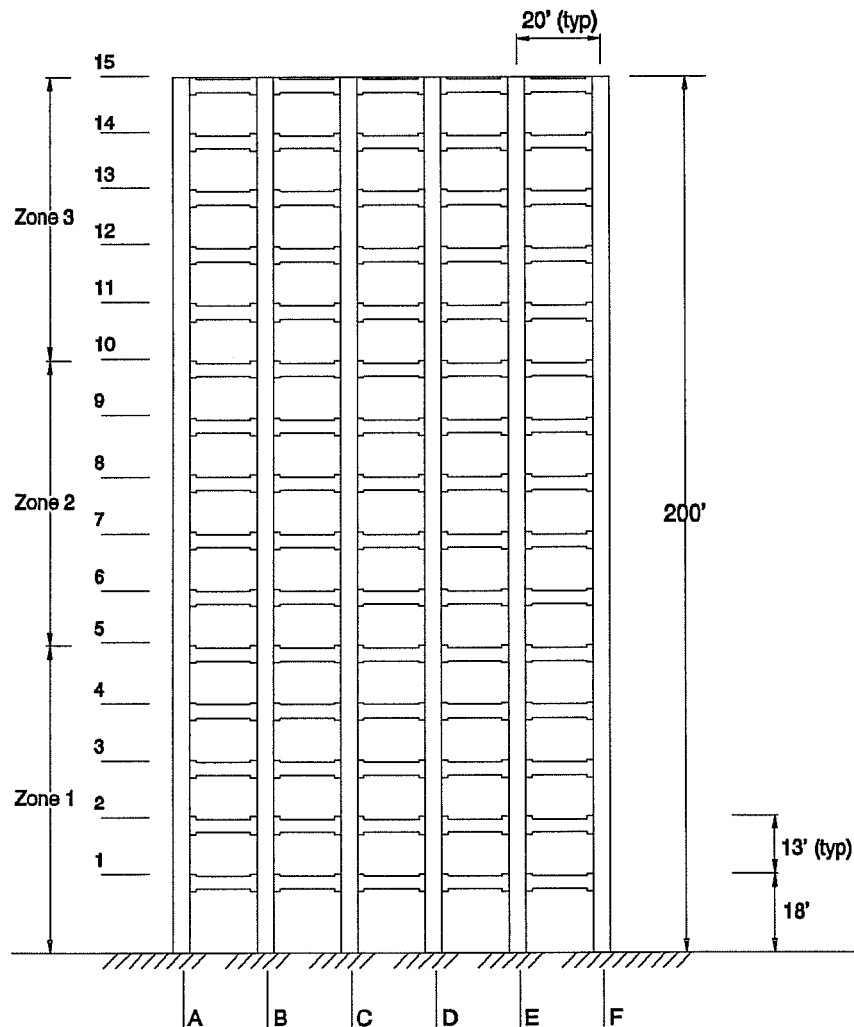


Figure 2.2 Elevation of 15-Story Prototype Structure.

The standard 50 psf live load for an office building was reduced to 20 psf, using a Uniform Building Code (UBC) live load reduction of 60% [30].

The U.S. prototype building has four exterior one-way moment-resisting frames, consisting of five bays each. In the longitudinal (long) direction of the building, the moment-frames consist of only the central five bays, thus uncoupling them from the transverse moment-frames. Internal frame elements are assumed to resist gravity loads only.

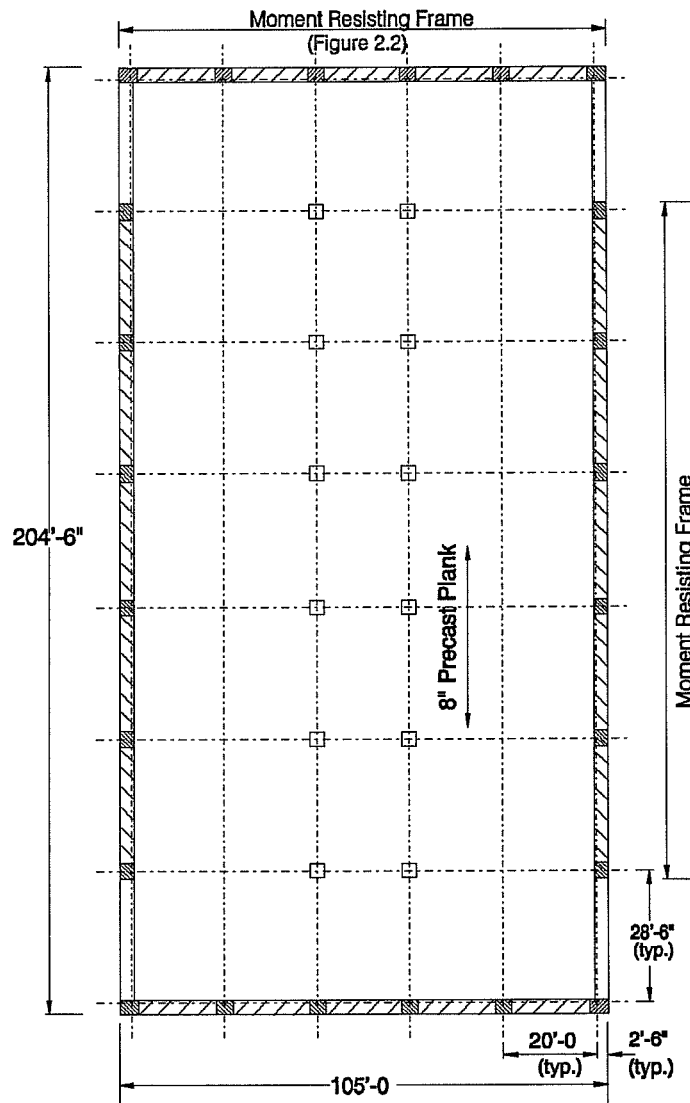


Figure 2.3 Plan of 15-Story Prototype Structure.

Each beam in the perimeter frames has enlarged end sections to provide space for the connecting elements (Fig. 2.5). (In the case of the prototype, 1 inch diameter threadbars were used.) The configuration is sometimes referred to as a "dogbone" connection, named for the shape of the beams (Fig. 2.2).

Table 2.1 Properties of Beam and Column Elements for 15-Story Frame.

		Cross-Sect. Area	Gross Mom. of Inertia	Shear Area	Yield Moment	Axial Yield in Tension	Axial Yield in Compr.
Zone 1	Cols.-Ext.	1728	331,776	1485	68,361	15,458	3182
	-Int.	1512	222,264	1287	57,832	13,739	3370
	Beams	1267	262,483	1039	Table 2.2	-	-
Zone 2	Cols.-Ext.	1728	331,776	1485	52,242	14,699	2246
	-Int.	1512	222,264	1287	45,933	12,749	2246
	Beams	1267	262,483	1039	Table 2.2	-	-
Zone 3	Cols.-Ext.	1728	331,776	1485	34,875	13,269	1310
	-Int.	1512	222,264	1287	30,272	11,514	1310
	Beams	1094	195,610	876	Table 2.2	-	-

Table 2.2 Yield Moments of Connection Elements for 15-Story Frame.

	Pos. Yield Moment	Neg. Yield Moment
Zone 1	27,742	27,742
Zone 2	23,206	23,206
Zone 3	18,588	18,588

Each frame is divided into three vertical zones of five floors each. The zones correspond with different capacities for the structural elements. Elements in the first zone (floors one through five) have the highest strength. Accordingly, zones two and three decrease in strength as story shears diminish with the height of the structure. Zone two has approximately 75% to 80% of the strength of zone

one elements, and zone three has approximately 60% to 70% of the strength of zone one elements. Table 2.1 catalogs the properties of the beams and columns. Table 2.2 lists the yield moments for the connection elements. Typical column and beam cross-sections are illustrated in Fig. 2.4.

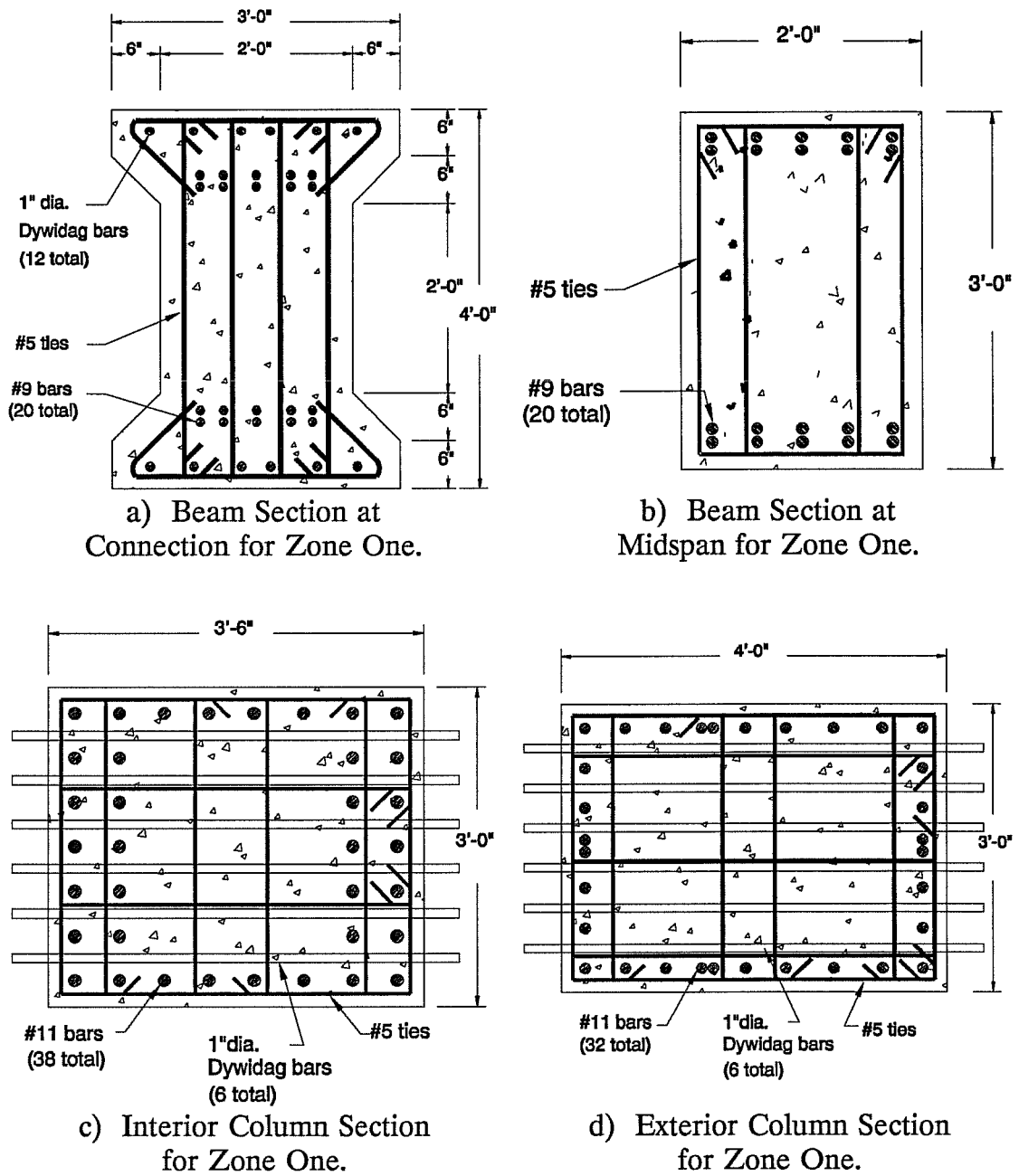


Figure 2.4 Typical Beam and Column Cross-Sections for 15-Story Prototype Structure.

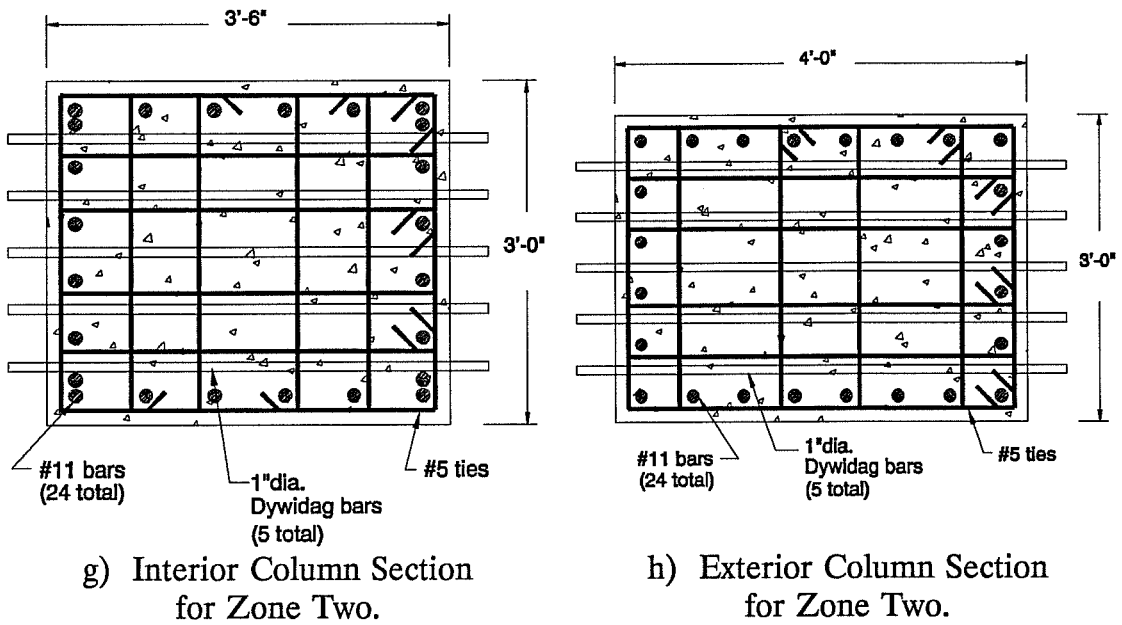
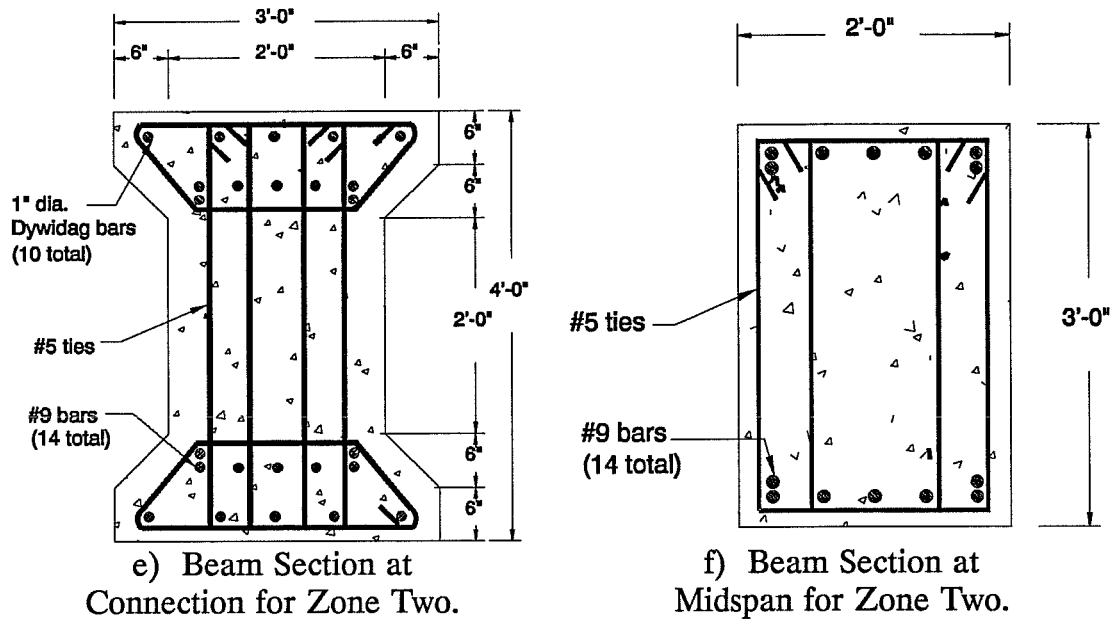
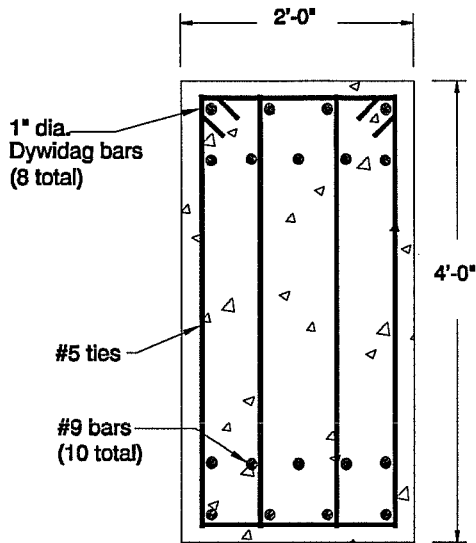
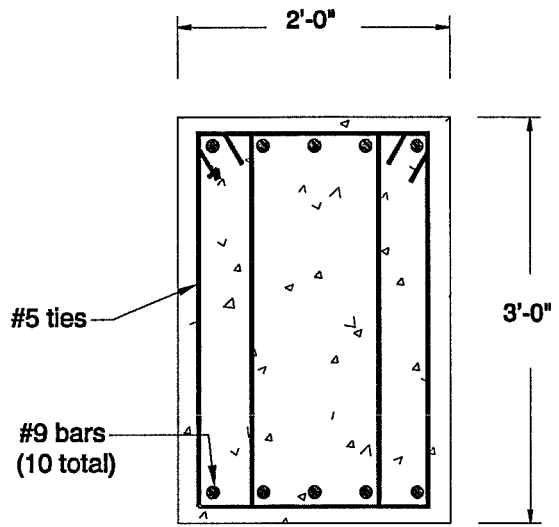


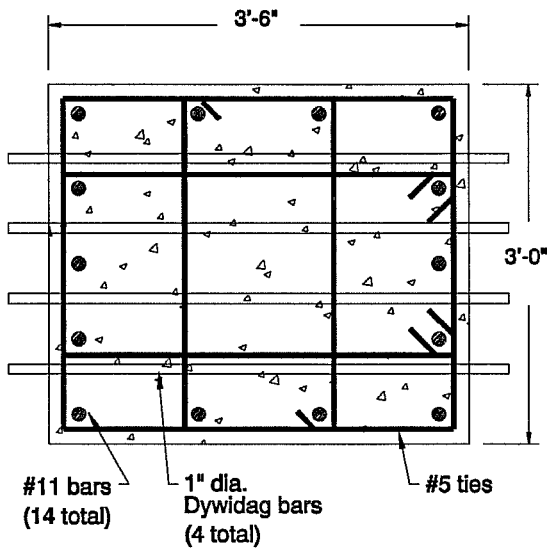
Figure 2.4 (cont'd) Typical Beam and Column Cross-Sections for 15-Story Prototype Structure.



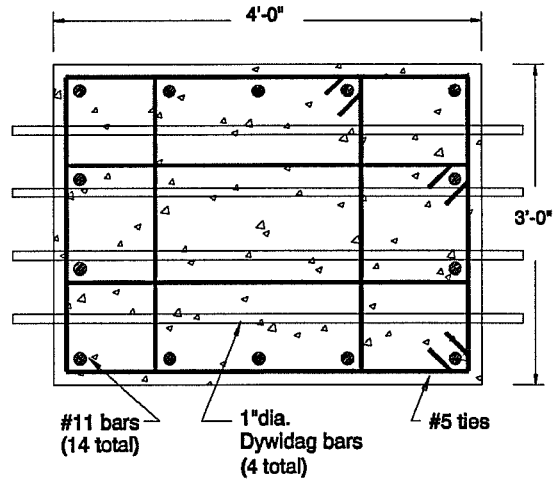
i) Beam Section at Connection for Zone Three.



j) Beam Section at Midspan for Zone Three.



k) Interior Column Section for Zone Three.



l) Exterior Column Section for Zone Three.

Figure 2.4 (cont'd) Typical Beam and Column Cross-Sections for 15-Story Prototype Structure.

A typical ductile connection is illustrated in Fig. 2.5. High-strength Dywidag threadbars (150 ksi ultimate strength) are used as the main reinforcement on each side of the connection. Depending on whether the threadbars are post-tensioned or only snug tight, and whether the ducts that contain the bars are grouted or ungrouted, it is possible the hysteretic behavior of the connections might resemble any of the models represented in Fig. 2.1.

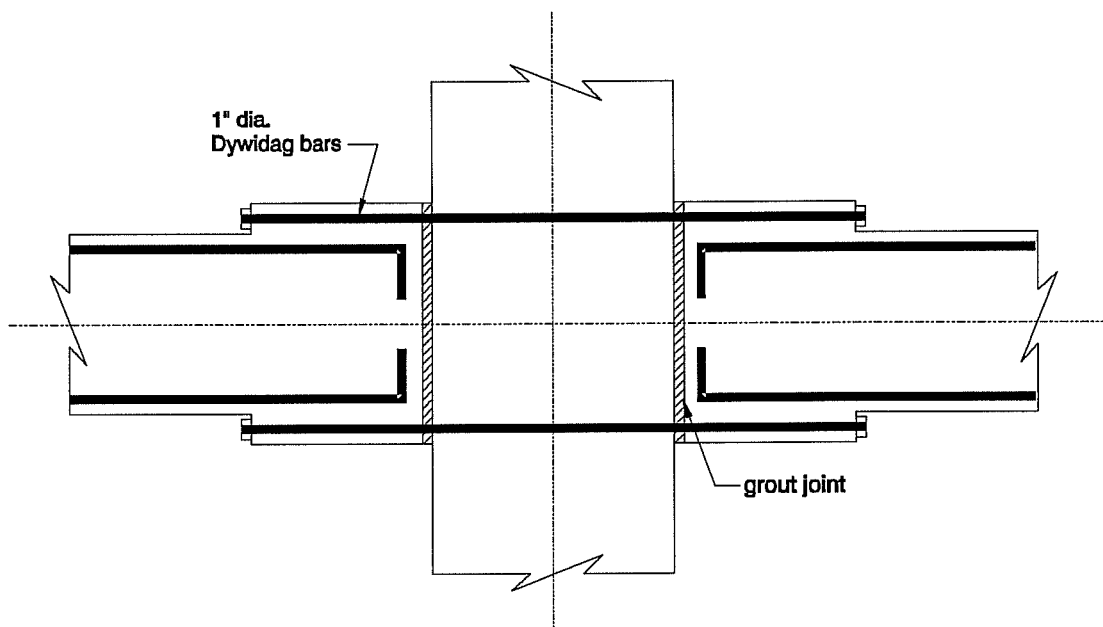


Figure 2.5 Typical Beam-Column Connection.

2.5 5-Story Structure

In addition to the 15-story structure, a 5-story building (Fig. 2.6) was proportioned and analyzed in this study. The building is identical to the prototype in its plan. For convenience, member sizes were kept identical to the prototype's first zone members, however, flexural capacities were decreased.

To determine the relative capacities for the shorter frame, static analyses for the 5-story and 15-story structures were conducted with lateral loads recommended from the UBC earthquake design procedure [30]. Member design

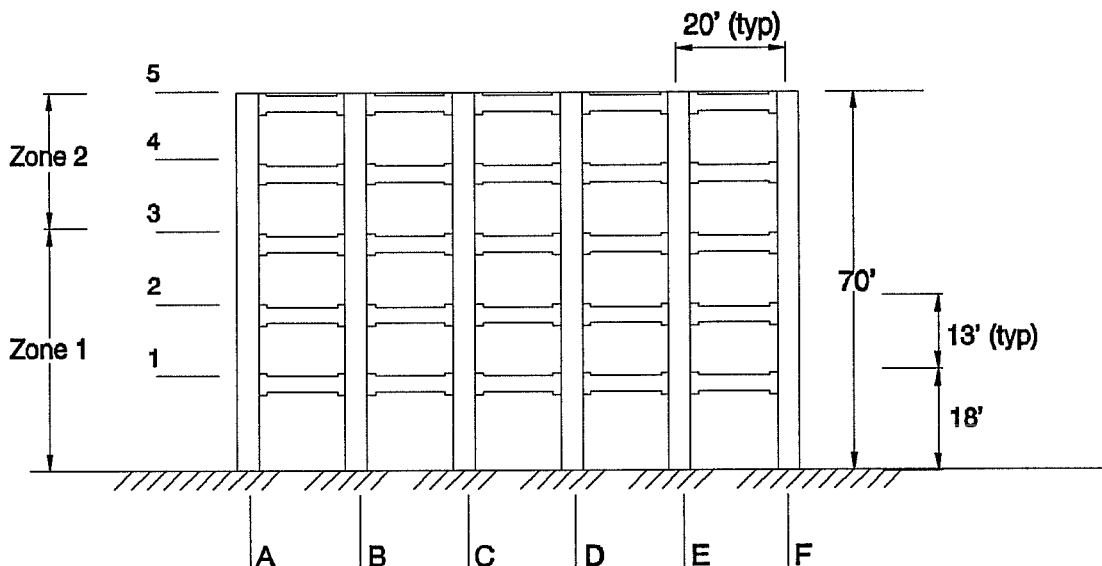


Figure 2.6 Elevation of 5-Story Structure.

Table 2.3 Properties of Beam and Column Elements for 5-Story Frame.

		Cross-Sect. Area	Gross Mom. of Inertia	Shear Area	Yield Moment	Axial Yield in Tension	Axial Yield in Compr.
Zone 1	Cols.-Ext.	1728	331,776	1485	47,852 (70%)	13,463 (87%)	2769 (87%)
	-Int.	1512	222,264	1287	34,699 (60%)	11,049 (80%)	2710 (80%)
	Beams	1267	262,483	1039	Table 2.4	-	-
Zone 2	Cols.-Ext.	1728	331,776	1485	41,016 (60%)	12,799 (83%)	2641 (83%)
	-Int.	1512	222,264	1287	23,133 (40%)	9936 (73%)	2460 (73%)
	Beams	1267	262,483	1039	Table 2.4	-	-

Table 2.4 Yield Moments of Connection Elements for 5-Story Frame.

	Pos. Yield Moment	Neg. Yield Moment
Zone 1	16,645 (60%)	16,645 (60%)
Zone 2	8323 (30%)	8323 (30%)

(*) percentage of first zone capacity for 15-story frame.

moments for the 5-story structure were computed by multiplying the flexural capacity of corresponding first zone members in the taller system by the ratio of moments computed as described above.

The 5-story structure is divided into two zones of member strengths.

The first zone comprises the bottom three stories and the second zone comprises the top two stories. Element properties are tabulated in Tables 2.3 and 2.4. The percentages shown reflect the comparisons between capacities for the 5-story building and the first zone capacities for the 15-story structure.

3. ANALYTICAL MODEL

3.1 Nonlinear Structural Analysis

Nonlinear structural analysis is pertinent for an earthquake analysis. Reinforced concrete buildings are expected and designed to enter the inelastic range during strong motion earthquakes. It is not reasonable to design a building (other than special structures, such as a nuclear reactor) to remain elastic during strong ground motion activity. Buildings, on the average, may experience forces five to six times their yield forces (Fig. 3.1) [10]. Inelastic response of structural members is relied upon to enable most buildings to withstand strong ground motions. In the ductile connection approach presented in this study, connection elements ideally dissipate all energy imported to the structure by an earthquake.

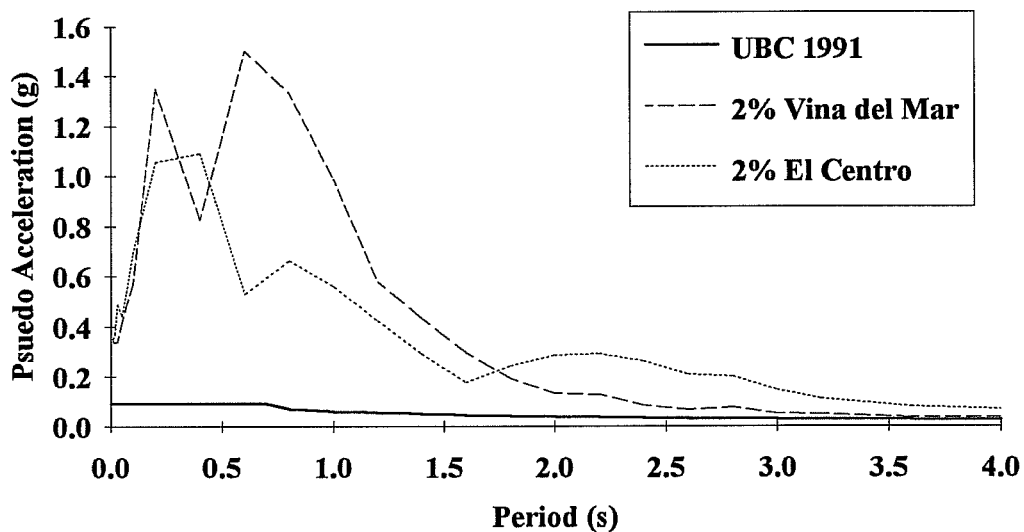


Figure 3.1 Ground Motion Acceleration Response Spectra Compared to 1991 UBC Design Values.

3.2 DRAIN-2DX Computer Program

The analytical models used in this investigation were developed with the aid of DRAIN-2DX [9, 18], a computer program for inelastic dynamic analysis of planar structures.

The structures were idealized as planar frame assemblages of discrete beam, column, and inelastic connection elements. Because the 5-bay frames are

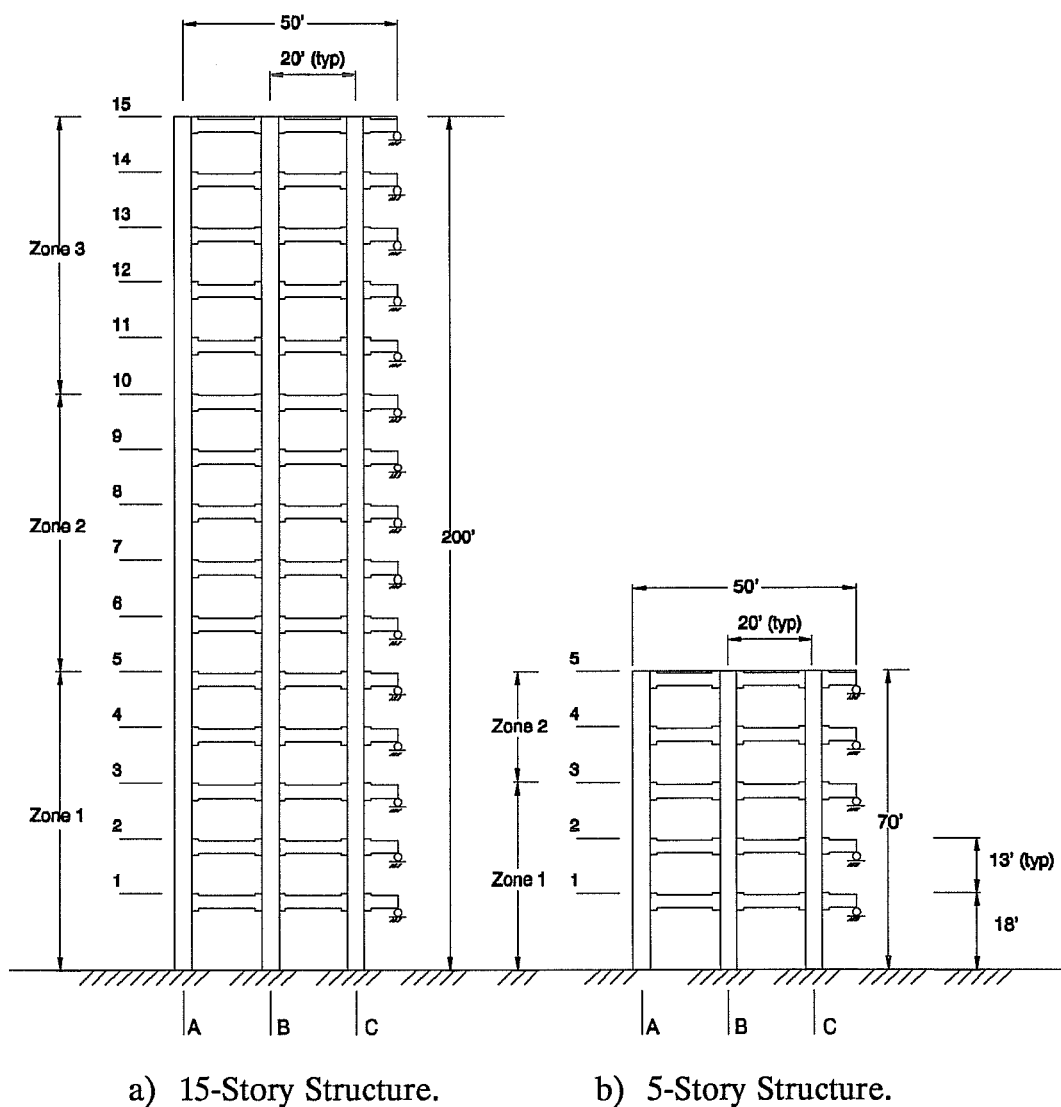


Figure 3.2 Typical Frames Input for Analyses.

symmetric about a central vertical axis and because of storage limitations written into the computer code, only one-half of a typical frame oriented in the transverse (short) direction was analyzed (Fig. 3.2). Rollers were assumed to be placed at midspan of the C-D (Figs. 2.2 and 2.6) beams to allow rotation and horizontal displacement.

Each node has three degrees of freedom: two translational in the X (horizontal) and Y (vertical) directions and one rotational. Degrees of freedom are reduced by slaving nodes with identical translational or rotational displacements. The Direct Stiffness Method is utilized in the DRAIN-2DX analysis to determine unknown structural displacements. Dynamic response is calculated by step-by-step integration [10, 18].

3.3 Direct Stiffness Method

For the Direct Stiffness Method, individual element stiffness matrices must be formed first. The local degrees of freedom of the element are related to the global structural degrees of freedom by a "location matrix". The structure stiffness matrix is then assembled from the element stiffness matrices.

Static loads (such as gravity loads) can be applied to the building, before it is subjected to the earthquake motion. Moments generated by static gravity loads are relatively insignificant in comparison to moments caused by earthquake loading (less than 12%) and were not included in this study.

3.4 Equations of Equilibrium

The equilibrium equations for static loads can be written as

$$[K] \cdot \{U\} = \{P\} \quad (3.1)$$

where $[K]$ = structure stiffness matrix, $\{U\}$ = unknown displacement vector, and $\{P\}$ = load vector.

For dynamic loading, the equilibrium equations become

$$[M] \cdot \{\ddot{U}_r\} + [C] \cdot \{\dot{U}_r\} + [K] \cdot \{U_r\} = \{P\} \quad (3.2)$$

where $[M]$, $[C]$, and $[K]$ denote the matrices for mass, tangent damping and tangent stiffness, respectively, and $\{\ddot{U}_r\}$, $\{\dot{U}_r\}$, and $\{U_r\}$ are the relative acceleration, velocity, and displacement of the structure at time t . The load vector at time t is represented by $\{P\}$.

For step-by-step integration the equation of motion must be written for an incremental time step,

$$[M] \cdot \{\Delta \ddot{U}_r\} + [C] \cdot \{\Delta \dot{U}_r\} + [K] \cdot \{\Delta U_r\} = \{\Delta P\} \quad (3.3)$$

For earthquake loading Equation 3.3 becomes

$$[M] \cdot \{\Delta \ddot{U}_{tot}\} + [C] \cdot \{\Delta \dot{U}_r\} + [K] \cdot \{\Delta U_r\} = \{0\} \quad (3.4)$$

where $\Delta \ddot{U}_{tot}$ is the total acceleration, the addition of the relative and ground accelerations, $\ddot{U}_r + \ddot{U}_g$. Equation 3.4 is usually written in the following form with the ground motion input as a load on the right-hand-side of the equation,

$$[M] \cdot \{\Delta \ddot{U}_r\} + [C] \cdot \{\Delta \dot{U}_r\} + [K] \cdot \{\Delta U_r\} = -[M] \cdot \{\Delta \ddot{U}_g\} \quad (3.5)$$

The equation for each time step has three unknowns: the incremental acceleration, velocity, and displacement values. Acceleration is assumed to be an average constant value over the time step, Δt , and the mass, damping, and stiffness are assumed to be constant. After applying the initial conditions and using kinematic relationships, the equation can be rewritten with only one unknown value (the incremental displacement, ΔU_r) and solved [10, 27]. The average constant acceleration method is stable for all periods and time steps and does not introduce additional damping. It is inaccurate for large time step-to-period ratios. This was not a problem in this study because the time steps were kept very small (less than 0.02 seconds).

3.5 Equilibrium Corrections

Errors in equilibrium may occur with changes in the structure state, such as yielding or unloading of an element. If an event (change in the structure state) occurs during a time step, the assumption that the element's tangent stiffness and damping are constant during that time increment is incorrect and an unbalanced moment will be calculated by the program.

The method of equilibrium correction is demonstrated in Fig. 3.3. Assume that at time t the moment and rotation are calculated to be at point A and at time $t + \Delta t$, the moment and rotation are computed at point B. This is clearly incorrect since the element must follow its defined primary moment-rotation curve. The corrective load vector is then formed to produce an unbalanced moment correction, ΔM_{unb} . The corrected point is then defined at point C. No

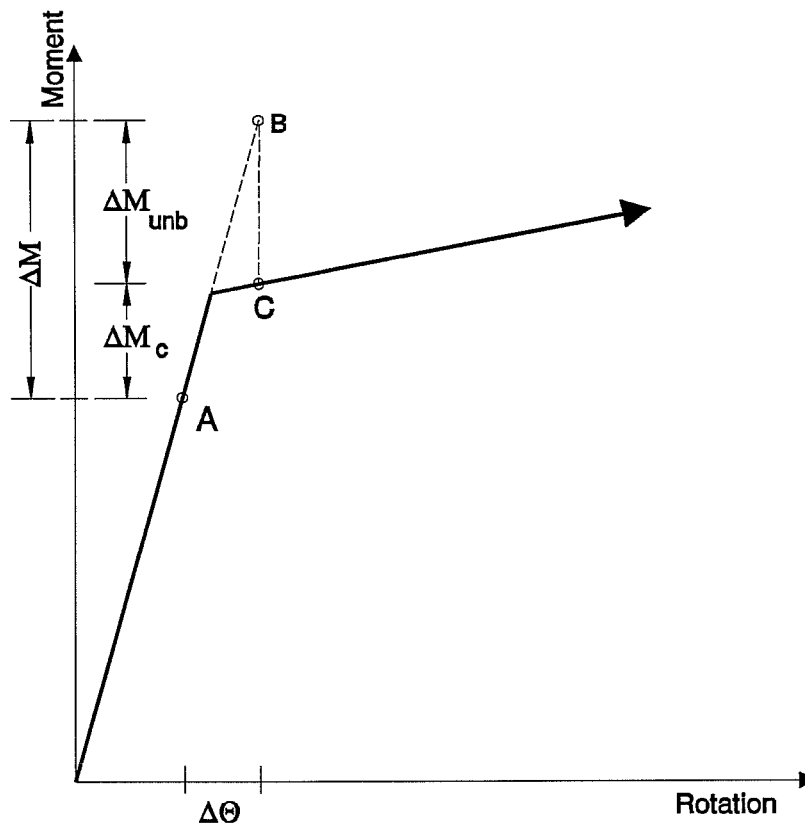


Figure 3.3 Corrections for Moment Unbalances.

correction in rotation is calculated for the member. The additional load is applied only for a short duration to satisfy equilibrium. Once the problem has been corrected, a load of equal and opposite magnitude is applied in the next time step to alleviate the effects of the first corrective load vector.

Moment overshoot tolerances are specified in the input file to control the unbalanced moments. If zero unbalanced moments are specified, the analysis will be more accurate, however, extensive analysis time is required. It is beneficial to specify small overshoot tolerance values and strike a balance between accurate results (moderate unbalanced moments) and reasonable analysis times.

A variable time step is also helpful in alleviating unbalanced moments. A starting time increment is specified and is then subdivided each time nonlinear behavior occurs. A minimum time step is also specified to save computation efforts. When the structure no longer is experiencing nonlinear action, the time step is increased to its original specified value. Variable time steps were utilized for this study. A starting time step of 0.02 seconds was specified for each analysis and minimum time steps between 0.001 and 0.005 seconds were used as required to allow the program to run efficiently.

3.6 Viscous Damping

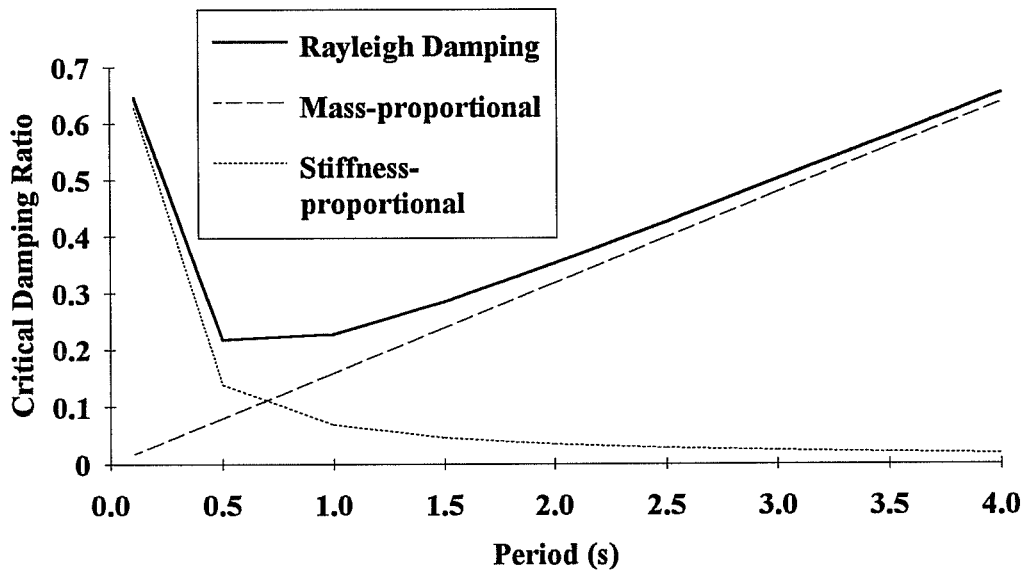
The damping matrix, $[C]$, must be solved directly for the step-by-step integration method. The Rayleigh damping method is applied [10, 27]. It assumes the following relationship

$$[C] = \alpha \cdot [M] + \beta \cdot [K] \quad (3.6)$$

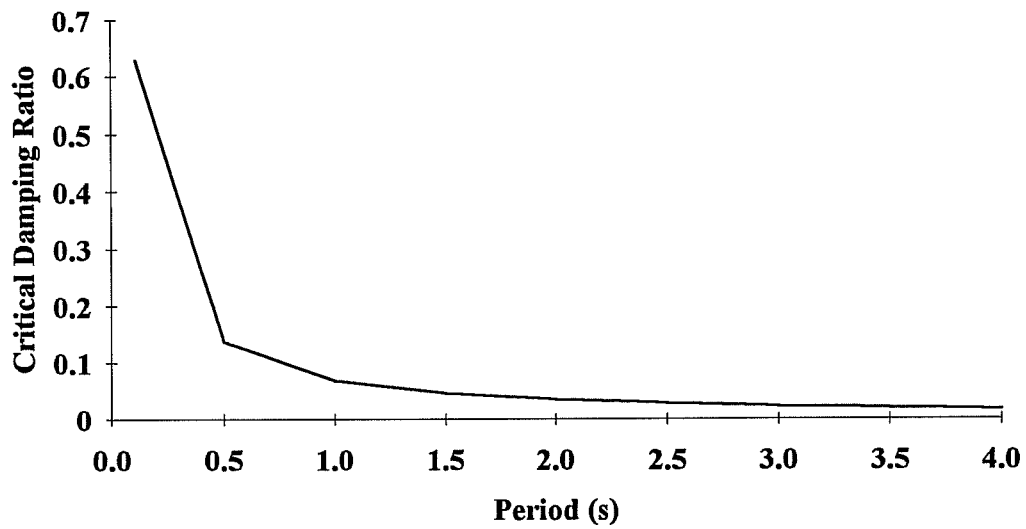
The relations between stiffness- and mass-dependent damping are plotted in Fig. 3.4a. For each mode of vibration, n , the equation becomes,

$$C_n^* = \alpha_n \cdot M_n^* + \beta_n \cdot K_n^* \quad (3.7)$$

where C_n^* , M_n^* , and K_n^* are the generalized damping, mass, and stiffness for the n th mode of vibration. Since the eigenvectors are orthogonal to the mass and stiffness matrices the principle of orthogonality can be used to uncouple the



a) Mass- and Stiffness-Proportional Damping.



b) Stiffness-Proportional Damping Only.

Figure 3.4 Rayleigh Damping.

equations. The coefficients, α and β , can then be calculated from the relationships,

$$C_1^* = 2 \cdot \xi_1 \cdot \omega_1 \cdot M_1^* \quad (3.8)$$

$$K_1^* = \omega_1^2 \cdot M_1^* \quad (3.9)$$

where ζ_1 is the critical damping ratio in the first mode and ω_1 is the circular frequency in the first mode. With a good approximation of ζ for the first and second modes of vibration, the following equations for α and β are generated,

$$\xi_1 = \frac{1}{2} \cdot \frac{\alpha}{\omega_1} + \frac{\beta}{2} \cdot \omega_1 \quad (3.9)$$

$$\xi_2 = \frac{1}{2} \cdot \frac{\alpha}{\omega_2} + \frac{\beta}{2} \cdot \omega_2 \quad (3.10)$$

As a reasonably conservative assumption, only stiffness-dependent damping, β , is specified for this study and mass-dependent damping, α , is not applied (Fig. 3.4b). This insures the damping will always increase with decreasing period lengths. As a result, responses of higher vibration modes will be reduced. The values suggested for ζ_1 in reinforced concrete buildings are within the range of 2% to 10%. For buildings with reasonable levels of cracking, Newmark [20] has suggested $\zeta_1 = 2\%$ to 5%. The value of ζ_1 employed for this study was 2%.

3.7 The P- Δ Effect

Secondary, or P- Δ , moments occur when axial loads act through an eccentricity due to a displaced structure. They should be considered in tall buildings and were included in this study. The geometric stiffness for each column element is constructed based on the axial force in the element acting through small displacements. It is then added to the elastic stiffness matrices for each column member.

3.8 State Determination

During any time step, fluctuations in member deformations are calculated. Yielding is assumed to take place suddenly. Yielding or unloading of a member is referred to as an event and causes a change in the slope of its force-deformation (or moment-rotation) plot and may or may not cause an unbalanced moment. Several events for an element may occur during one time step.

An element's maximum and accumulated inelastic deformations are monitored to give an indication of its ductility demand. The accumulated plastic deformations refer to excursions on the plastic plateau. Each time an element is loaded past its flexural yield point, the inelastic deformations are summed. Negative and positive actions are computed separately. Accumulated plastic deformations are a means of identifying the locations and level of inelastic activity in the structure.

3.9 Beam and Column Elements

This element model is based on the inelastic girder model proposed by Clough [6] (Fig. 3.5). It consists of an elastic and an inelastic component acting in parallel to achieve a bilinear strain hardening moment-rotation behavior along the member. The inelastic component has an elastic-perfectly plastic moment-rotation relationship. The initial stiffness of the element is the sum of the stiffnesses of the two components. Once the yield moment of element is reached in the analysis, a plastic hinge is introduced to the inelastic component. After a plastic hinge forms, the stiffness is reduced as the inelastic component continues on a plastic plateau with a constant moment and the elastic component continues as before with a linear elastic moment-rotation behavior.

Three element deformations are considered for a beam or column element. These include axial deformation and flexural rotations at each end of the member (Fig. 3.6). Yielding can only take place at the ends of the member as concentrated plastic hinges. Accumulated flexural plastic deformations are the summation of the plastic hinge rotations.

If the bending moment along the element is constant (Fig. 3.7a) its moment-rotation curve will parallel its moment-curvature relationship. The two

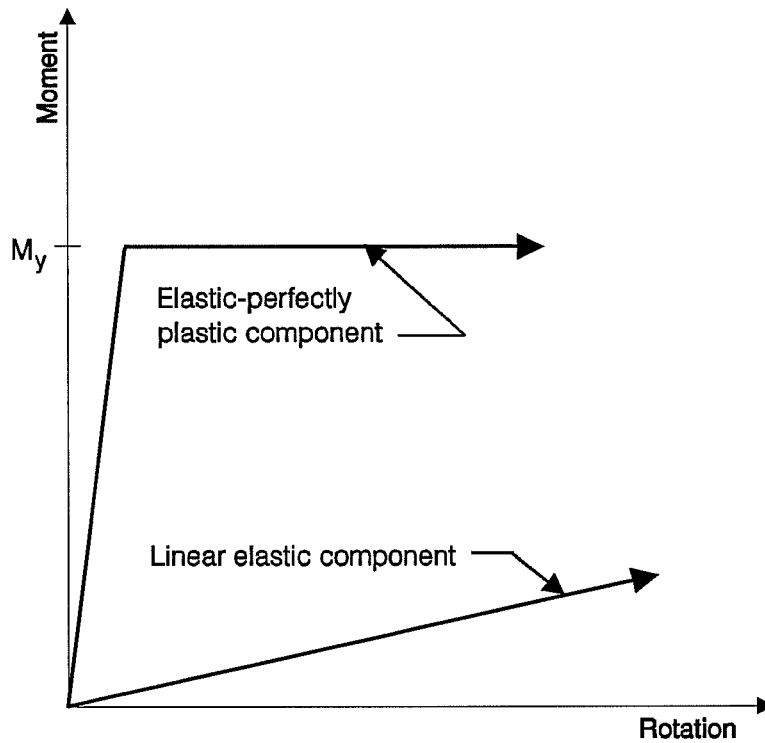


Figure 3.5 Two-Component Element Model.

curves will be proportionally related by the value of the elastic stiffness, EI . If moment varies along the member (Fig. 3.7b), rotation will no longer be proportional to curvature.

The following properties were assigned to each beam and column element: cross-sectional area, moment of inertia, flexural stiffness factors, shear area,

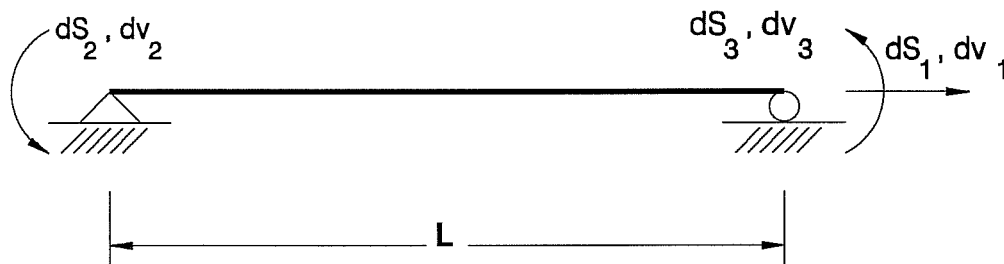


Figure 3.6 Beam or Column Element [9, 18].

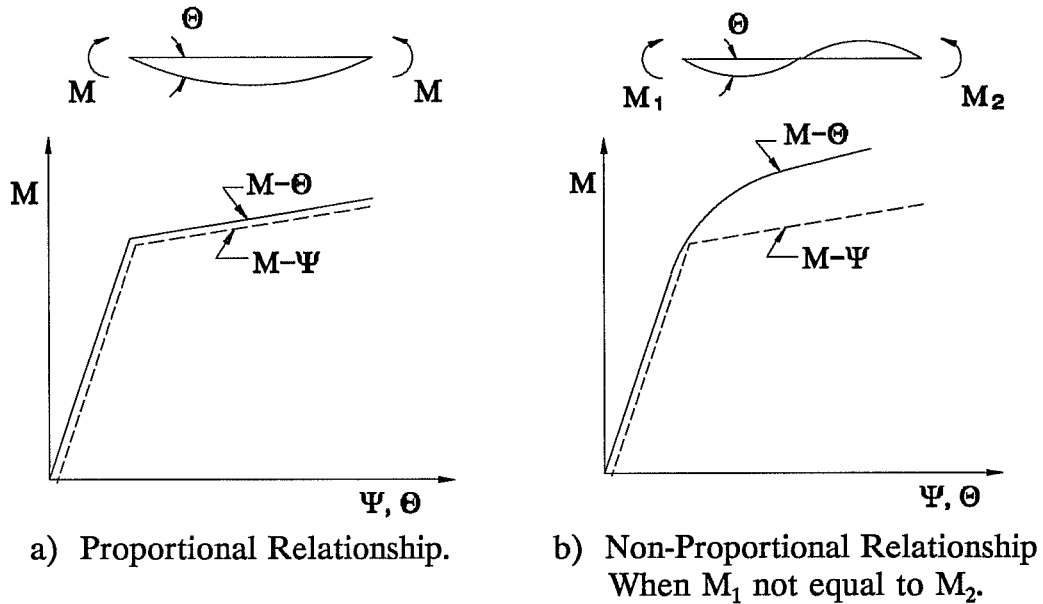
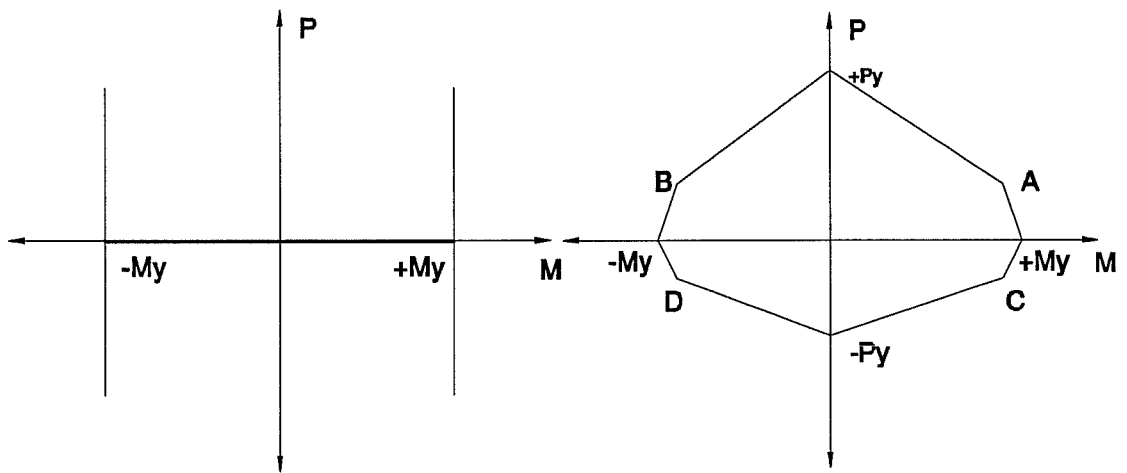


Figure 3.7 $M-\theta$ and $M-\Psi$ Relationships for Beam and Column Elements [9, 18].

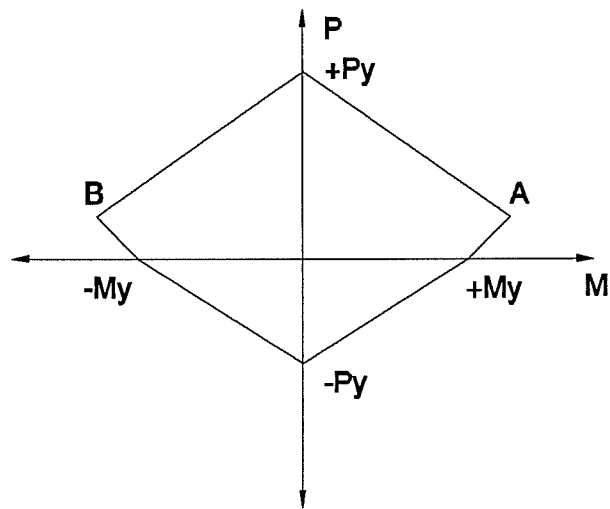
Young's modulus, strain-hardening ratio, and moment overshoot tolerance. (Some of these properties are listed in Tables 2.1 and 2.3.) For a column, the axial load-moment ($P-M$) interaction diagram can be described for the member. For a beam, only positive and negative yield moments are required, since axial deformation is considered to be negligible.

The $P-M$ interaction surface for the inelastic component is designated as a beam, a steel column, or a reinforced concrete column interaction surface. The beam surface (Fig. 3.8a) actually has no interaction between axial load and moment and only positive and negative yield moments are considered. Yielding will occur in the beam when the yield moment is reached. A steel column interaction surface (Fig. 3.8b) or a reinforced concrete column interaction surface (Fig. 3.8c) is defined by axial and moment yield and balance points. The member is assumed elastic if the moment and axial load combination plots within the defined interaction surface. If a combination plots outside this surface, a plastic hinge is introduced to the column element.



a) Beam Interaction Surface.

b) Steel Column Interaction Surface.



c) Concrete Column Interaction Surface.

Figure 3.8 P-M Interaction Surfaces for Beam or Column Element [9, 18].

Inelastic axial deformations are not accounted for in the program. Theoretically, axial stiffness should change with flexural stiffness after yielding occurs. However, to simplify the analysis procedure, only flexural stiffness is corrected following inelastic behavior.

The equilibrium unbalances due to inelastic behavior in beam and column elements are corrected by applying corrective loads in succeeding time steps (Fig. 3.9). If after time $t + \Delta t$, an element's axial load and moment combination plots outside the interaction surface, the moment is corrected while axial load remains constant.

The elastic flexural stiffness for each beam-column member (Fig. 3.6) is given by Equation 3.11,

$$\begin{Bmatrix} dS_1 \\ dS_2 \\ dS_3 \end{Bmatrix} = \begin{bmatrix} \frac{E \cdot A}{L} & 0 & 0 \\ 0 & k_{ii} & k_{ij} \\ 0 & k_{ji} & k_{jj} \end{bmatrix} \cdot \begin{Bmatrix} dv_1 \\ dv_2 \\ dv_3 \end{Bmatrix} \quad (3.11)$$

where E = modulus of elasticity, A = area, I = moment of inertia, L = length, $k_{ii} = 4EI/L^3$, $k_{jj} = 4EI/L$ and $k_{ij} = k_{ji} = 2EI/L^2$. After the member forms a plastic hinge, flexural stiffness factors for the inelastic component change. For a plastic hinge at node i of a member equation 3.11 becomes

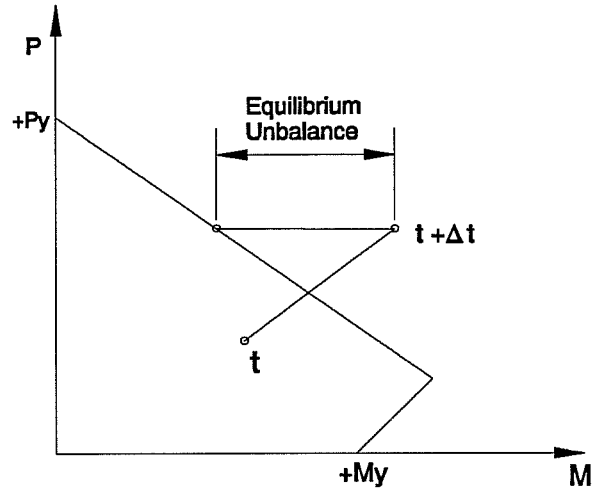


Figure 3.9 Beam or Column Equilibrium Correction for Inelastic Behavior.

$$\begin{Bmatrix} dS_1 \\ dS_2 \\ dS_3 \end{Bmatrix} = \begin{bmatrix} \frac{E \cdot A}{L} & 0 & 0 \\ 0 & 0 & 0 \\ 0 & 0 & \frac{3 \cdot EI}{L} \end{bmatrix} \cdot \begin{Bmatrix} dv_1 \\ dv_2 \\ dv_3 \end{Bmatrix} \quad (3.12)$$

Correspondingly, for a hinge at node j of a member, $k_{ii} = 3EI/L$ and $k_{jj} = k_{ij} = k_{ji} = 0$. For a member with hinges at both ends, $k_{ii} = k_{jj} = k_{ij} = k_{ji} = 0$, because there will be no additional moment contribution from a member with a hinge at each end.

In DRAIN-2DX, a stiffness-proportional Rayleigh damping, βK , is modeled by adding a viscous damping component in parallel with the elastic component. It develops axial and flexural resistant damping during earthquake analysis. A damping geometric stiffness is not included.

Beam and column elements are defined from node to node, not accounting for the finite width of members and joint regions. To correct for this misconception, end eccentricities can be defined for each member, in effect moving plastic hinge locations to the joint faces. The joint region is assumed to be a rigid link between the end of the member and the theoretical joint centerline. It was modeled, for this study, with the following connection elements.

3.10 Simple Connection Element

The DRAIN-2DX simple connection element connects translational or rotational displacements. For the analyses of precast ductile connections, the rotational element (Fig 3.10) was utilized. It has zero length, and connects two nodes having the same X-Y coordinates with a rotational spring. The spring was modeled to be rigid until yielding in flexure (Tables 2.2 and 2.4) and then allow deformation (zero strain-hardening was assumed). The relative rotation (deformation) for a connection element is defined as

$$\theta = \theta_I - \theta_J \quad (3.13)$$

where θ_I and θ_J are rotations of the connected nodes.

The hysteretic behavior of the connection may be specified to be nonlinear, nonlinear-elastic, or gap-opening (Fig. 2.1).

As with the beam and column elements the stiffness-proportional Rayleigh damping, βK , adds a viscous damping element in parallel with the elastic element. Since the damping stiffness is based on the original elastic stiffness of the connection, which was very high, a β value of zero was input for the connection elements to avoid unusually high viscous damping. The viscous damping was solely accounted for in the beam and column elements.

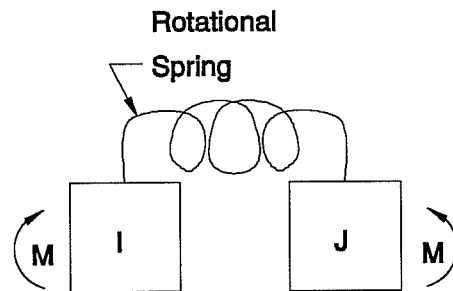


Figure 3.10 Simple Rotational Connection Element [9, 18].

3.11 Assumptions Used in Analyses

The following general assumptions were made to allow DRAIN-2DX to efficiently analyze a planar frame:

- Only horizontal earthquake ground motion was considered; vertical accelerations were ignored.
- Symmetry was used to model only half of the lateral-force-resisting systems in the transverse (short) direction of the buildings.
- The structure's mass was lumped at the nodes and was calculated from plan tributary areas.
- A concrete strength of 6000 psi was used for all members.
- P- Δ effects were included.

- Poisson's ratio of 0.20 was assumed.
- The concrete stress-strain relationship according to Scott, Park and Priestley was employed [26].
- Each floor slab acted as a rigid diaphragm, so each floor level had only one horizontal degree of freedom. Axial deformations of the beam elements were considered negligible.
- Foundation and soil conditions were not included in the analyses. First-story columns were fixed at the base.
- During the earthquake loading, all support points moved in phase.
- The translational degrees of freedom of the pair of nodes comprising a connection element were slaved. They behaved translationally rigid and rotationally flexible.
- Ultimate strength of the Dywidag bars was 150 ksi and the yield strength was assumed to be 85% of ultimate. All other reinforcement had a yield strength of 60 ksi.
- Connections were assumed to be rigid until they yielded in flexure.
- No strain hardening was assumed for the connection elements.
- Strain hardening for the beam and column elements was 1.0% of the elastic stiffness.
- Axial load and moment interaction was specified for column members only. It was not considered for the beams since axial deformations were assumed to be negligible.

4. RESULTS OF DYNAMIC ANALYSIS

Two precast frame buildings, 15 stories and 5 stories tall, and having beam-column connections with three distinctly different types of nonlinear behavior were subjected to different earthquake base motions. Results of the dynamic analyses are presented and discussed in this chapter.

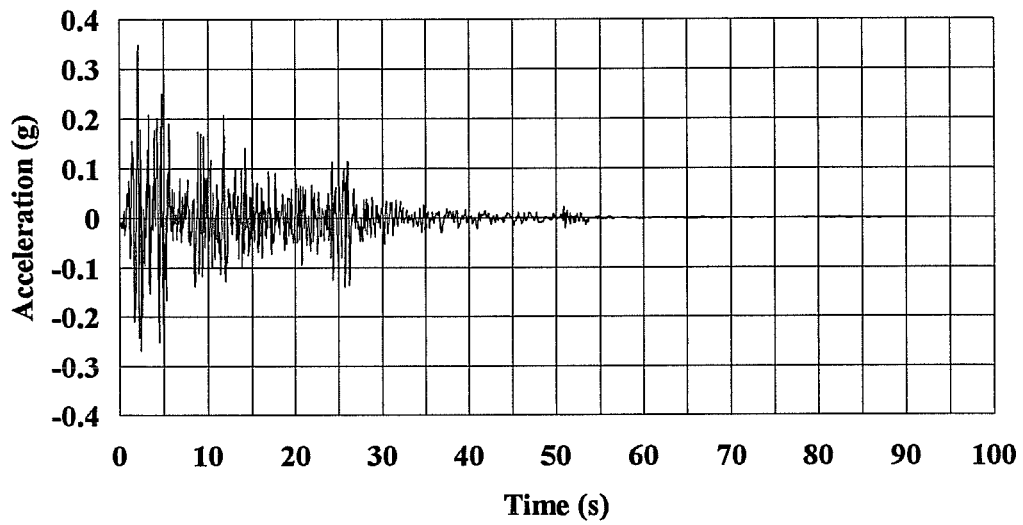
4.1 Earthquake Ground Motions

The 15-story prototype and 5-story moment-resisting precast frames (Figs. 2.2 and 2.6) were subjected to three earthquake ground motions. The N-S component of El Centro, California, 1940, El Centro scaled by 1.43, and Viña del Mar, Chile, 1985, were the records selected to evaluate dynamic response of the frames. More information about the earthquake records is listed in Table 4.1. The El Centro record was chosen because of its wide-band spectrum and because it is representative of a "moderate" West Coast earthquake. The scaled El Centro and Viña del Mar ground motions were selected to represent more severe West Coast earthquakes.

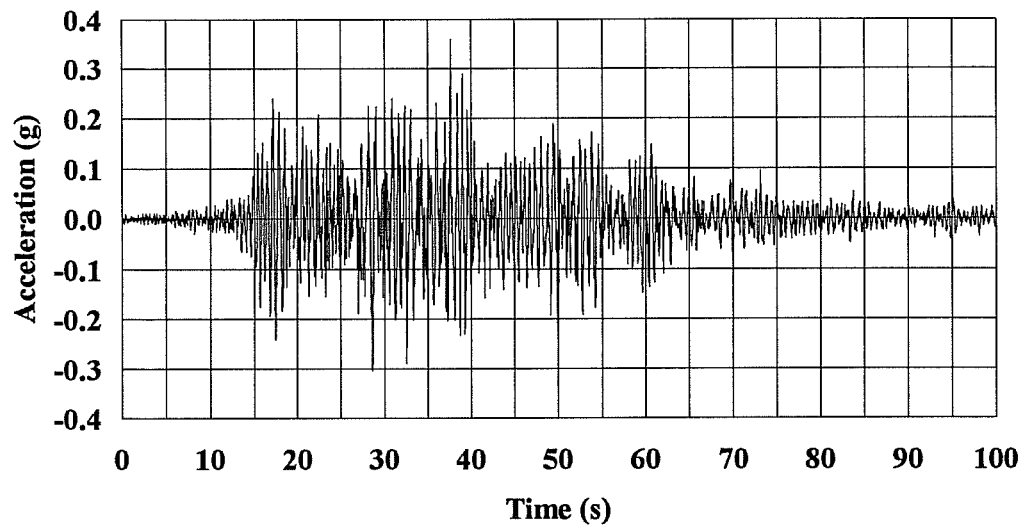
Table 4.1 Earthquake Ground Motions.

Earthquake Record	Direction	Soil Type	Maximum Acceleration	Magnitude, Ms
El Centro, Imperial Valley, California, 1940.	N 0 E	Alluvial Deposits	0.35g	7.1
El Centro (Scaled), Imperial Valley, CA, 1940.	N 0 E	Alluvial Deposits	0.50g	-
Vina del Mar, Chile, 1985.	S 20 W	Alluvial Deposits	0.36g	7.8

The acceleration records for the El Centro and Viña del Mar ground motions are shown in Fig. 4.1 [2]. Only the initial 50 seconds of El Centro and the first 75 seconds of Viña del Mar were used for the analyses. Accelerations beyond these points were trivial and did not cause significant changes in the results.



a) El Centro N-S, 1940.



b) Viña del Mar, S20W, 1985.

Figure 4.1 Acceleration Time Histories.

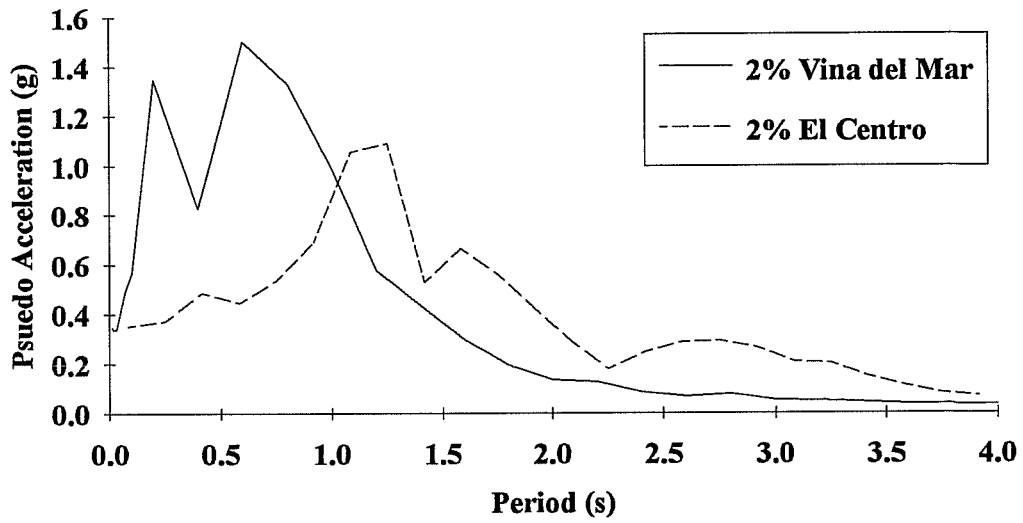


Figure 4.2 Ground Motion Acceleration Response Spectra.

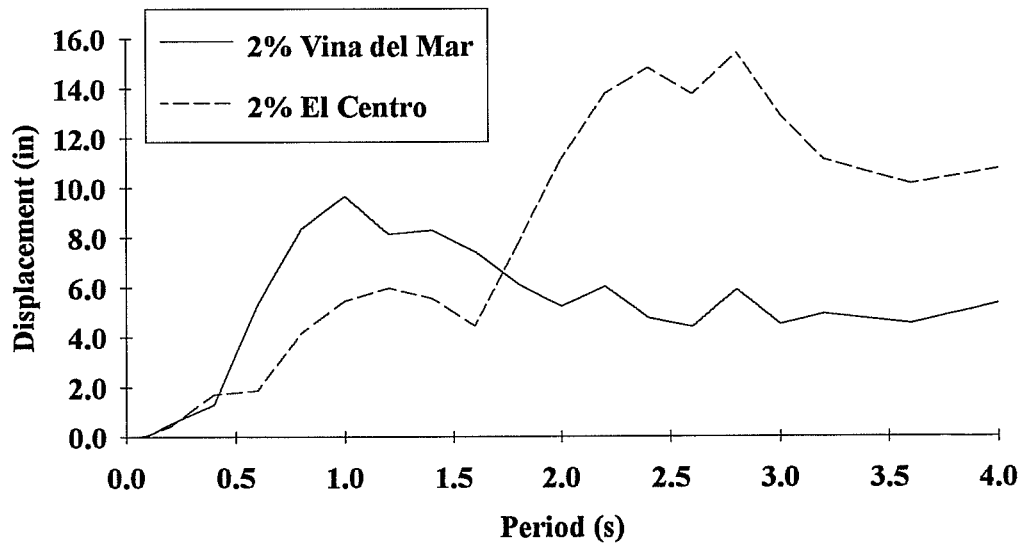


Figure 4.3 Ground Motion Displacement Response Spectra.

The elastic pseudo-acceleration and displacement spectra for 2% critical damping are shown in Figs. 4.2 and 4.3, respectively, for the El Centro and Viña del Mar records. Acceleration response was substantially larger for the Viña del Mar record for periods less than 1 second. Displacement response for the El Centro record was more than double that for the Viña del Mar record for periods exceeding approximately 1.7 seconds. The significance of these observations will be evident later.

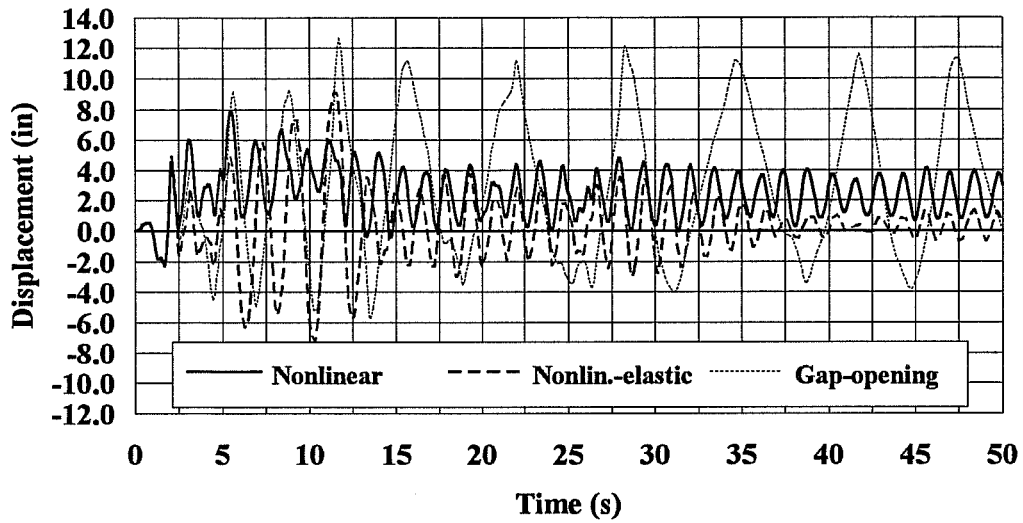
4.2 15-Story Prototype Frame

For each ground motion the prototype frame was analyzed three times using the different hysteretic models described in Chapter 2 (nonlinear, nonlinear-elastic, and gap-opening) for the connection elements. The method of analysis and the element parameters are discussed in Chapter 3.

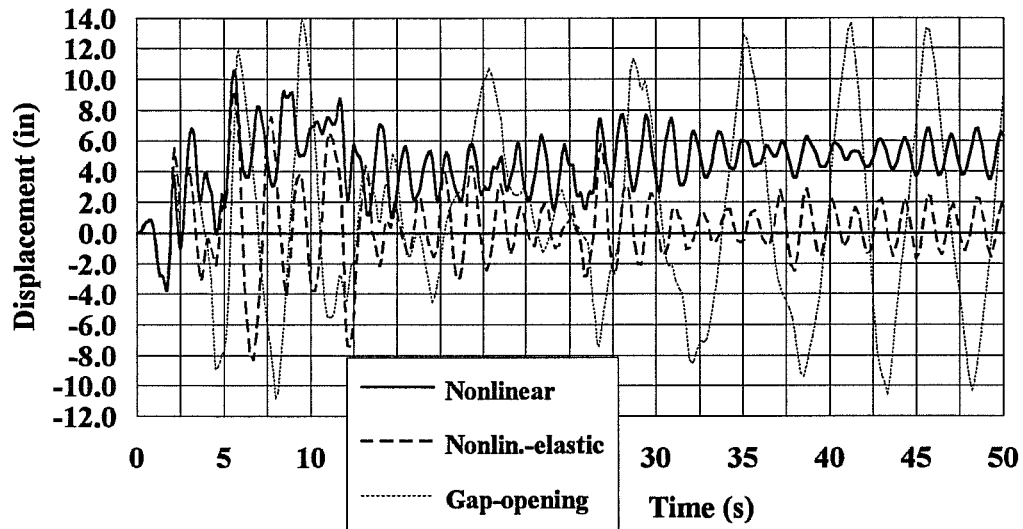
4.2.1 Structural Displacement Results

The displacement histories for the 15th story (roof) level are shown in Fig. 4.4 for the different base motions and hysteretic models. Maximum floor displacement envelopes are shown in Fig. 4.5, and Table 4.2 tabulates the maximum roof displacements and total drifts of the structure. The maximum roof displacement calculated for all connection models of 13.97 inches (0.58% drift) occurred for the gap-opening hysteresis and the scaled El Centro ground motion.

The frame with nonlinear-elastic connection behavior demonstrated consistent displacement history records. Maximum building drift in each of the earthquakes was very comparable and ranged from 0.31% to 0.39% (Table 4.2). Maximum building drift of 0.39% (a 9.27 inch maximum roof displacement) occurred for the scaled El Centro ground motion. For all ground motions, the response dissipated quickly after the maximum displacement occurred (Fig. 4.4). Little to no residual drifts occurred. However, the inelastic response of individual structural members (discussed in later sections) may not be as favorable for this type of hysteretic behavior.

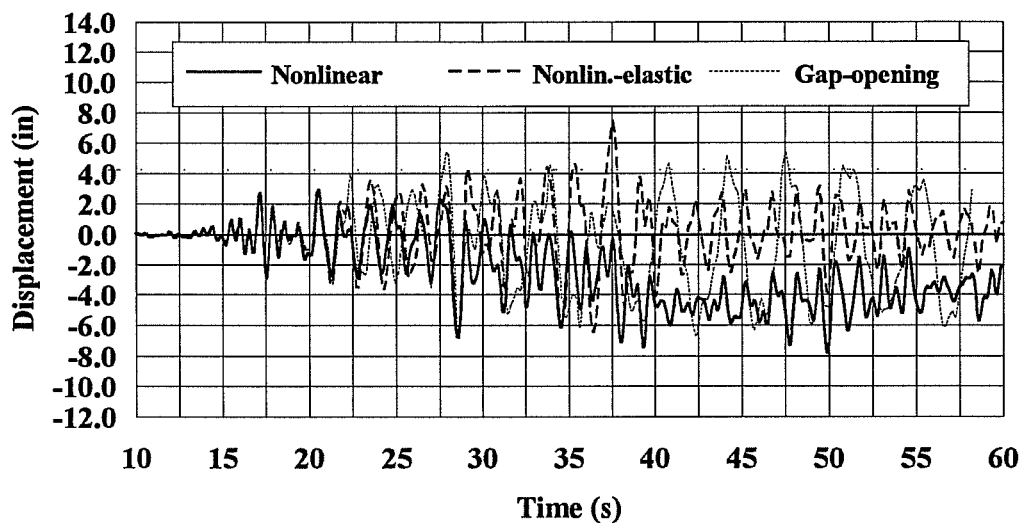


a) El Centro.



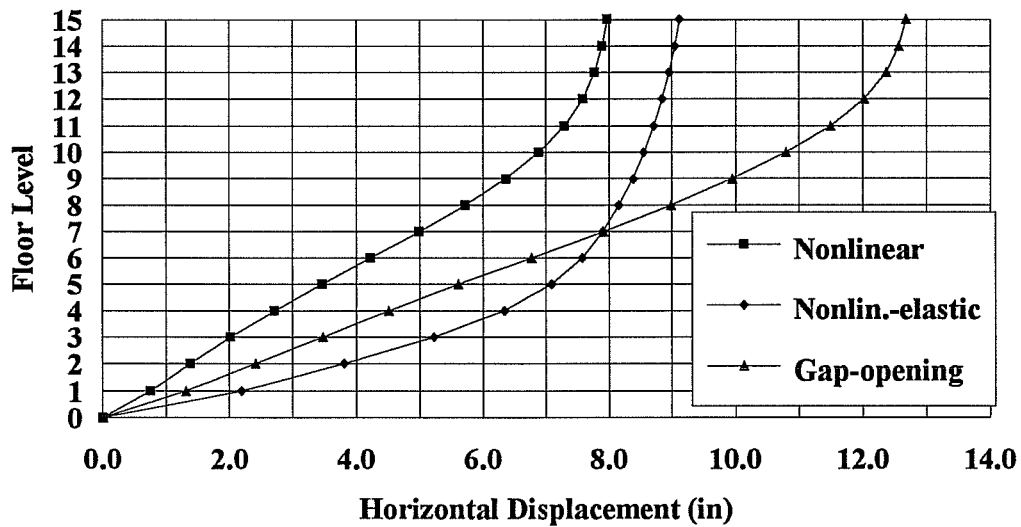
b) Scaled El Centro.

Figure 4.4 Displacement Histories of 15th Story.



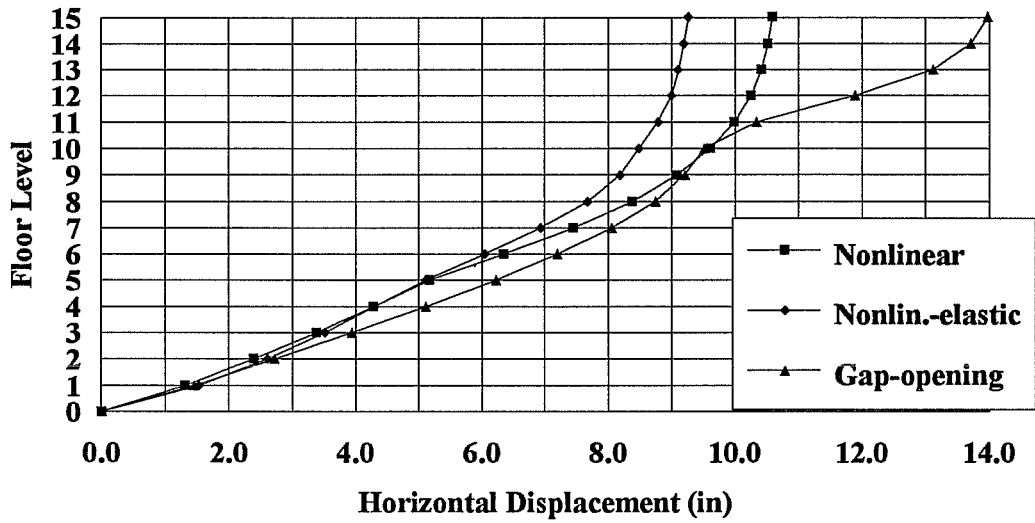
c) Viña del Mar.

Figure 4.4 (cont'd) Displacement Histories of 15th Story.

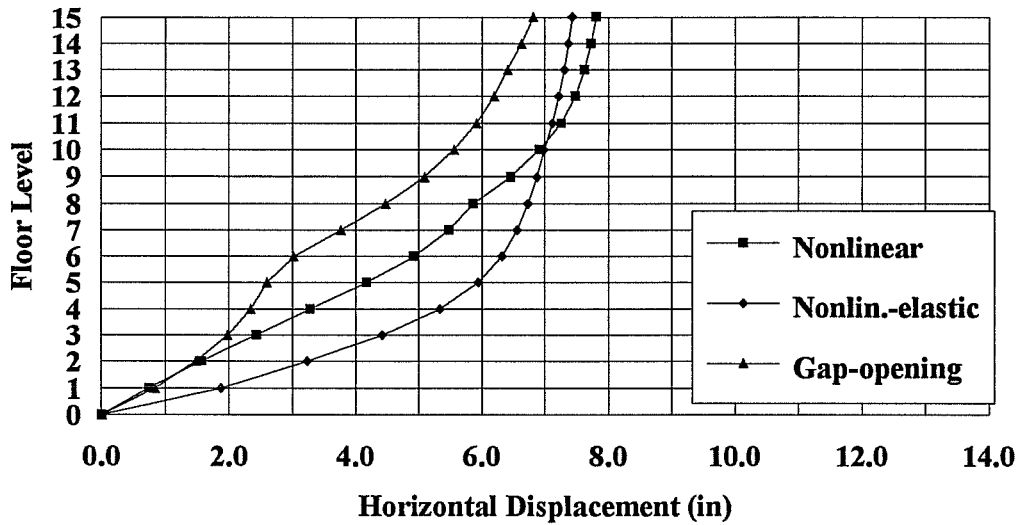


a) El Centro.

Figure 4.5 Floor Displacement Envelopes.



b) Scaled El Centro.



c) Viña del Mar.

Figure 4.5 (cont'd) Floor Displacement Envelopes.

Table 4.2 Maximum Displacements of 15th Story and Maximum Building Drifts.

	Nonlinear Behavior		Nonlinear-elastic Behavior		Gap-opening Behavior	
	Max Disp (in)	Drift (%)	Max Disp (in)	Drift (%)	Max Disp (in)	Drift (%)
El Centro	7.97	0.33	9.12	0.38	12.67	0.53
El Centro (Sc.)	10.59	0.44	9.27	0.39	13.97	0.58
Vina del Mar	7.81	0.33	7.43	0.31	6.81	0.28

The frame with nonlinear connection behavior experienced small permanent inelastic deformations for each ground motion (Fig. 4.4). The calculated residual drifts of 0.08% (El Centro) to 0.21% (scaled El Centro) could be considered tolerable in most structures. The peak-to-peak displacements were relatively small after the plastic deformations occurred. The number of displacement cycles was comparable to the nonlinear-elastic case. This implies, in a very crude way, that the average period of vibration was approximately the same for the nonlinear and nonlinear-elastic cases. The maximum drift for the building with nonlinear connections was comparable for each ground motion (Table 4.2). The maximum drift of 0.44% occurred for the scaled El Centro base motion.

Maximum building displacements when connections behave like the gap-opening hysteretic model were 12.67 inches and 13.97 inches for the two El Centro records. Not only do the deflections exceed the maximum deflections experienced by the structures with connections having nonlinear or nonlinear-elastic behavior, but the structure with gap-opening connections continued to experience many cycles of large deflections well after the maximum deflection was experienced.

The very different displacement responses can be rationalized by considering the effective stiffness of the structure leading up to the peak response. Considering an average of the duration between displacement cycles approaching the maximum displacements in Fig. 4.4, the apparent period of the structure with gap-opening connections was approximately 2.0 seconds (Viña del Mar) to 2.7 seconds (El Centro). The building with nonlinear connections demonstrated an

approximate period of 1.2 seconds, and the nonlinear-elastic case had a period of approximately 1.6 seconds. Using the period approximation for the gap-opening behavior and considering the displacement response spectra for the ground motions (Fig 4.3), the structure can be predicted to experience large displacements with these connections during the El Centro ground motions. Similarly, it can also be predicted from Fig. 4.3 that the structure with nonlinear or nonlinear-elastic connections will have larger displacements during the Viña del Mar base motion than during the El Centro motion. However, maximum displacements for the nonlinear and nonlinear-elastic cases were approximately the same or reduced for the Viña del Mar base motion (Table 4.2).

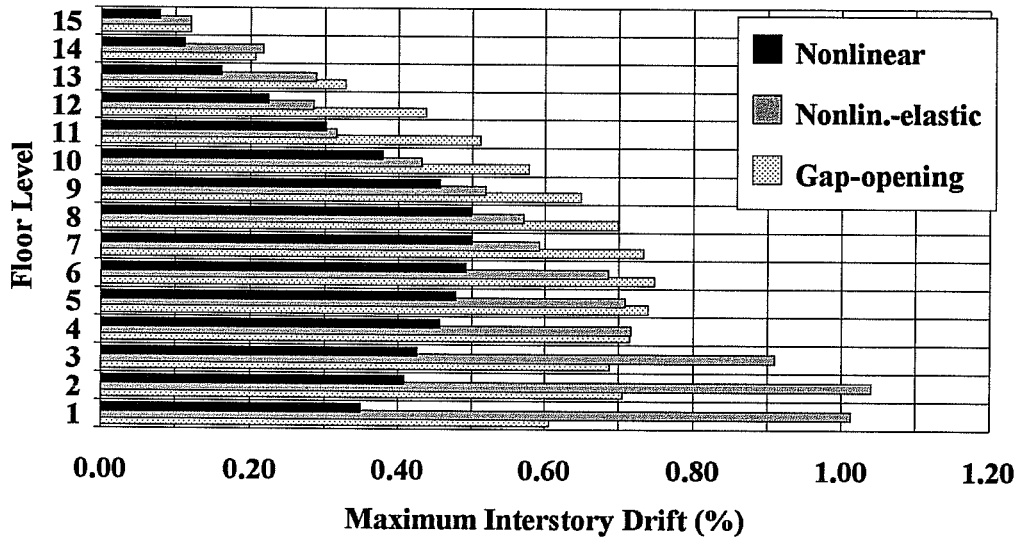
4.2.2 Strength Discontinuities

The prototype building design has three zones of strength that decrease with height (Section 2.4). This is typical of modern design and construction techniques. Because discontinuities of strength or stiffness sometimes result in larger displacements and rotations above the discontinuities, the response of the building as it relates to member strength reductions is examined here.

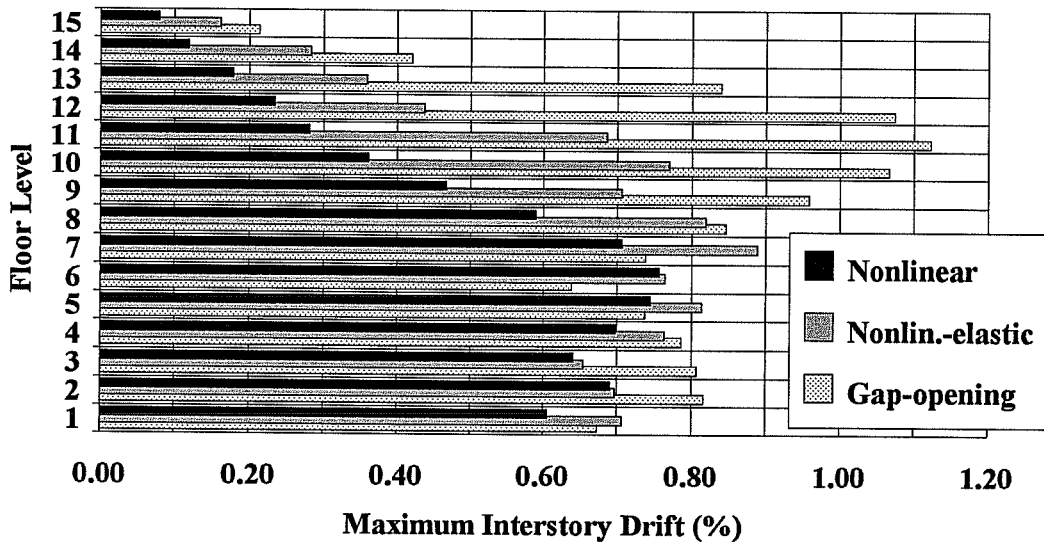
The strength discontinuities between the 5th and 6th and 10th and 11th levels (Tables 2.1 and 2.2) resulted in enhanced displacements for the gap-opening connection model in the stories above the discontinuities (Fig. 4.5) during the scaled El Centro and Viña del Mar records. In the scaled El Centro base motion, much larger displacements occurred in the top four stories above the strength discontinuity, indicating that common practice may not be appropriate for proportioning frames with this type of connection.

4.2.3 Interstory Drifts

Interstory drift is calculated by dividing the relative horizontal displacement between two levels by the story height (18 feet for the first story and 13 feet for all other stories). The envelopes plotted in Fig. 4.6 are the maximum interstory drifts experienced at each level during the dynamic analysis.

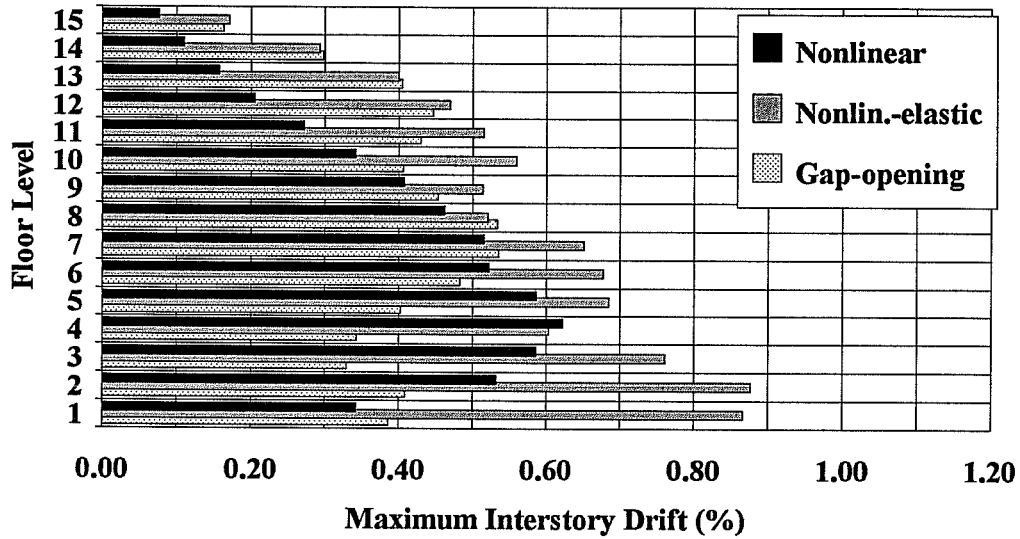


a) El Centro.



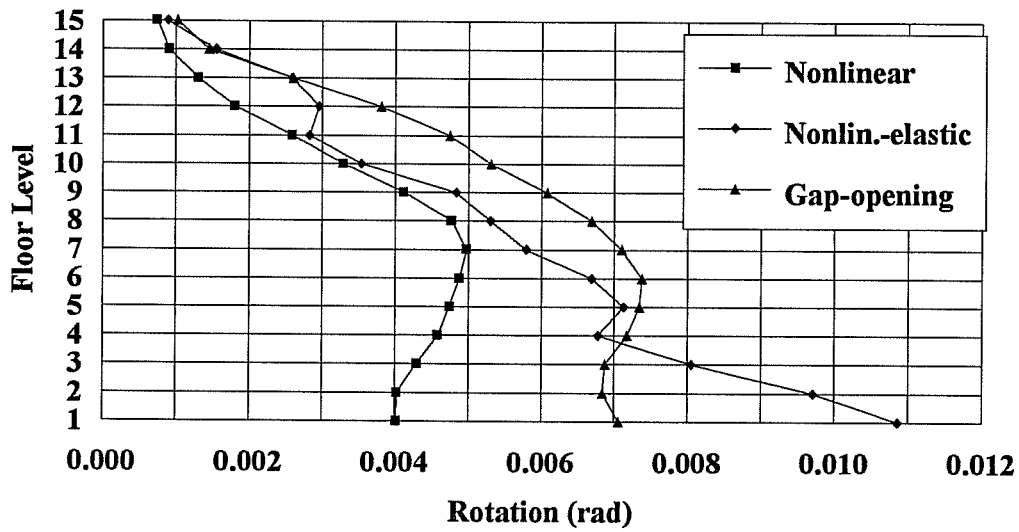
b) Scaled El Centro.

Figure 4.6 Interstory Drift Envelopes.



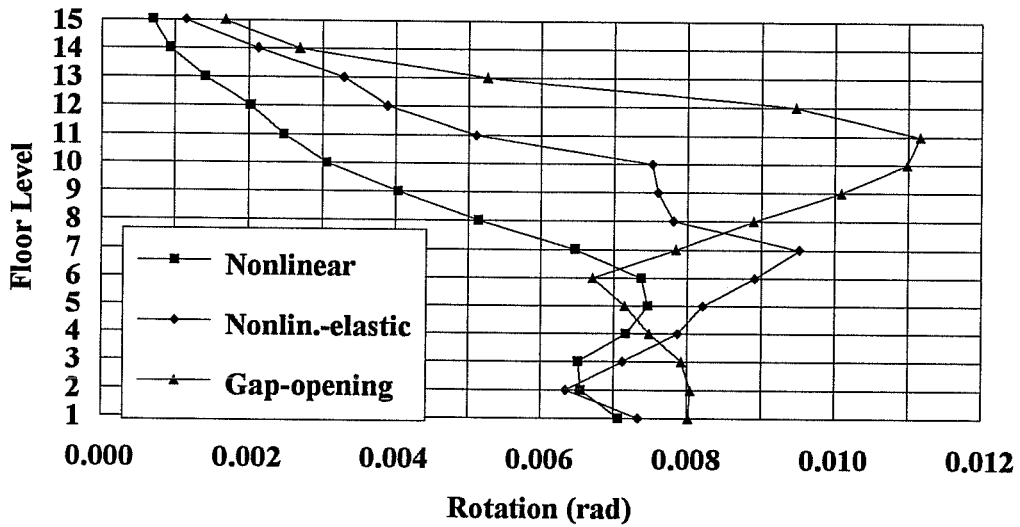
c) Viña del Mar.

Figure 4.6 (cont'd) Interstory Drift Envelopes.

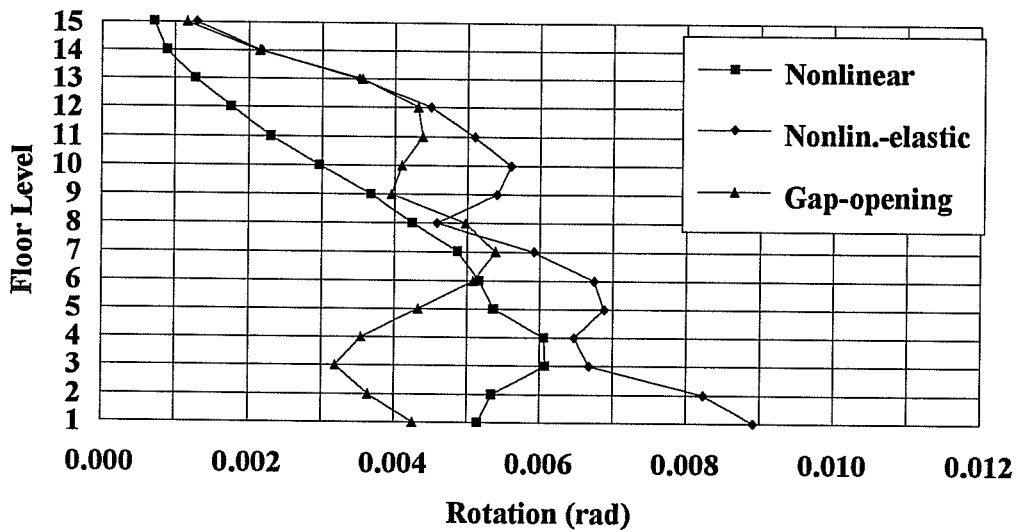


a) El Centro.

Figure 4.7 Rotation Envelopes of Column Line A Nodes.



b) Scaled El Centro.



c) Viña del Mar.

Figure 4.7 (cont'd) Rotation Envelopes of Column Line A Nodes.

The maximum rotation envelopes of the floor level nodes in column line A are shown in Fig. 4.7. The nodes are located at the intersection of the centerlines of column line A and the beams. Rotations at only these nodes were plotted since maximum rotations occur at this exterior column line. Similar trends are visible in the maximum rotation envelopes and the interstory drift envelopes.

Smaller and less sporadic interstory drifts and maximum rotations were observed for the structure with nonlinear connections. For this type of connection, the largest drifts occurred between the 4th and 8th floors for the three base motions considered. Rotation envelopes also were maximum around these locations.

The nonlinear-elastic and gap-opening hysteretic behaviors generated the largest interstory drifts. They were both highly influenced by strength discontinuities in the structure. The structure with nonlinear-elastic connections experienced large drifts and large rotations in the lower floors for the basic El Centro and Viña del Mar records. For the scaled El Centro ground motion the drifts were curiously smaller in the lowest three stories and escalated above the 4th floor.

For the scaled El Centro ground motion, the frame with gap-opening connections experienced relatively large interstory drifts (greater than 1.1%) in the 10th through 12th stories due to large rotations and inelastic action in the columns at the beginning of the third strength zone. For Viña del Mar, the drifts and rotation envelopes were more favorable, again due to the long periods of vibration.

Maximum interstory drift at each level occurred at different times in the analyses. If the maximum interstory drifts for the nonlinear-elastic connection had occurred simultaneously, the overall drifts for the three base motions would have been 0.57% for El Centro, 0.64% for scaled El Centro, and 0.58% for Viña del Mar. These are increases of 1.5 to 2.0 times the maximum overall drifts calculated to occur during the earthquakes (Table 4.2). Summation of the interstory drifts for the other two connection types also produced higher overall

drifts, but these were not as exaggerated as for the nonlinear-elastic case. The maximum story drifts did not occur simultaneously because of higher-mode contributions to the overall response.

It would appear from the plots of drift envelopes that drift control in an attempt to limit non-structural damage is best for frames with connections having the nonlinear hysteretic response. For the Viña del Mar record the nonlinear-elastic connection case had the largest interstory drifts and for the scaled El Centro ground motion the gap-opening case exhibited the largest interstory drifts.

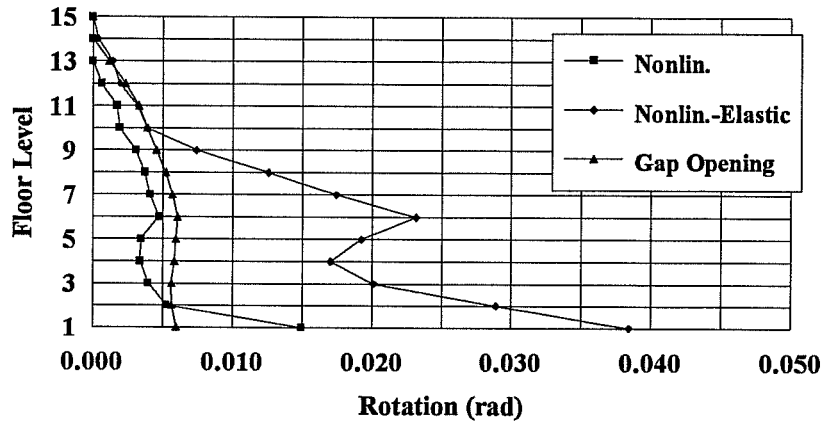
4.2.4 Inelastic Action

The deformation of a connection element is defined as the relative rotation between the two nodes joined by the connecting element. Each connecting element joins the end of a beam (at the face of the column) and the geometric center of the column. The accumulated plastic rotation is the summation of the excursions on the plastic plateau described by the hysteretic model under consideration (Section 3.8). The maximum negative and positive accumulated plastic rotations are tabulated by DRAIN-2DX. Only the maximum absolute rotation (positive or negative) is plotted. The maximum absolute relative rotation between two connected nodes and the maximum absolute accumulated plastic rotation for each type of connection element and each ground motion are tabulated in Table 4.3.

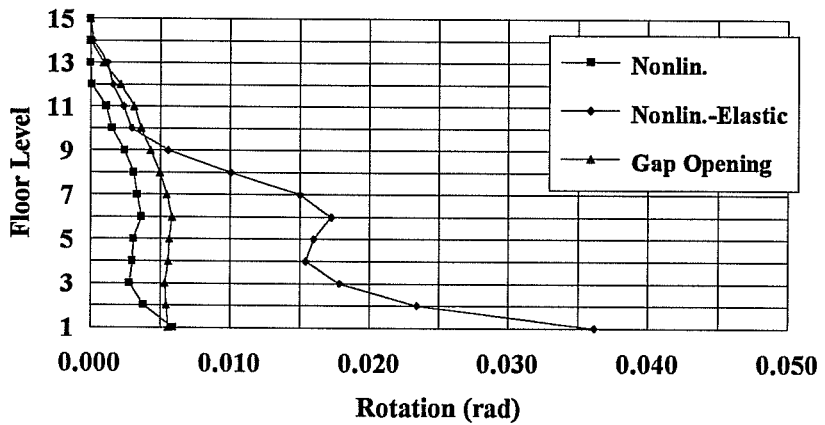
Distributions of accumulated plastic rotations over the height of the structure are shown for connection elements at the ends of beams in bays A-B, B-C, and C-D in Figs. 4.8 through 4.10. While examining these plots, particular attention will be paid to relative comparisons between plots for the nonlinear-

Table 4.3 Maximum Plastic Rotations and Maximum Accumulated Plastic Rotations for Connection Elements.

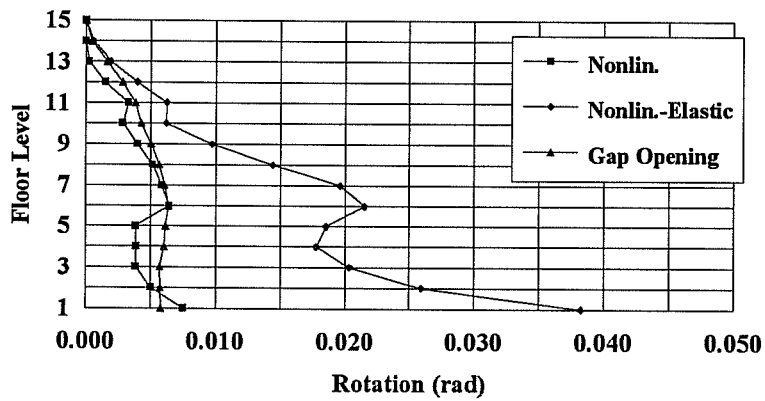
	Nonlinear Behavior		Nonlinear-elastic Behavior		Gap-opening Behavior	
	Max (rad)	Accum. (rad)	Max (rad)	Accum. (rad)	Max (rad)	Accum. (rad)
El Centro	0.0042	0.0149	0.0101	0.0407	0.0067	0.0065
El Centro (Sc.)	0.0067	0.0241	0.0085	0.0481	0.0105	0.0103
Vina del Mar	0.0052	0.0173	0.0082	0.0368	0.0047	0.0044



a) Left End of Beam A-B

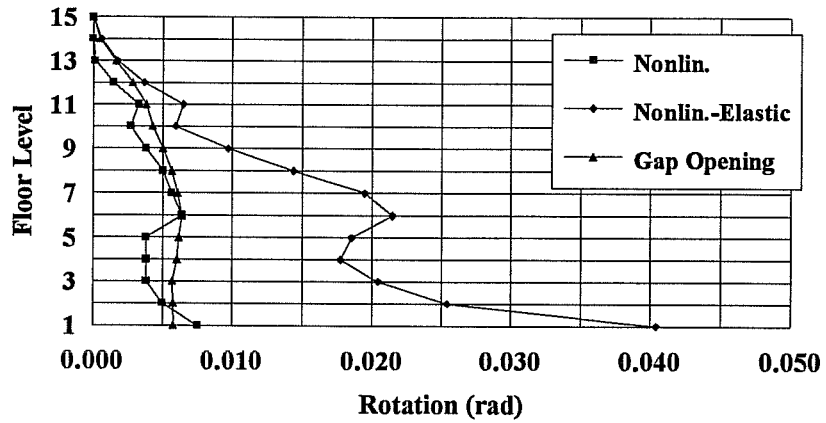


b) Right End of Beam A-B.

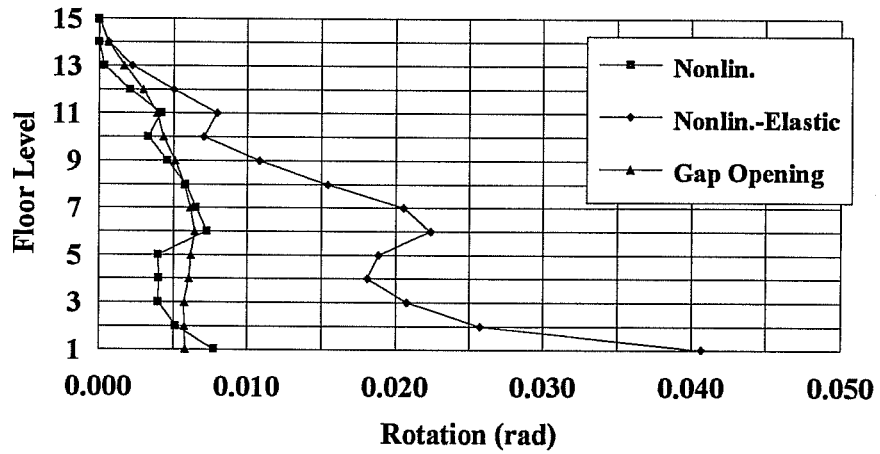


c) Left End of Beam B-C.

Figure 4.8 Accumulated Plastic Rotations, El Centro.

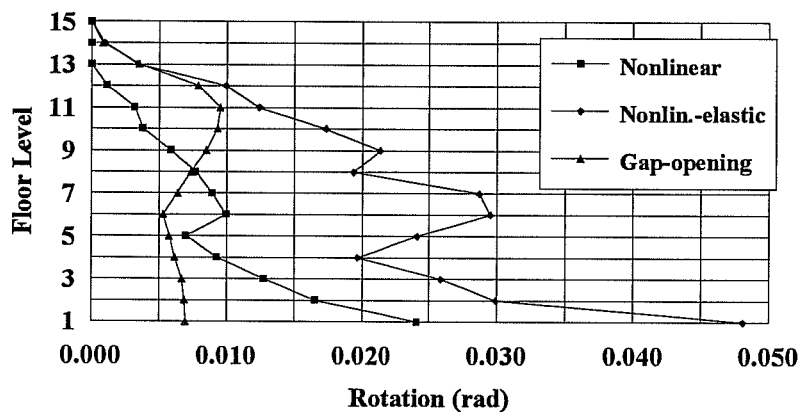


d) Right End of Beam B-C.

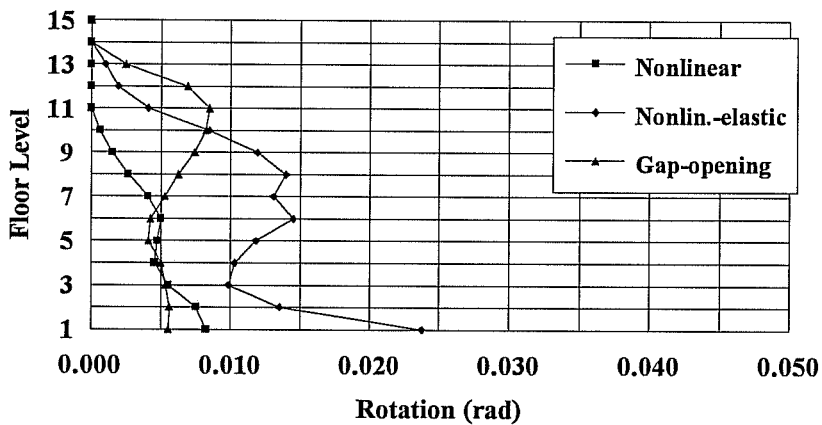


e) Left End of Beam C-D.

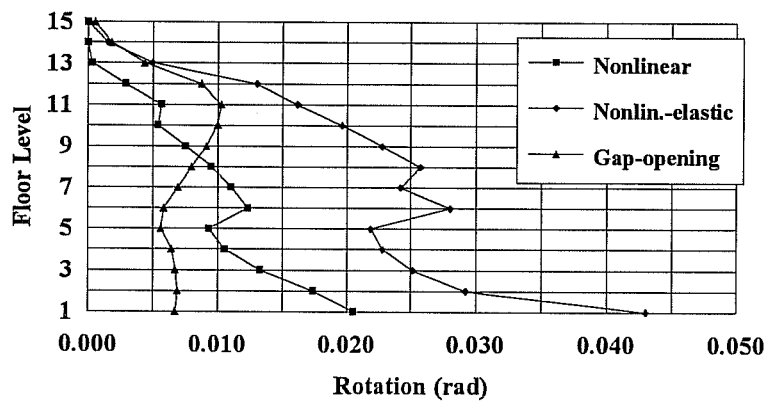
Figure 4.8 (cont'd) Accumulated Plastic Rotations, El Centro.



a) Left End of Beam A-B.

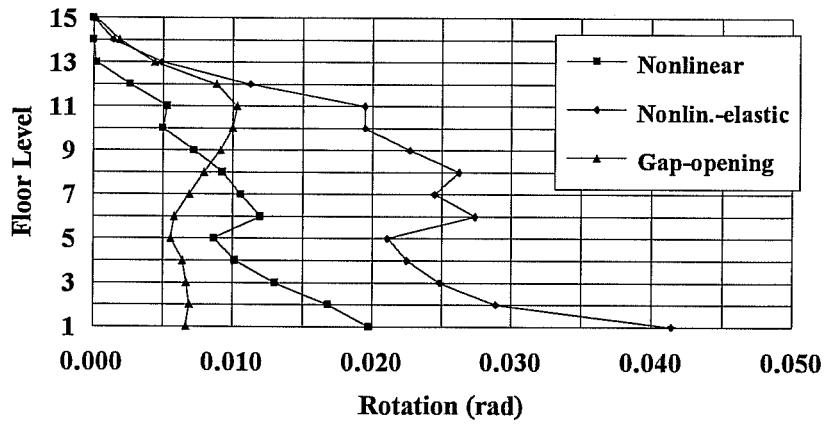


b) Right End of Beam A-B.

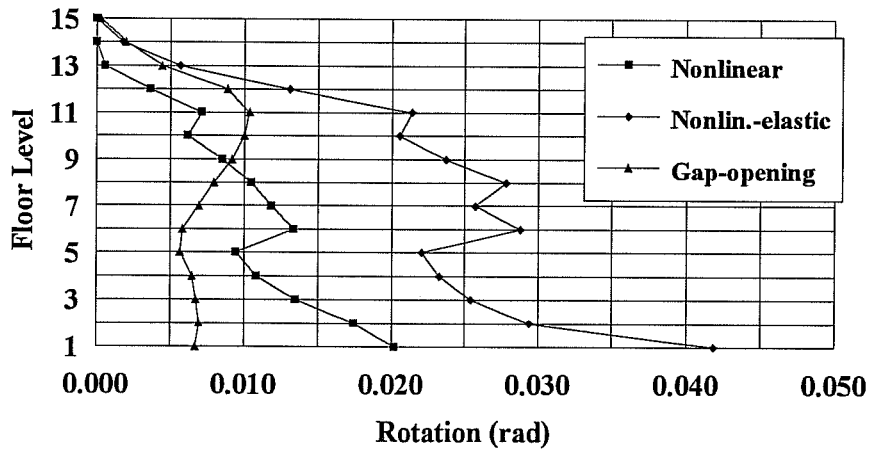


c) Left End of Beam B-C.

Figure 4.9 Accumulated Plastic Rotations, Scaled El Centro.

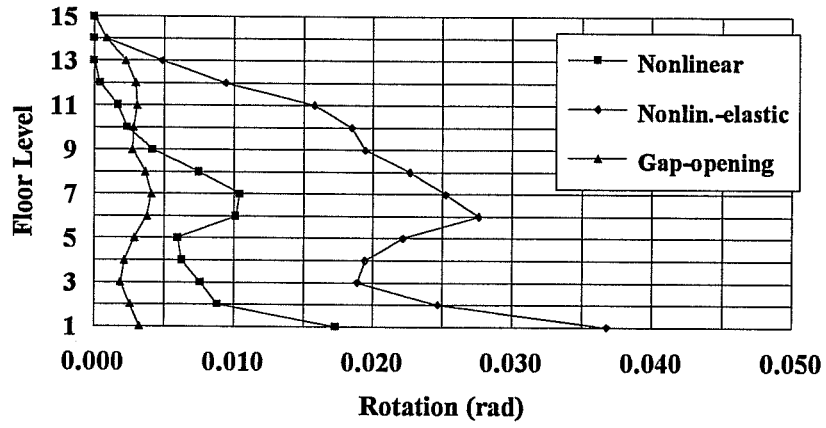


d) Right End of Beam B-C.

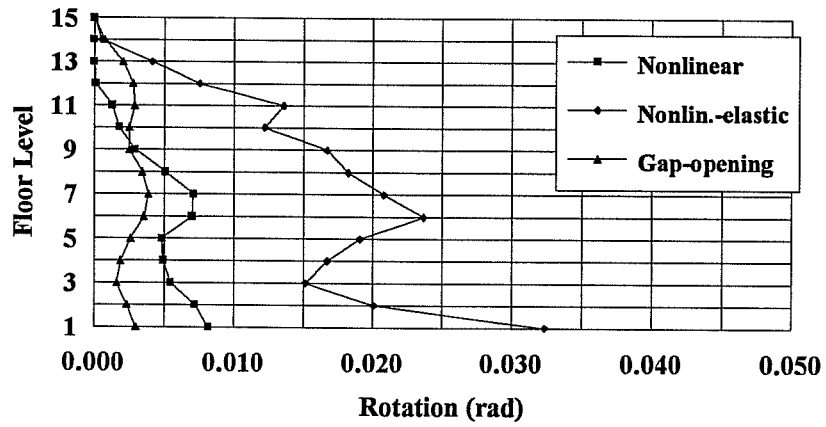


e) Left End of Beam C-D.

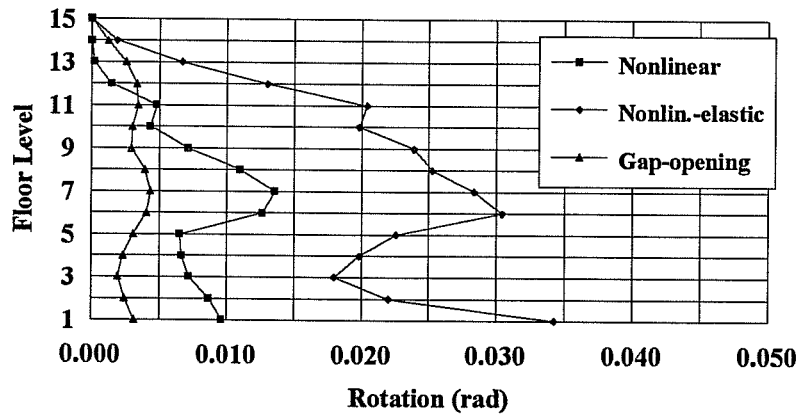
Figure 4.9 (cont'd) Accumulated Plastic Rotations, Scaled El Centro.



a) Left End of Beam A-B.

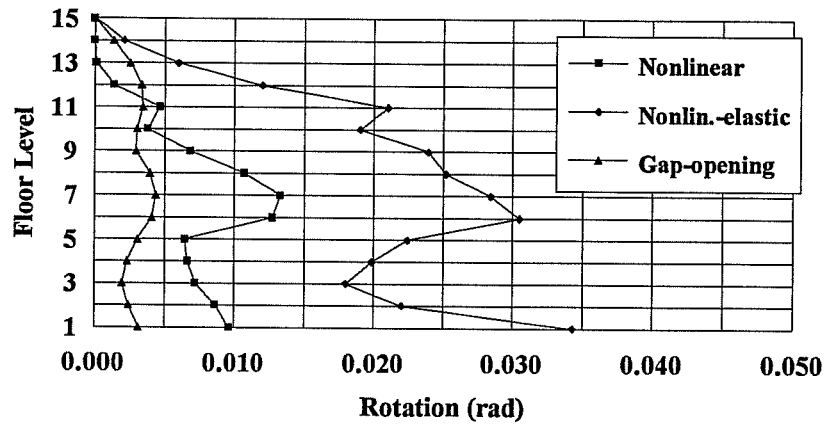


b) Right End of Beam A-B.

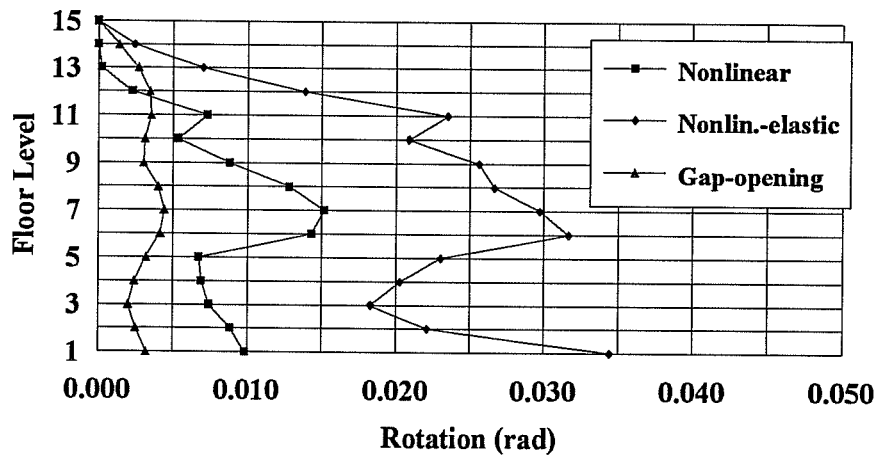


c) Left End of Beam B-C.

Figure 4.10 Accumulated Plastic Rotations, Viña del Mar.



d) Right End of Beam B-C.



e) Left End of Beam C-D.

Figure 4.10 (cont'd) Accumulated Plastic Rotations, Viña del Mar.

elastic and gap-opening systems versus the nonlinear system. The use of relative comparisons is based on the premise that the building having nonlinear connection behavior will emulate a well-detailed reinforced concrete structure.

The inelastic actions of the nonlinear connections were comparatively small in part due to the ability of the connection to absorb energy with large moment-rotation hysteresis loops. Also, the structure had small peak-to-peak displacement cycles after it had acquired a residual drift (Fig. 4.4). In effect, the origin of the moment-rotation cycles for many of the connections moved and the connections began to act about a shifted origin with the same stiffness as the initial elastic stiffness. Due to the small peak-to-peak displacements of the structure after the residual drift was acquired, the yield moment of each connection was rarely exceeded and inelastic action was limited. As a result, accumulated plastic deformations were relatively small. The maximum relative rotation (Table 4.3) of 0.0067 radians occurred during the scaled El Centro record. For this ground motion it was the smallest maximum rotation recorded for the three hysteresis types.

The structure having gap-opening connections demonstrated very minimal inelastic activity and distributed it well over the height of the structure (Fig. 4.8 through Fig. 4.10). Maximum recorded accumulated plastic rotations for this connection (0.0044 to 0.0103 radians) (Table 4.3) were the smallest for each ground motion. This was due largely to the fact that the structure underwent a very limited number of inelastic cycles due to its long period of vibration. In effect, it had fewer chances to accumulate plastic deformations. The smaller number of cycles this hysteretic behavior produced is evident in Fig. 4.4. The maximum plastic rotation of 0.0105 radians which occurred during the scaled El Centro record was approximately 1.5 times the maximum inelastic rotation calculated for the connections having nonlinear hysteretic behavior. This indicates that such a connection may need to be designed to accommodate larger ductility demands.

The accumulated plastic rotations for the nonlinear-elastic connections were higher for all ground motions than those calculated for the other hysteretic

models. Maximum values exceeded those calculated for the nonlinear connections by factors ranging from 2.0 to 2.7. Because of the "pinched" nature of the nonlinear-elastic model, minimal energy was absorbed by the connections. The structure moved through greater peak-to-peak displacements than for the nonlinear connection case and experienced a greater number of load cycles than for the gap-opening case (Fig. 4.4). Therefore, connections reached the "yield moment" more often and spent considerable time on the plastic plateau. The nonlinear-elastic connections experienced large maximum rotations during all three earthquake records (Table 4.3). The maximum plastic rotation of 0.0101 radians was 2.4 times the maximum calculated for the nonlinear connection model.

Although the behavior of the nonlinear-elastic connections appears to be by far the worst, consideration of the behavior of actual connections that will behave like the nonlinear-elastic model should alleviate many of these concerns. Unbonded post-tensioned connections tested by the National Institute of Standards and Technology [5] demonstrated that opening of precast joints produced a dramatic change in connection stiffness that resembled yielding of a normal reinforced concrete connection. However, because tendons in the beams were unbonded, no yielding was actually experienced by the reinforcement. When the calculated responses from this study for the nonlinear-elastic connection case are viewed in light of these tests, the accumulated plastic rotations lose significance because the reinforcement in the connections does not actually experience nonlinear behavior.

Maximum accumulated plastic rotations in columns at each floor level are compared in Fig. 4.11. Only results for the scaled El Centro record are plotted as a worst case scenario. For the nonlinear connection case, hinges formed only at the ground level of the columns. The nonlinear-elastic and gap-opening cases experienced plastic hinge rotations in columns located in other stories in addition to first-story columns. The plastic hinges appear to follow and may have been initiated by the strength discontinuities.

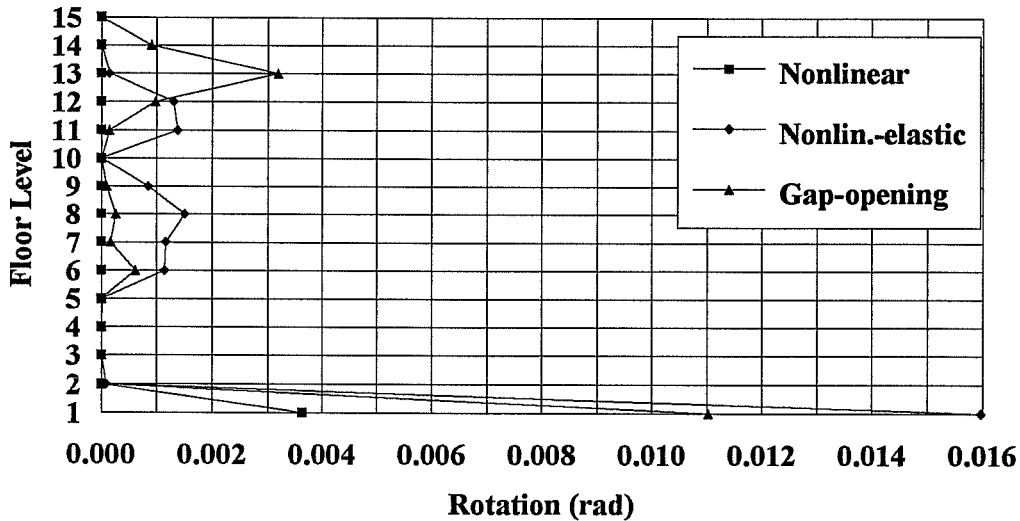
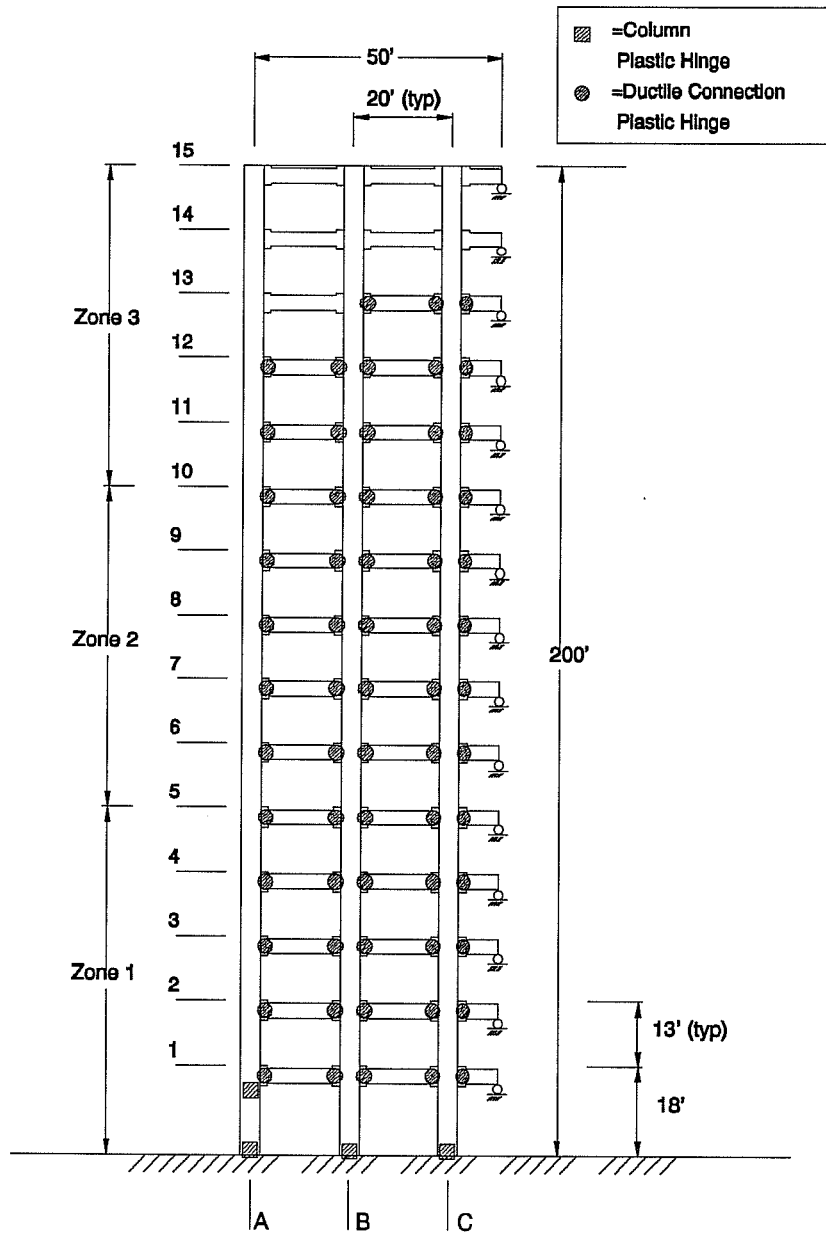


Figure 4.11 Accumulated Plastic Rotations in Columns, Scaled El Centro.

The locations of column and beam connection plastic hinges are marked in Figs. 4.12 through 4.14. The number of beam connection hinges was slightly fewer for the nonlinear connection case. In the other two cases, more hinges formed in the top floors. (Keep in mind that for the nonlinear-elastic case these are not really hinges.) The structure with nonlinear connections exhibited the least number of column hinges, with a maximum of two upper-story hinges formed in column line A during the Viña del Mar ground motion.

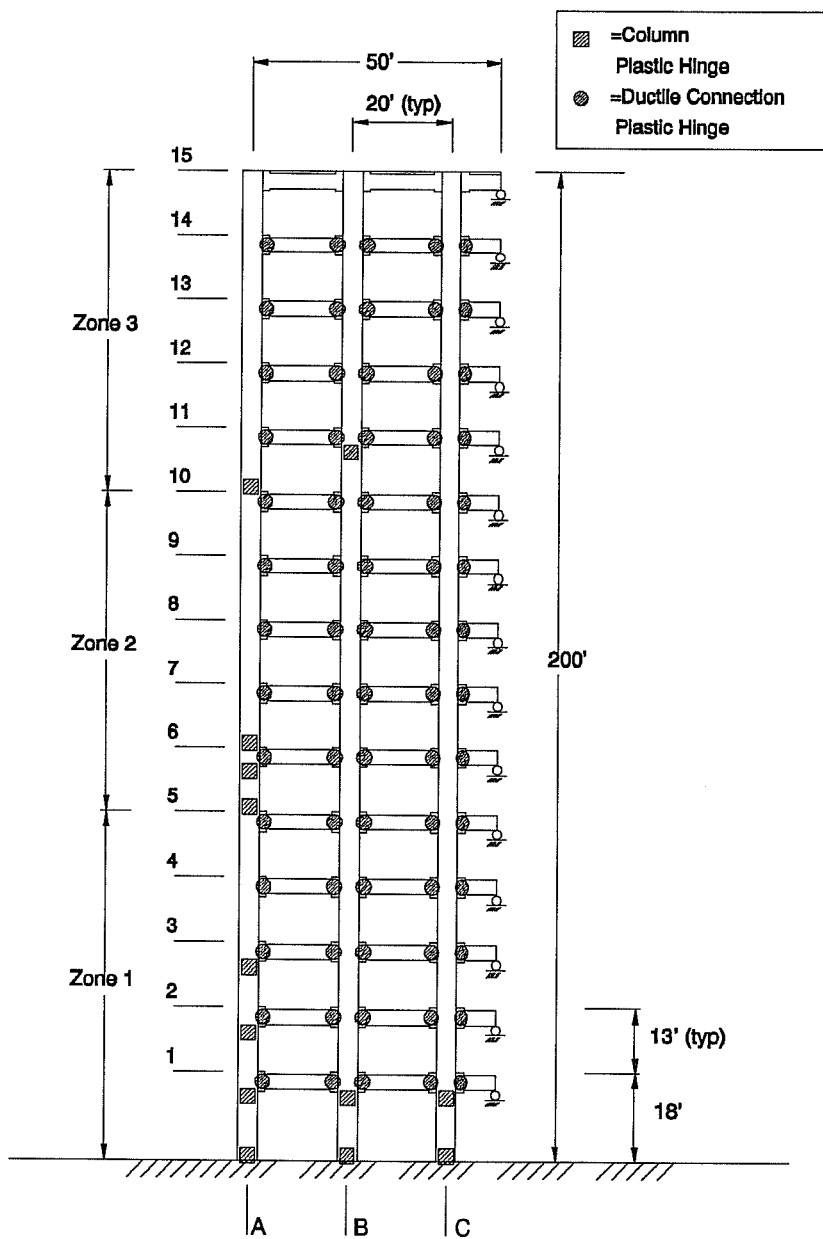
The nonlinear-elastic and gap-opening cases developed substantially larger numbers of plastic hinges in the columns. In many cases, the member strength discontinuities were denoted by column plastic hinges formed just above the zone changes. Column line A experienced the most inelastic action, as expected, because maximum rotations occurred in this column line.

In order to further understand the differences in nonlinear behavior that occurred, story shear envelopes for the three connection cases and three base motions are plotted in Fig 4.15. For all ground motions, the nonlinear-elastic connection case developed the highest lateral forces, resulting in higher strength



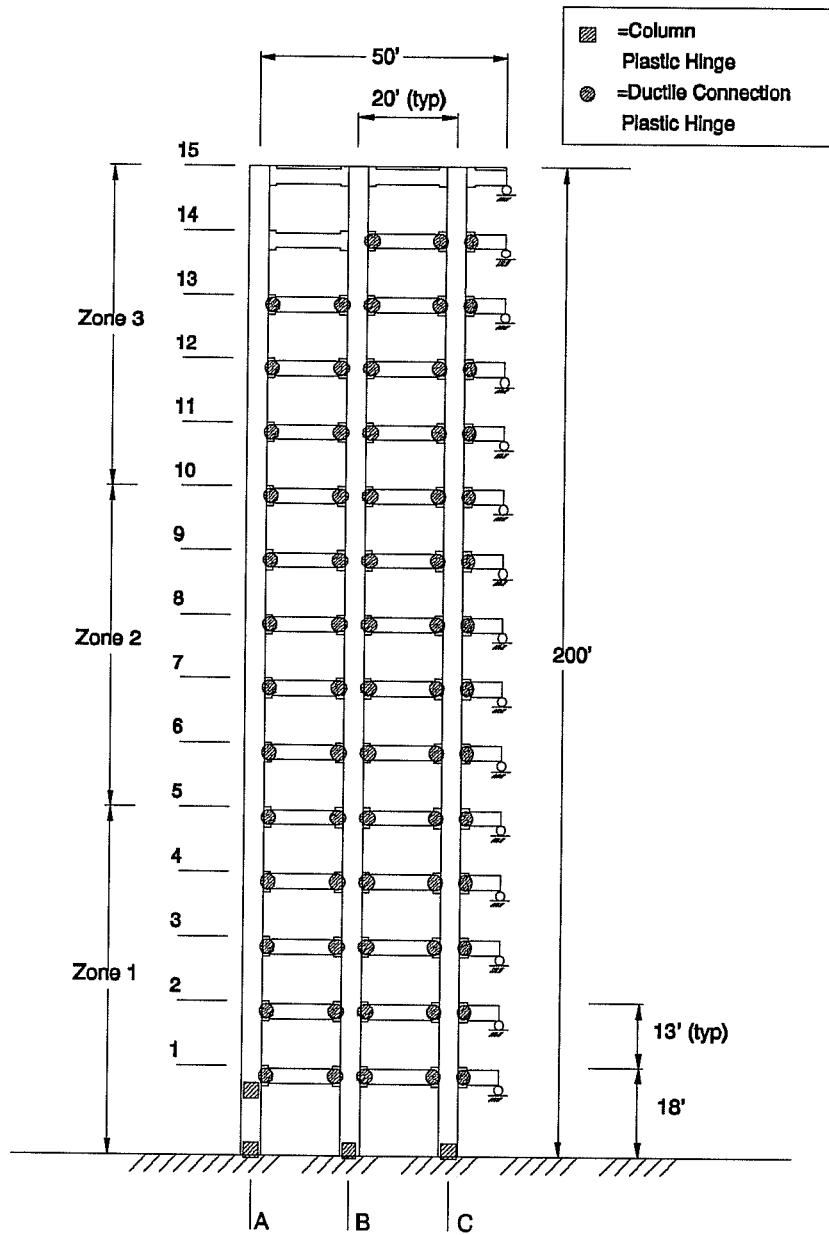
a) Nonlinear Behavior.

Figure 4.12 Locations of Plastic Hinges, El Centro.



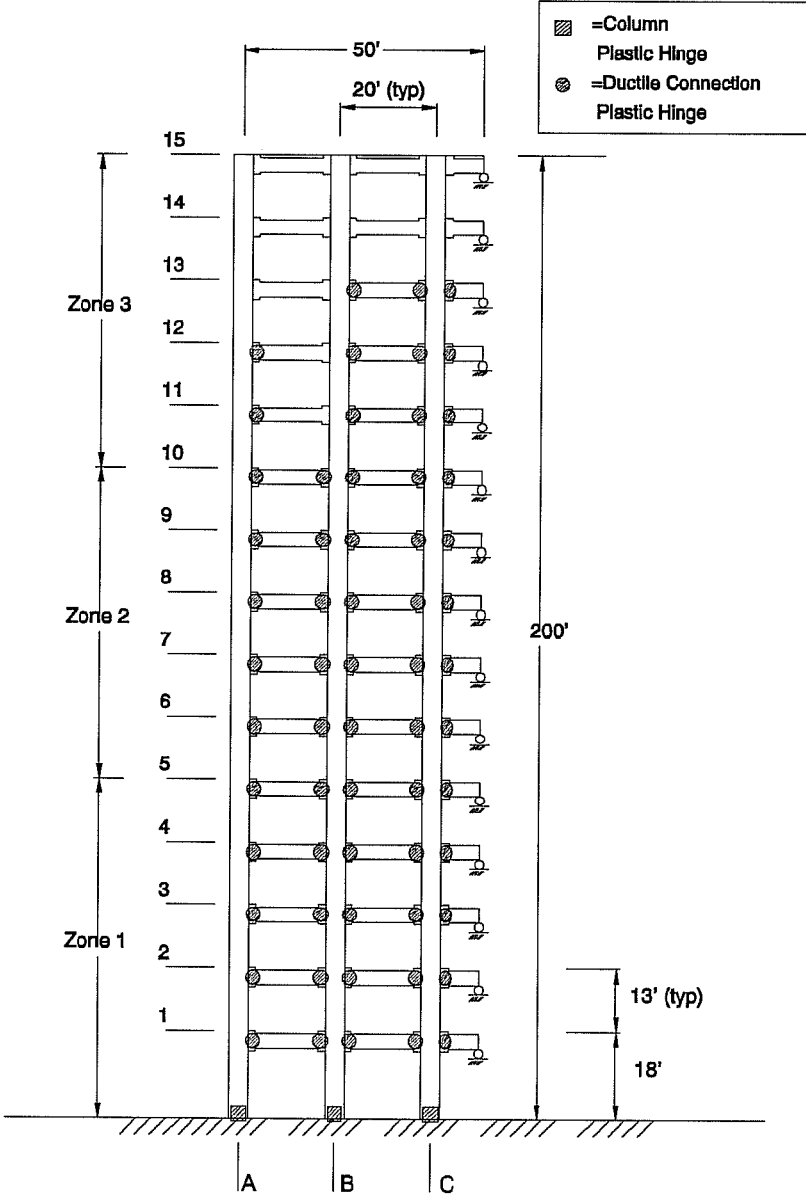
b) Nonlinear-Elastic Behavior.

Figure 4.12 (cont'd) Locations of Plastic Hinges, El Centro.



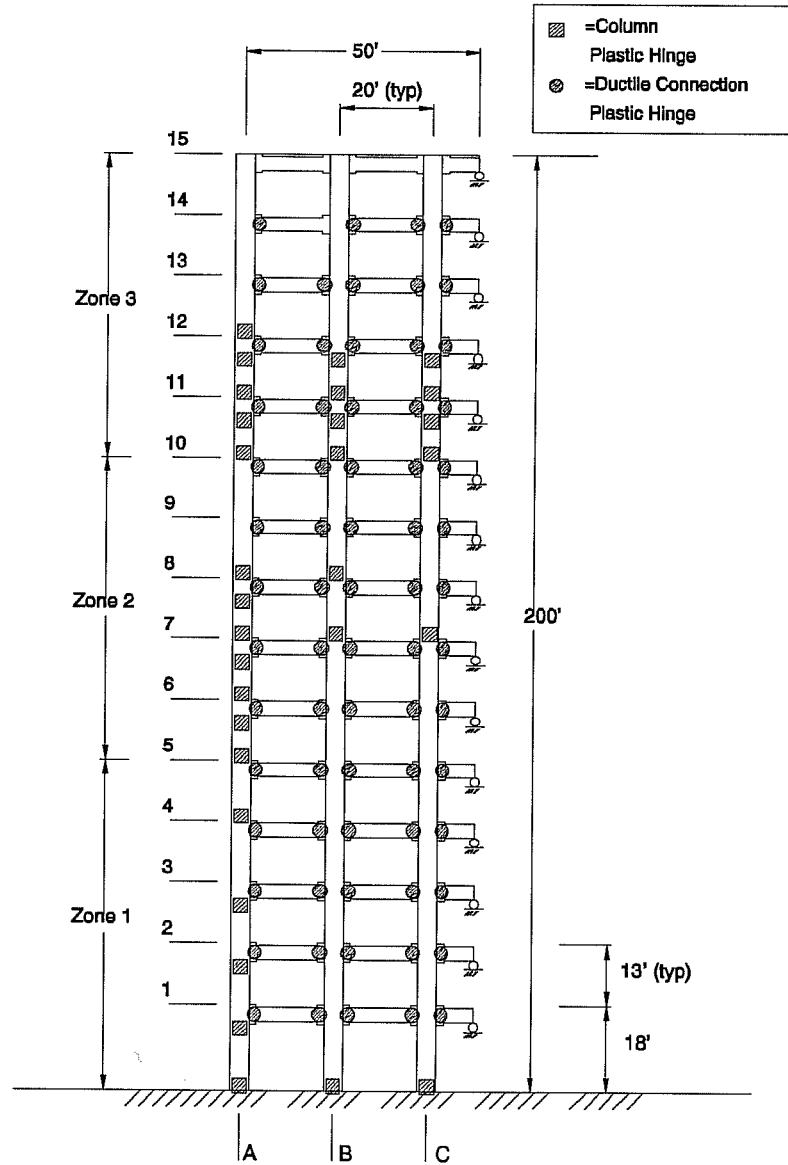
c) Gap-Opening Behavior.

Figure 4.12 (cont'd) Locations of Plastic Hinges, El Centro.



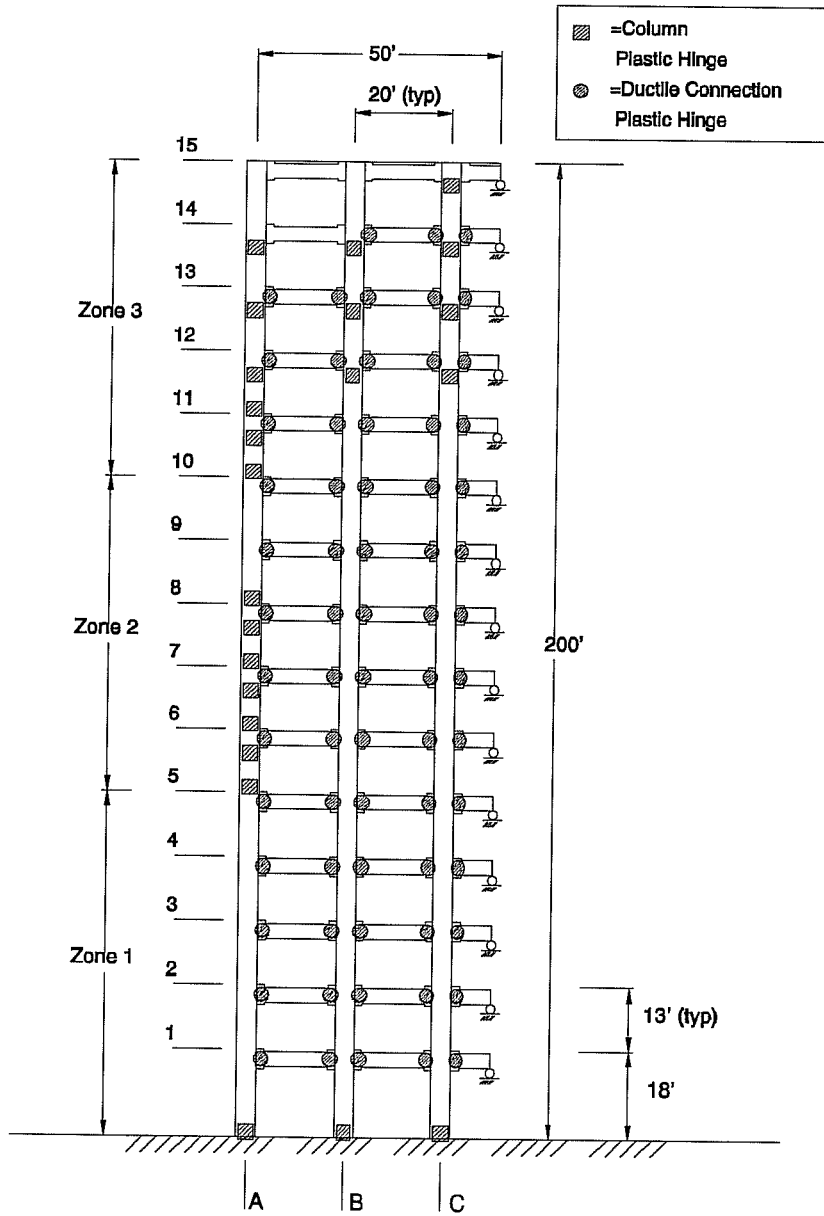
a) Nonlinear Behavior.

Figure 4.13 Locations of Plastic Hinges, Scaled El Centro.



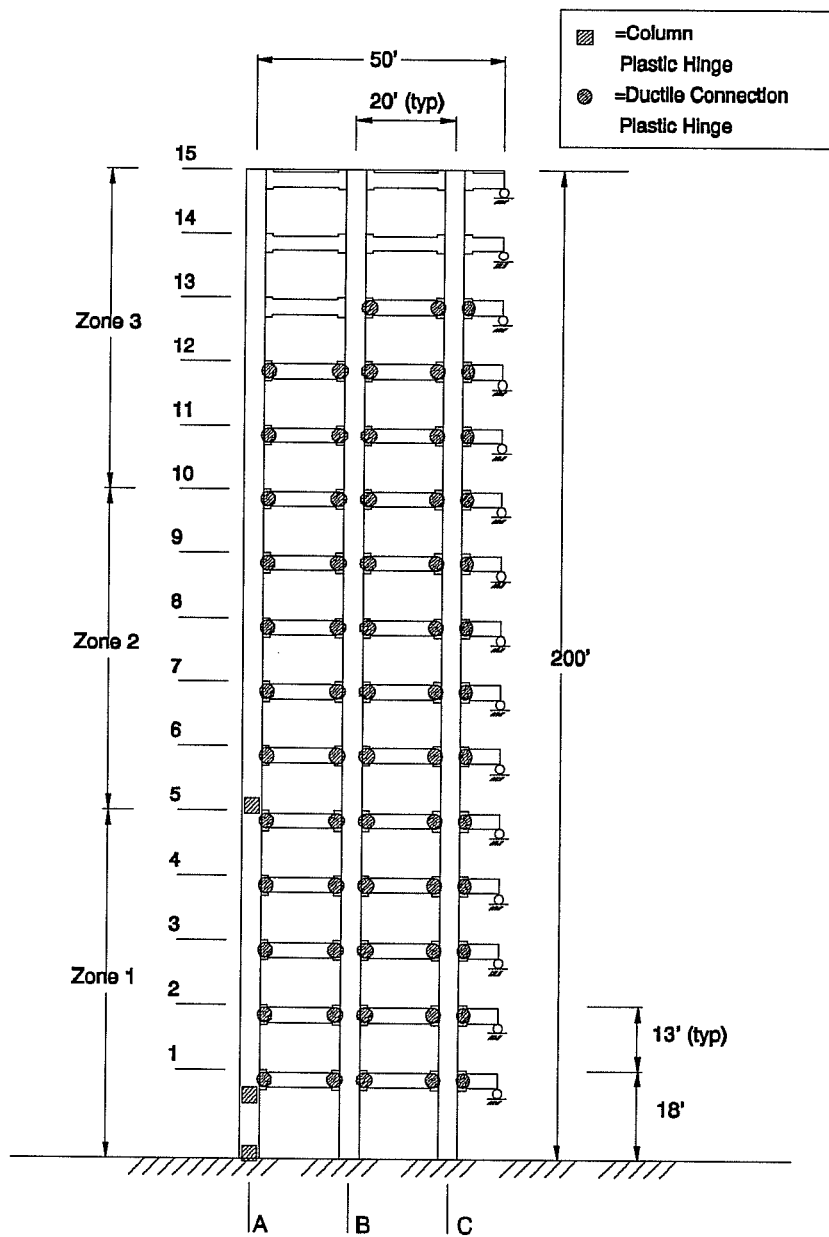
b) Nonlinear-Elastic Behavior.

Figure 4.13 (cont'd) Locations of Plastic Hinges, Scaled El Centro.



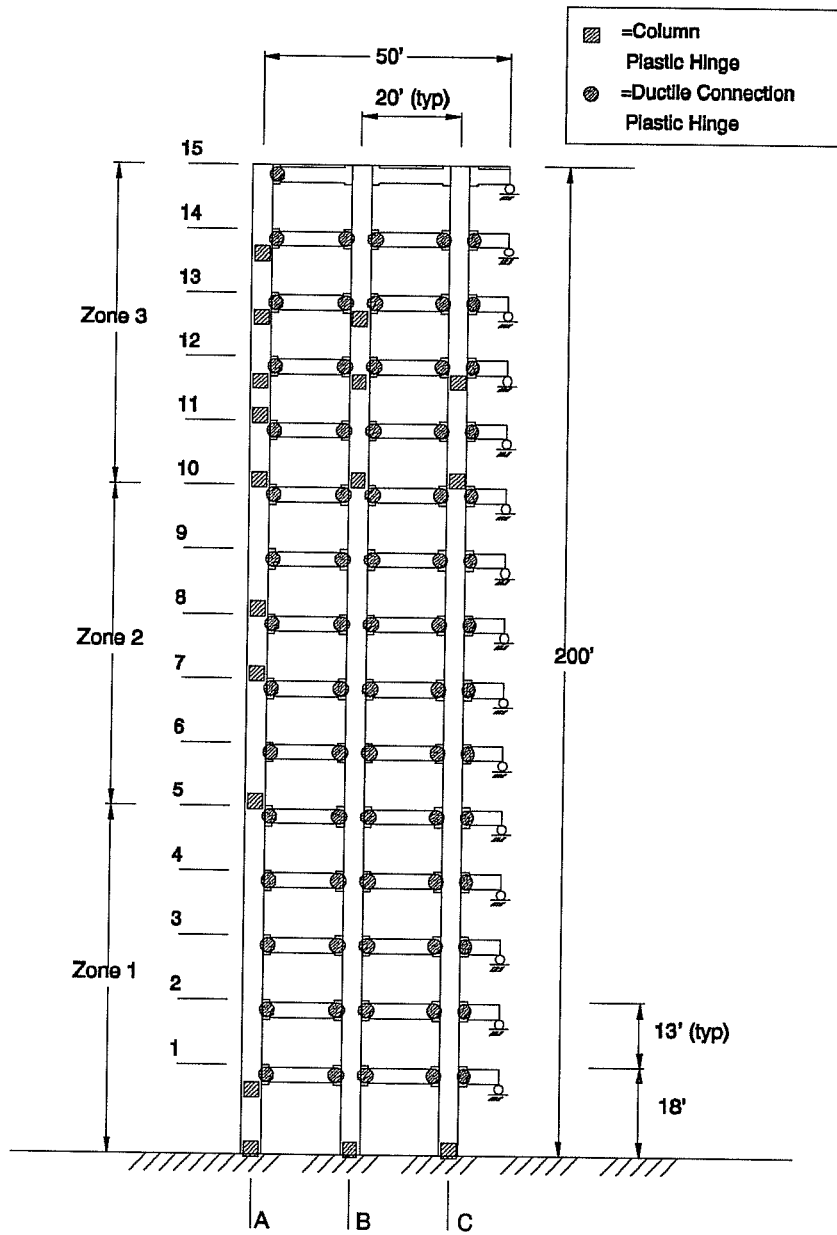
c) Gap-Opening Behavior.

Figure 4.13 (cont'd) Locations of Plastic Hinges, Scaled El Centro.



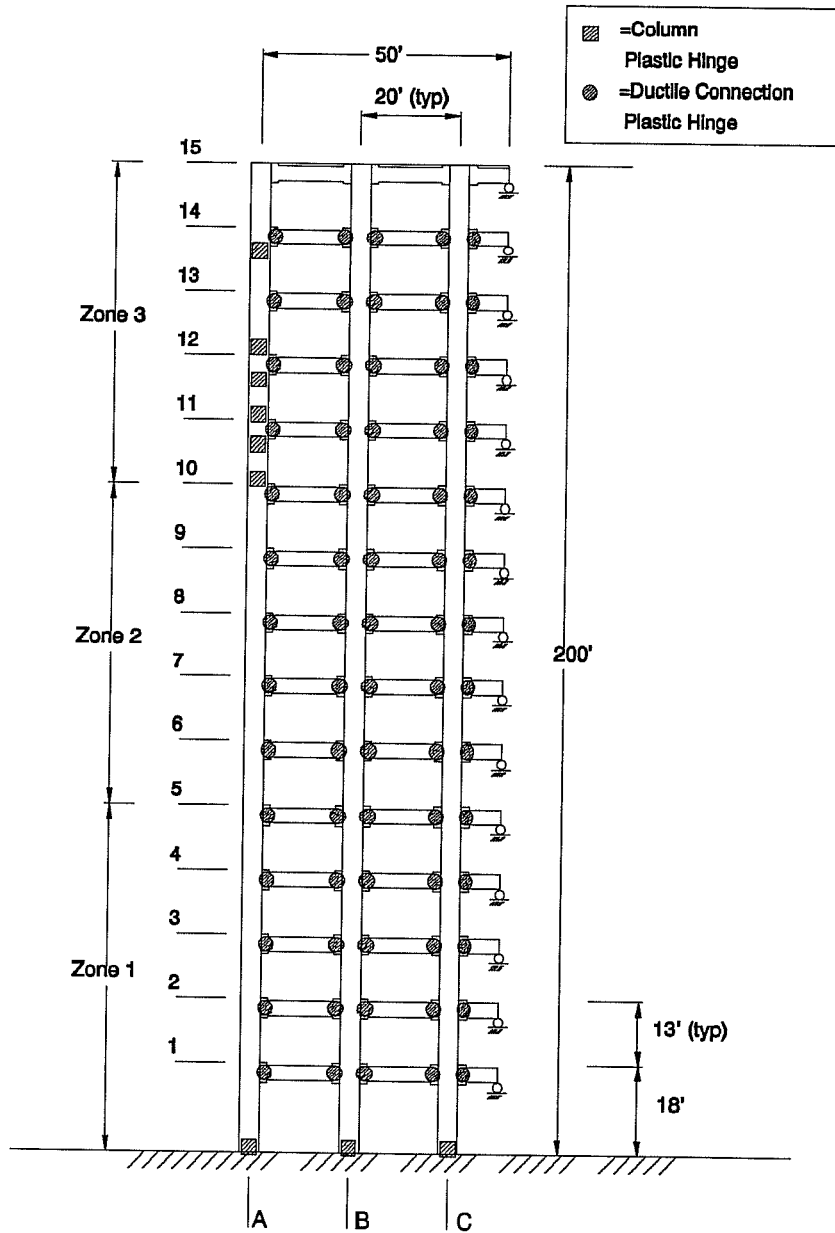
a) Nonlinear Behavior.

Figure 4.14 Locations of Plastic Hinges, Viña del Mar.



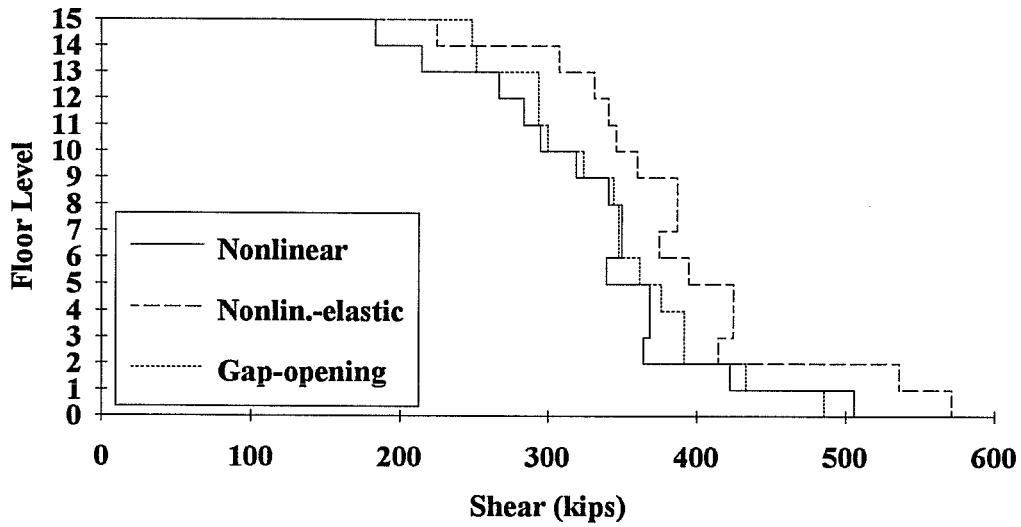
b) Nonlinear-elastic Behavior.

Figure 4.14 (cont'd) Locations of Plastic Hinges, Viña del Mar.

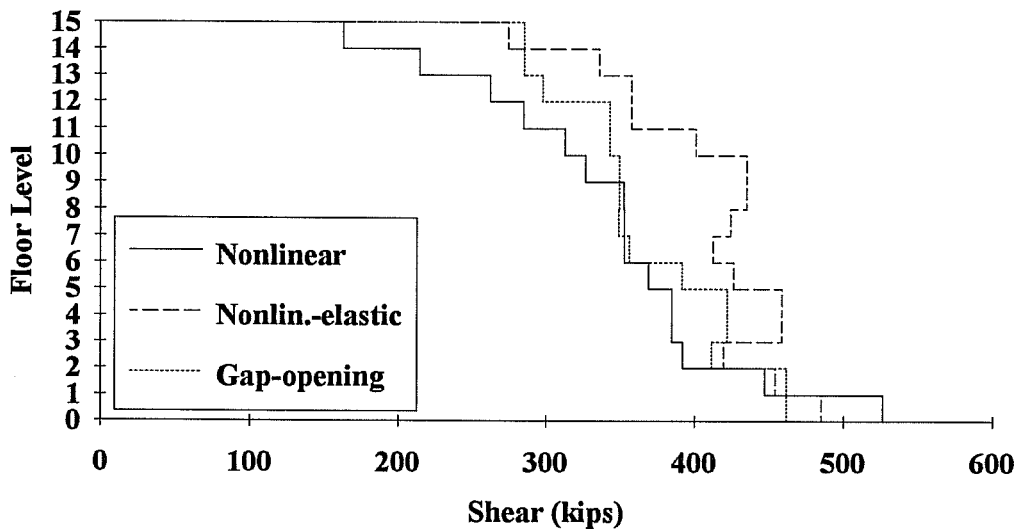


c) Gap-Opening Behavior.

Figure 4.14 (cont'd) Locations of Plastic Hinges, Viña del Mar.

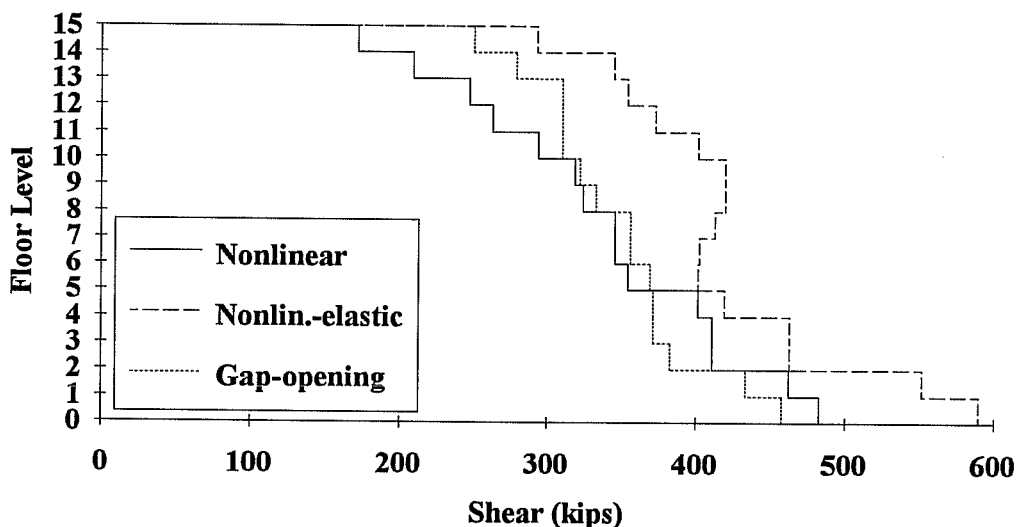


a) El Centro.



b) Scaled El Centro.

Figure 4.15 Story Shear Envelopes.



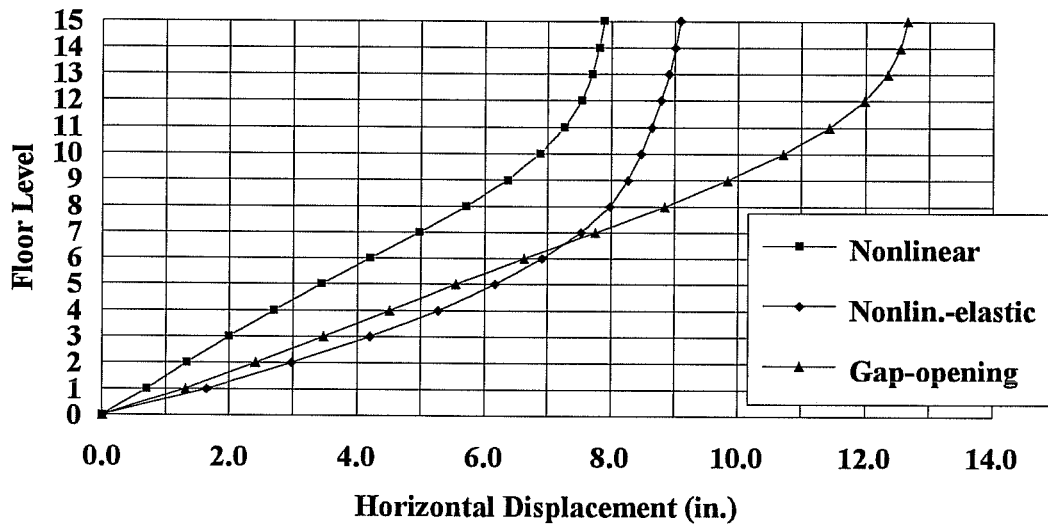
c) Viña del Mar.

Figure 4.15 (cont'd) Story Shear Envelopes.

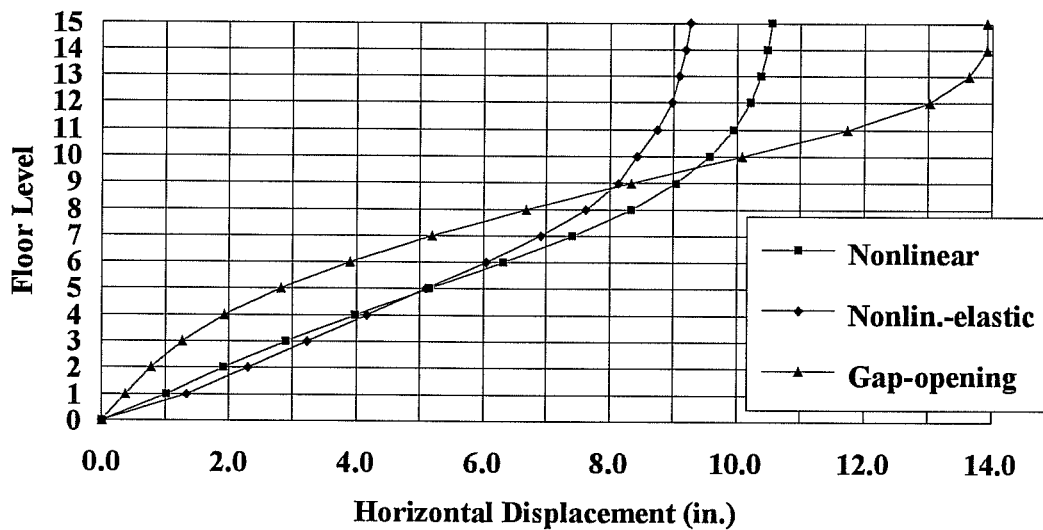
members needed for this type of behavior. Nonlinear connection behavior developed the smallest story shears, most notably in the upper stories.

4.2.5 Higher Mode Vibrations

Due to the long-period response for the gap-opening hysteretic case, higher modes of response were observed. In Fig. 4.16 the floor displacements are plotted for when the roof reached maximum displacement. A deformed shape with higher-mode components is visible in Fig 4.16c. In this figure, the first floor has displaced a small amount in the negative direction while the roof reached its maximum positive displacement. Another unusual deformed shape was observed at the peak response for the gap-opening case during the scaled El Centro base motion. Figure 4.17 shows structure displacements coinciding with the maximum displacement of the first story. Once again, the gap-opening connections displayed higher mode responses, as seen in Figs. 4.17a and 4.17c.

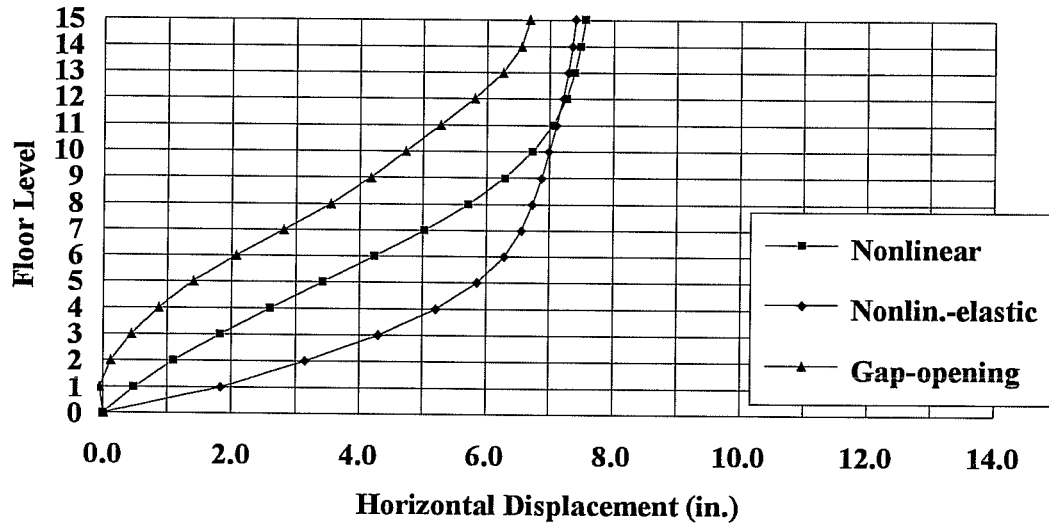


a) El Centro.



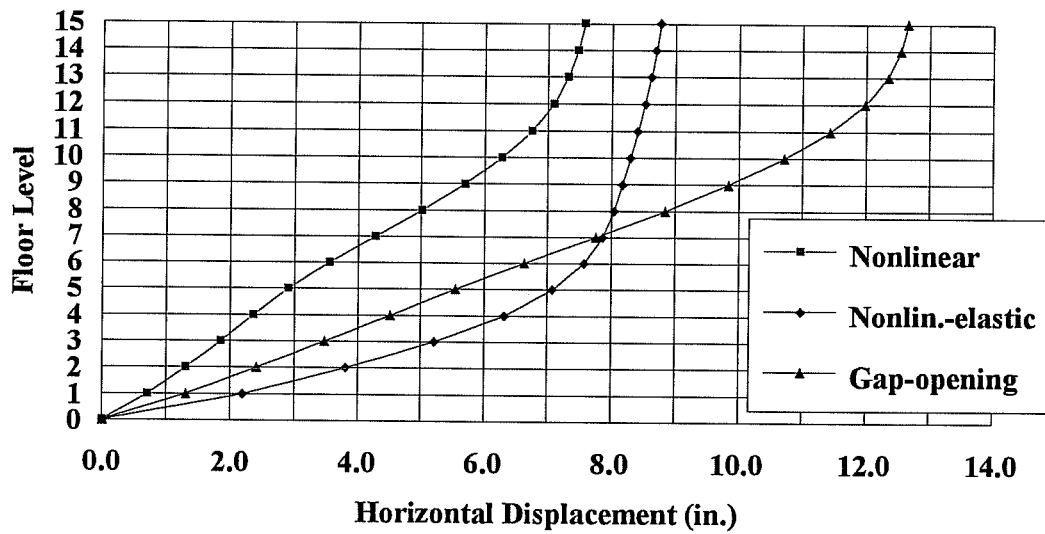
b) Scaled El Centro.

Figure 4.16 Floor Displacements when the 15th Story is at its Maximum Displacement.



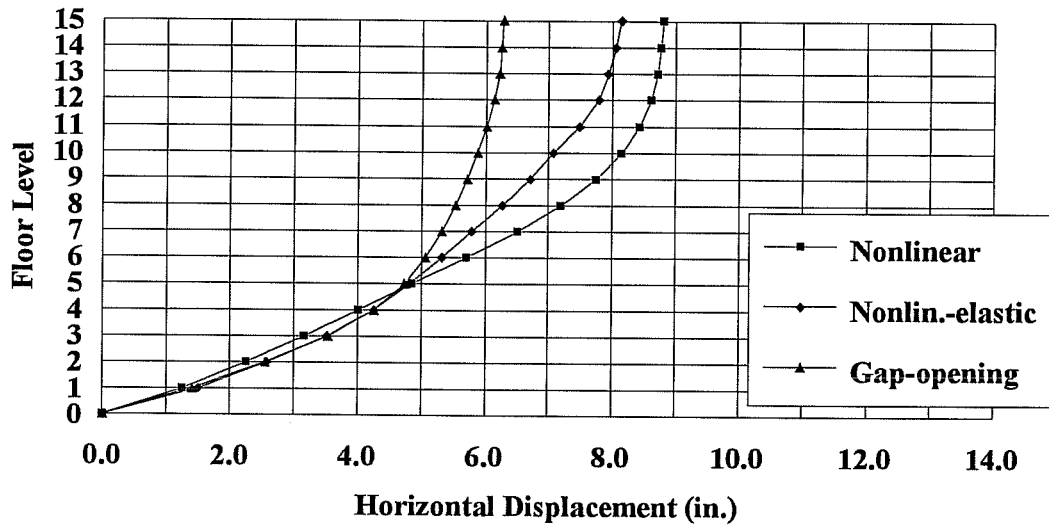
c) Viña del Mar.

Figure 4.16 (cont'd) Floor Displacements when the 15th Story is at its Maximum Displacement.

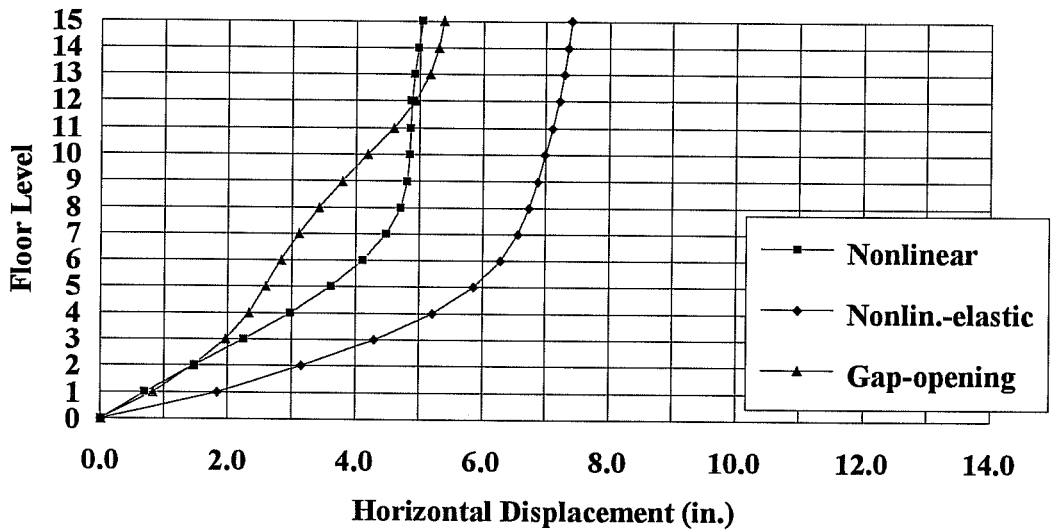


a) El Centro.

Figure 4.17 Floor Displacements when the 1st Story is at its Maximum Displacement.



b) Scaled El Centro.



c) Viña del Mar.

Figure 4.17 (cont'd) Floor Displacements when the 1st Story is at its Maximum Displacement.

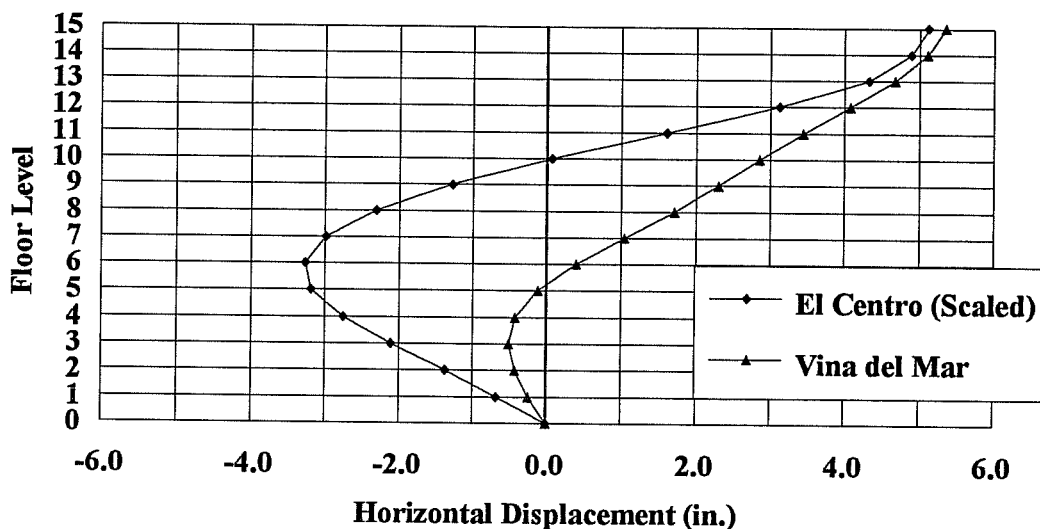


Figure 4.18 Floor Displacements, Higher Mode Response for Gap-Opening Behavior.

Figure 4.18 depicts the displaced shape for the structure with gap-opening connections at 48.84 seconds during the Viña del Mar record and at 14.73 seconds during the scaled El Centro record. The structure is responding with what appears to be a second mode shape. For the weaker El Centro ground motion, only primary mode shapes were detected.

4.3 5-Story Frame

The smaller frame was also analyzed for each type of connection and for the three ground motions. The parameters were kept the same as for the 15-story prototype building. The structure was designed with two zones of member strengths. The first zone consisted of the 1st through 3rd floor levels and the second zone contained the top two stories. Strengths for the two zones were established as described in Section 2.5.

The 5-story frame subjected to gravity loads had a period, based on elastic properties, of approximately 0.55 seconds in comparison to 1.42 seconds for the

15-story frame. The dramatic shortening of period length for the smaller frame is the primary reason for examining the dynamic response of the structure.

4.3.1 Structural Displacement Results for the 5-Story Frame

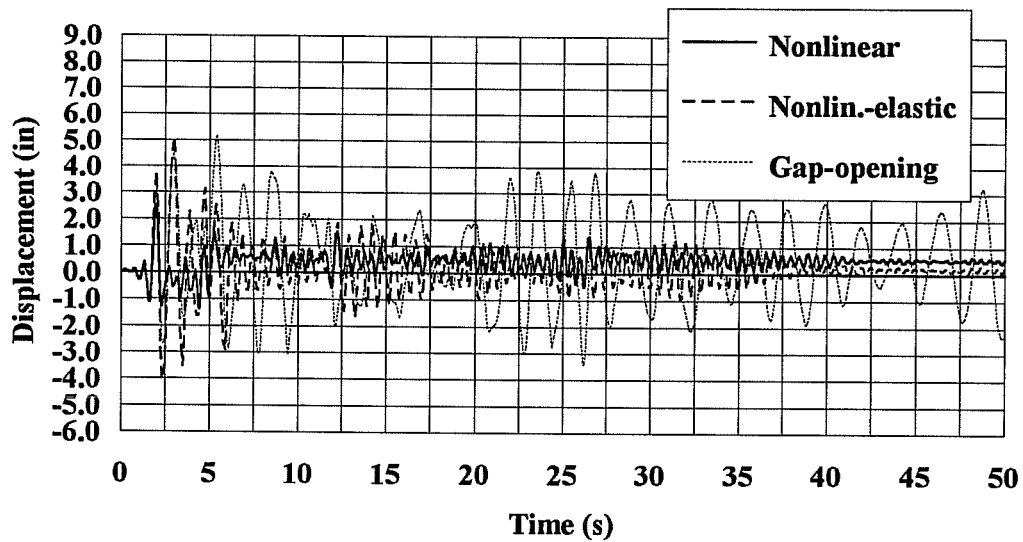
The 5th level displacement histories are shown in Fig. 4.19. Envelopes for displacements over the height of the structure are displayed in Fig. 4.20, and tabulated maximum displacements and building drifts are cataloged in Table 4.4.

The structure with nonlinear connections experienced relatively small displacements and had permanent deformations as did the 15-story structure (Fig. 4.4). Residual drifts were smaller though, with values between 0.01% and 0.02%.

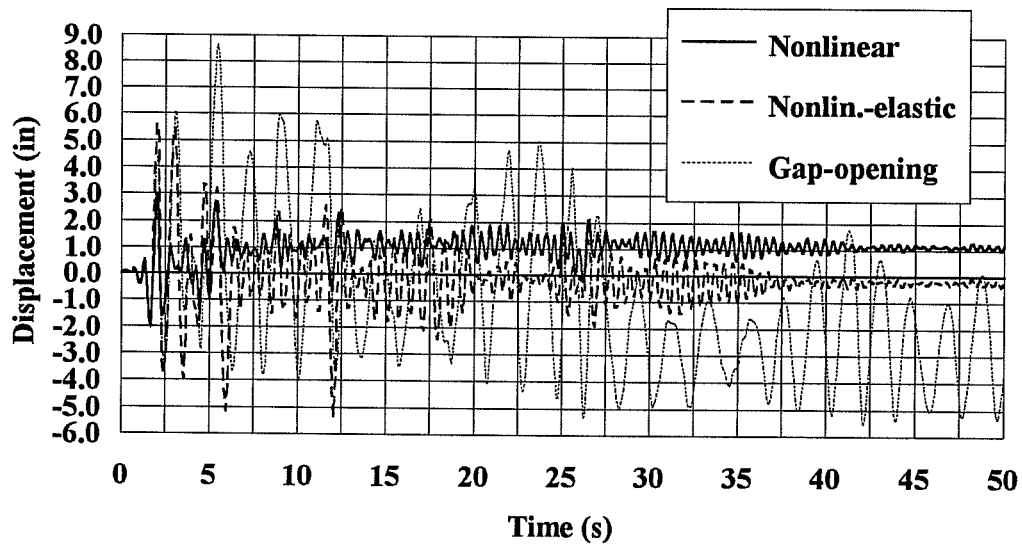
The gap-opening case performed poorly for all ground motions, but especially so for the scaled El Centro earthquake record where an approximate residual drift of 0.35% occurred (Fig. 4.19b). The predominant period for this type of hysteretic behavior was approximately 1.5 to 2.0 seconds, compared to predominant periods of approximately 0.5 to 1.0 second for the other two connection types. The longer periods resulting from the gap-opening connections are clear in the roof displacement plots (Fig. 4.19). The periods are not as long as those estimated earlier for the 15-story frame (2.0 to 2.7 seconds), and as a result the taller frame experienced smaller building drifts during the Viña del Mar record (Tables 4.2 and 4.4).

The nonlinear-elastic case performed poorest for the Viña del Mar record, experiencing a maximum building drift of nearly 1%. It produced small permanent deformations, which were not evident in the taller frame, for all the ground motions.

Drifts for the 5-story frame (Table 4.4) were generally larger than drifts tabulated for the 15-story frame (Table 4.2). Frames having nonlinear-elastic and gap-opening connections generated structural drifts from 1.8 to 3.2 times the drifts generated in the taller frame for the Viña del Mar and scaled El Centro ground motions. The largest drift of 1.03% occurred for the scaled El Centro record and with the gap-opening hysteresis. Only frames with nonlinear connection behavior

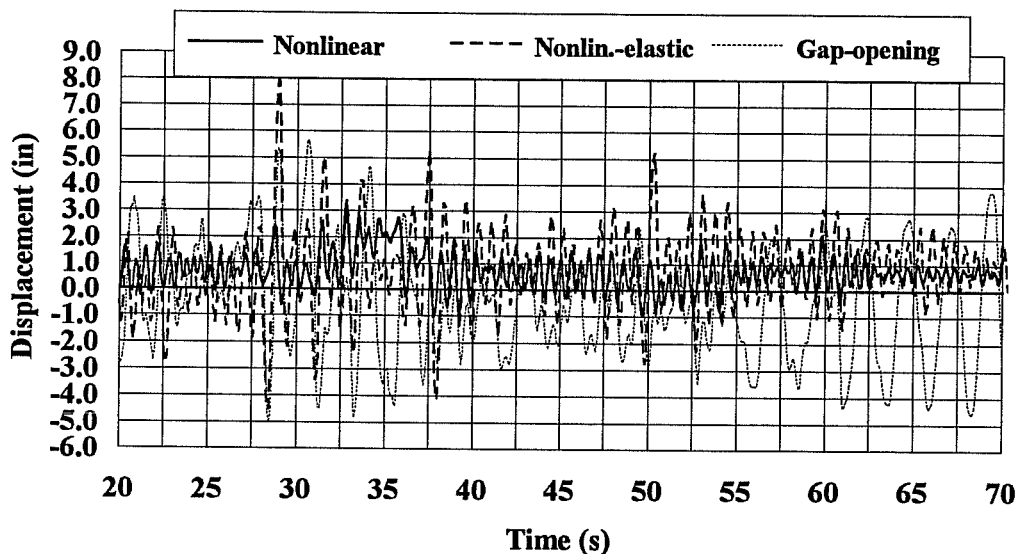


a) El Centro.



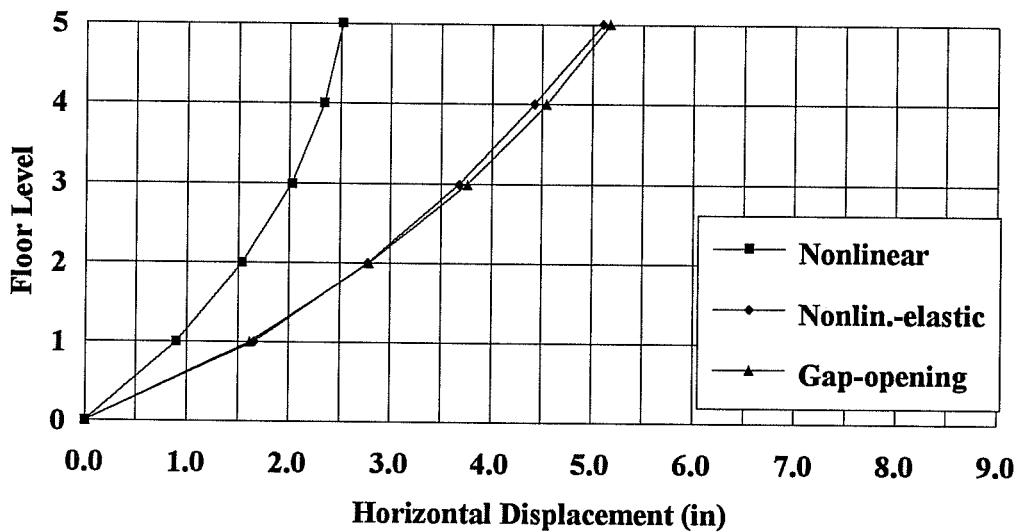
b) Scaled El Centro.

Figure 4.19) Displacement Histories of 5th Story.



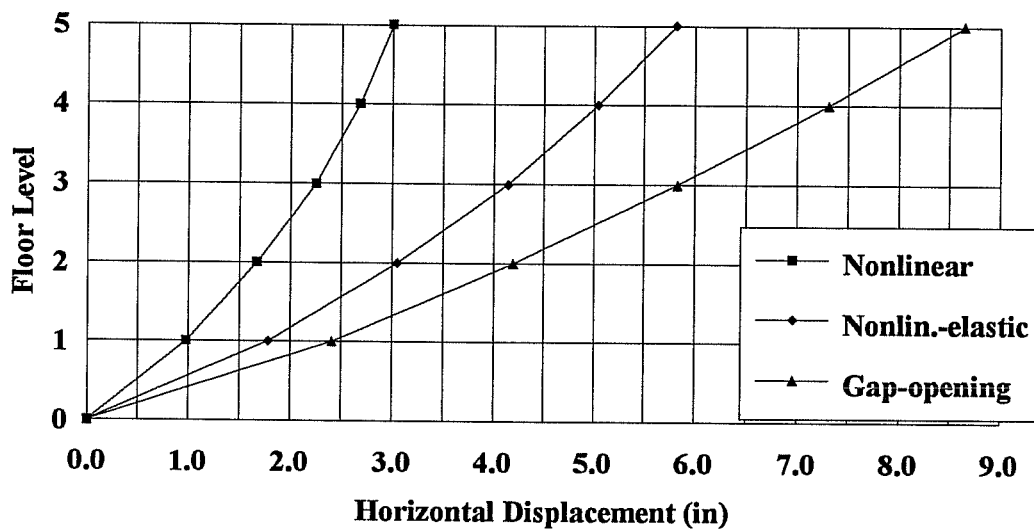
c) Viña del Mar.

Figure 4.19 (cont'd) Displacement Histories of 5th Story.

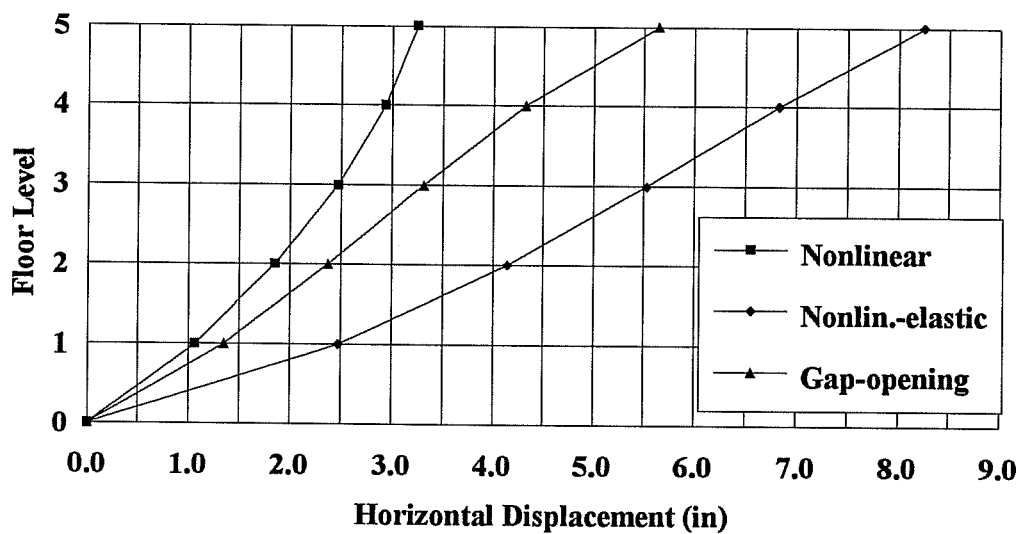


a) El Centro.

Figure 4.20 Floor Displacement Envelopes, 5-Story Frame.



b) Scaled El Centro.



c) Viña del Mar.

Figure 4.20 (cont'd) Floor Displacement Envelopes, 5-Story Frame.

Table 4.4 Maximum Displacements of 5th Story and Maximum Building Drifts.

	Nonlinear Behavior		Nonlinear-elastic Behavior		Gap-opening Behavior	
	Max Disp (in)	Drift (%)	Max Disp (in)	Drift (%)	Max Disp (in)	Drift (%)
El Centro	2.52	0.30	5.10	0.61	5.17	0.62
El Centro (Sc)	3.00	0.36	5.81	0.69	8.64	1.03
Vina del Mar	3.24	0.39	8.25	0.98	5.64	0.67

had similar drifts for both size buildings. Drifts for these connections ranged from 0.30% to 0.39%.

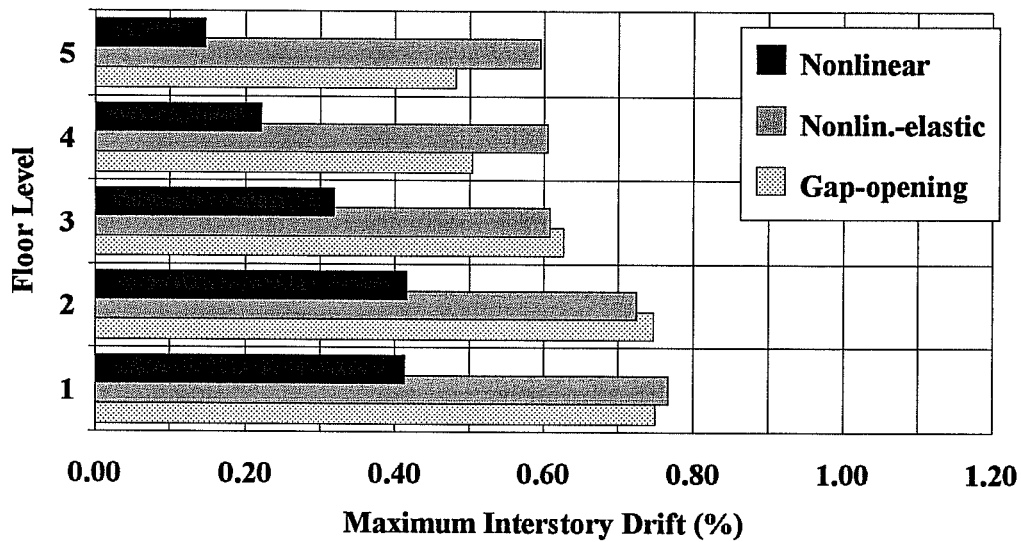
Interstory drift envelopes shown in Fig. 4.21 closely resemble the 15-story trends (Fig. 4.6). The nonlinear connection case consistently exhibited the smallest interstory drifts. The case of gap-opening behavior resulted in the largest interstory drifts for the scaled El Centro base motion, and the nonlinear-elastic case displayed the largest interstory drifts for the Viña del Mar ground motion as was observed for the taller frame.

The strength discontinuity between the 3rd and 4th stories is hardly detectable in the displacement envelopes or interstory drift envelopes, presumably because of the smaller number of floors and the fact that the second zone only contains two floor levels. However, the frame with gap-opening connections appeared to be influenced by the discontinuity; in Fig 4.21c interstory drifts increased with height of the building for the Viña del Mar ground motion.

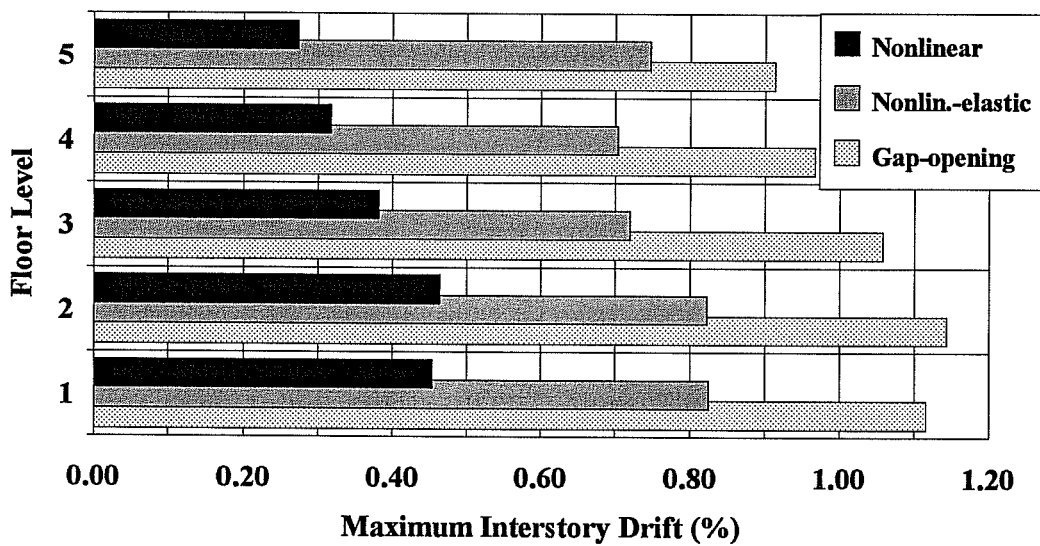
The envelopes of interstory drifts were closely related to the rotation envelopes of the column line A nodes shown in Fig. 4.22. The rotation envelopes along the building height were larger and more evenly distributed than the maximum rotations for the 15-story frame (Fig. 4.7). Due to the consistently large rotations in the 5-story frame, all connection elements formed hinges during each ground motion.

4.3.2 Inelastic Action in the 5-Story Frame

To examine the inelastic behavior of the structure, accumulated plastic rotations are plotted in Figs. 4.23 through 4.25 for the connection elements and in Fig. 4.26 for the columns during the scaled El Centro and Viña del Mar base

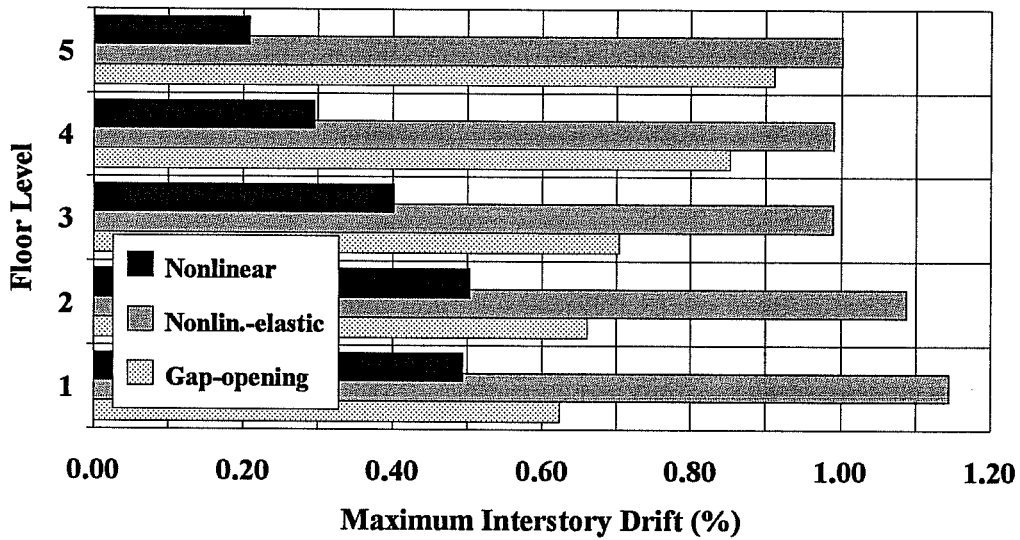


a) El Centro.



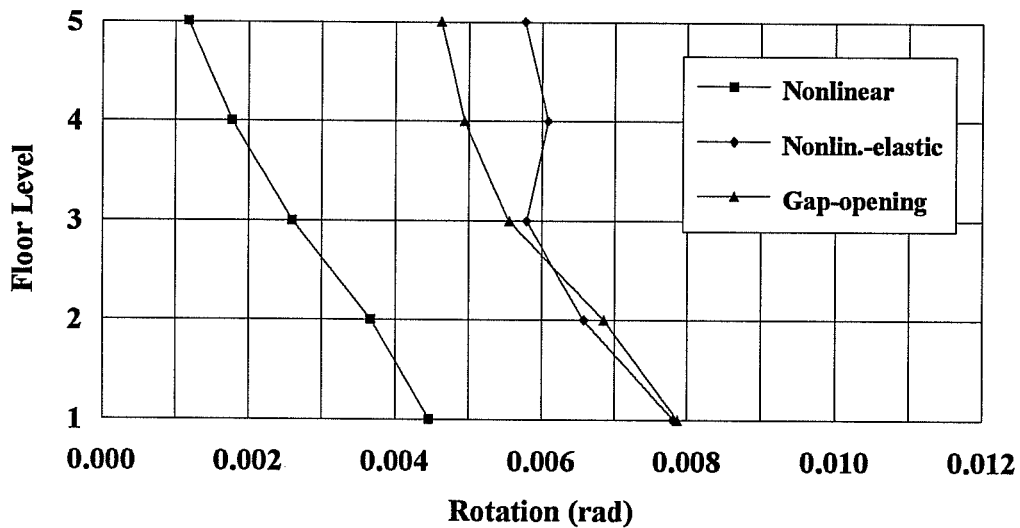
b) Scaled El Centro.

Figure 4.21 Interstory Drift Envelopes, 5-Story Frame.



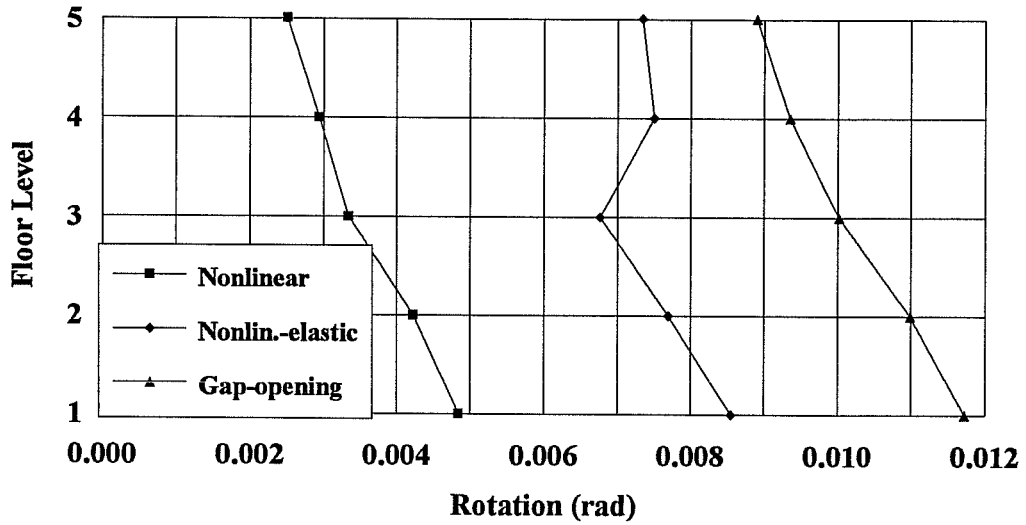
c) Viña del Mar.

Figure 4.21 (cont'd) Interstory Drift Envelopes, 5-Story Frame.

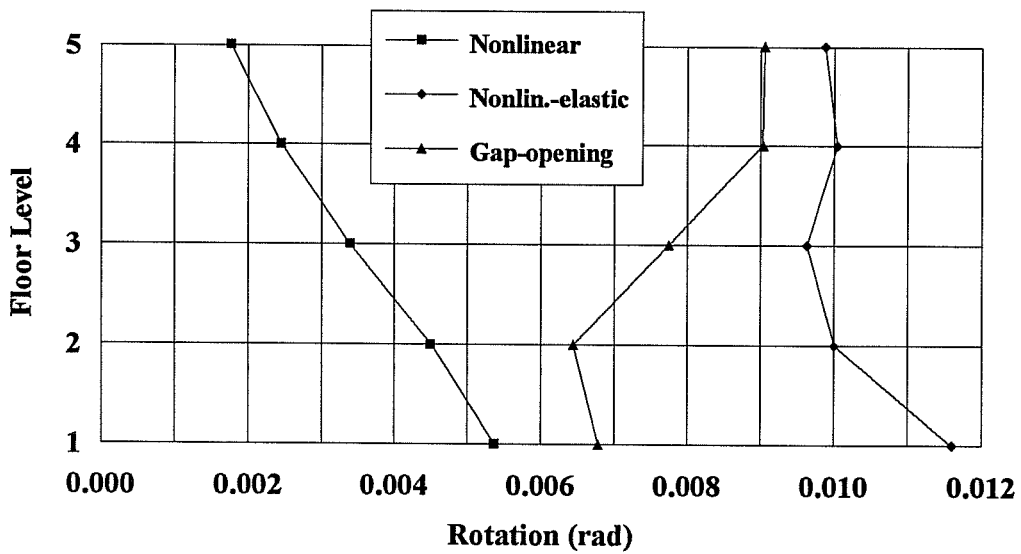


a) El Centro.

Figure 4.22 Rotation Envelopes of Column Line A Nodes, 5-Story Frame.

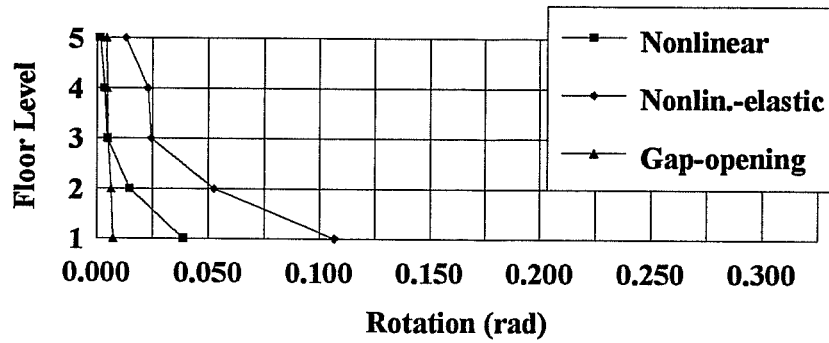


b) Scaled El Centro.

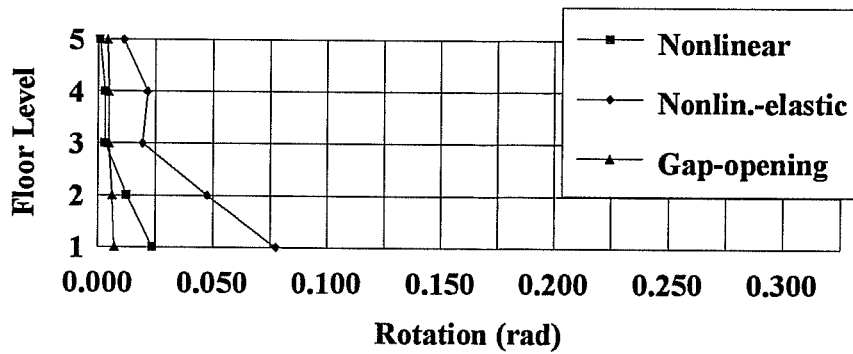


c) Viña del Mar.

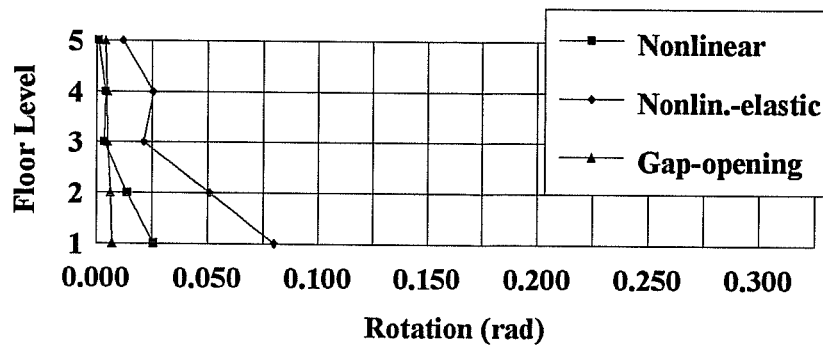
Figure 4.22 (cont'd) Rotation Envelopes of Column Line A Nodes, 5-Story Frame.



a) Left End of Beam A-B.

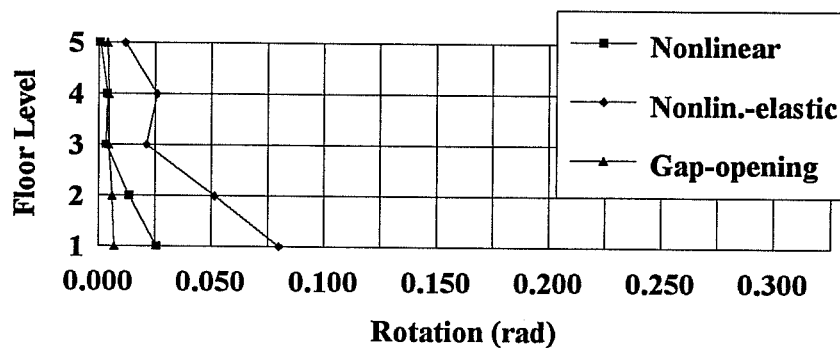


b) Right End of Beam A-B.

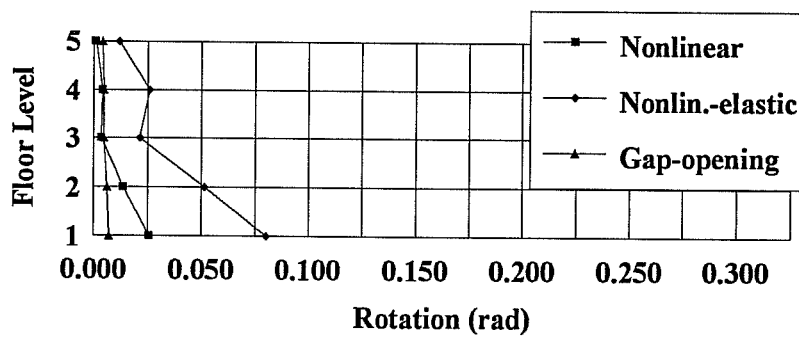


c) Left End of Beam B-C.

Figure 4.23 Accumulated Plastic Rotations, El Centro, 5-Story Frame.

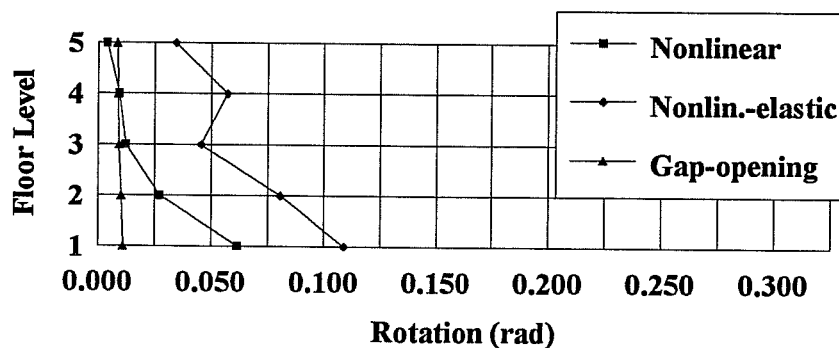


d) Right End of Beam B-C.

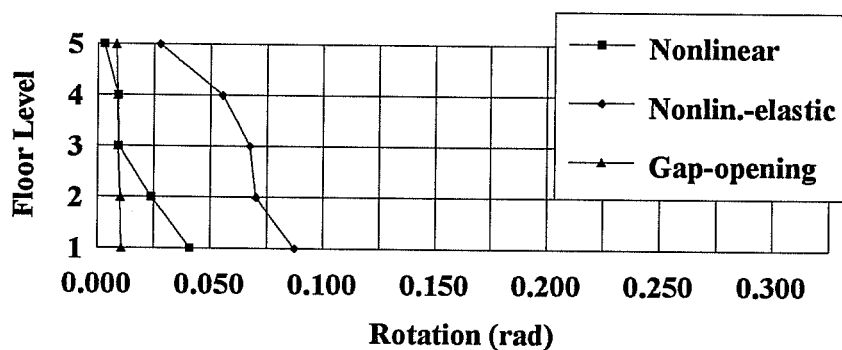


e) Left End of Beam C-D.

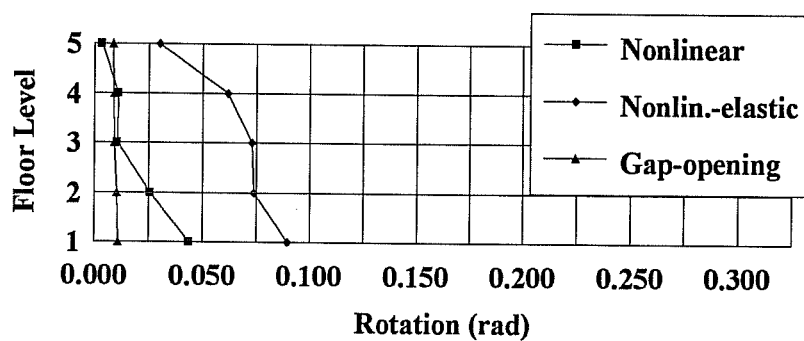
Figure 4.23 (cont'd) Accumulated Plastic Rotations, El Centro, 5-Story Frame.



a) Left End of Beam A-B.

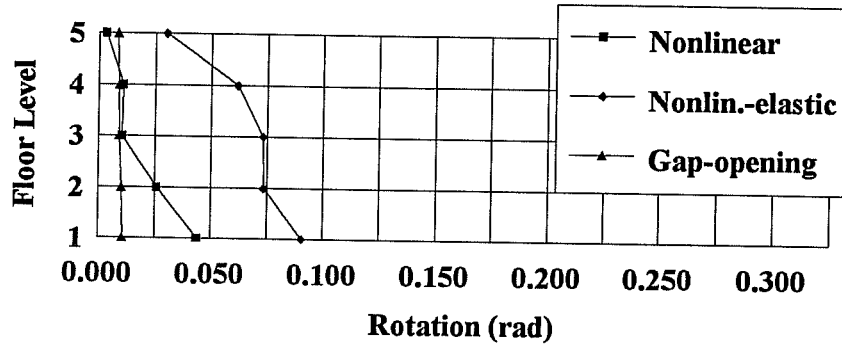


b) Right End of Beam A-B.

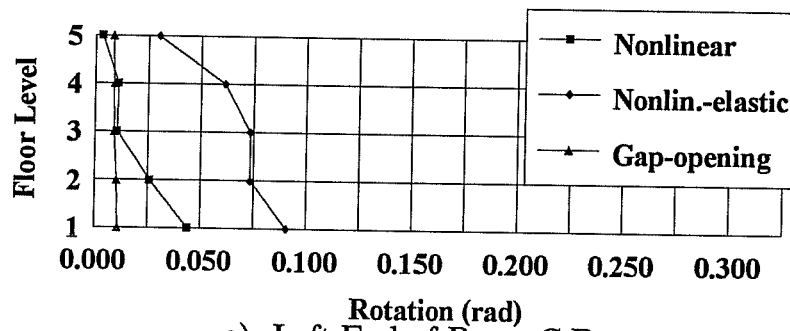


c) Left End of Beam B-C.

Figure 4.24 Accumulated Plastic Rotations, Scaled El Centro, 5-Story Frame.

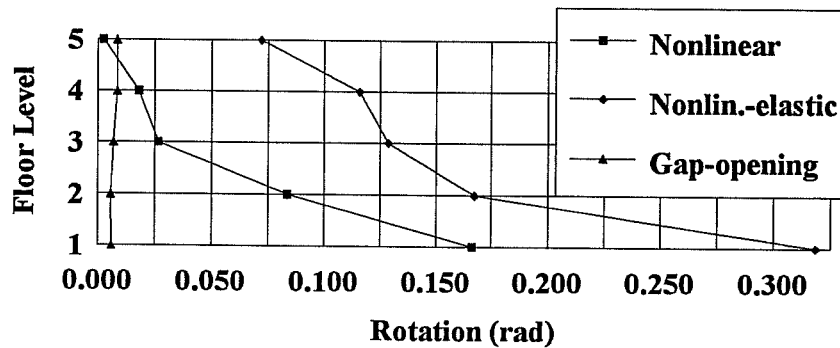


d) Right End of Beam B-C.

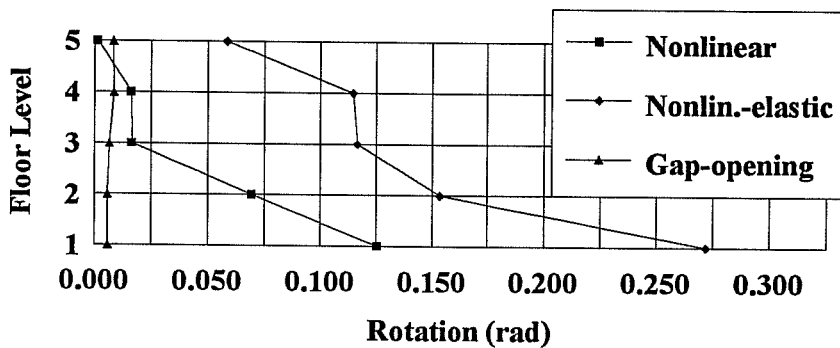


e) Left End of Beam C-D.

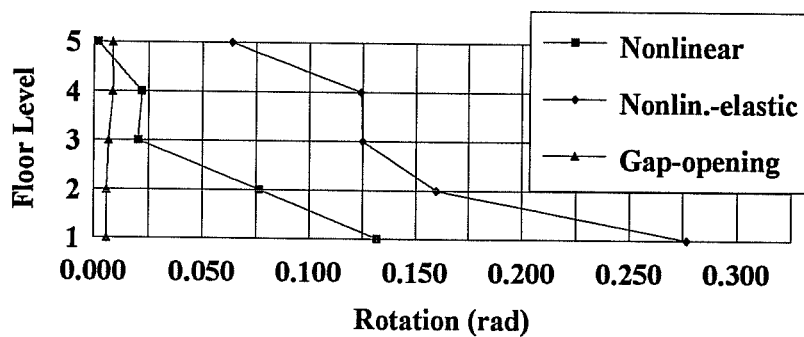
Figure 4.24 (cont'd) Accumulated Plastic Rotations, Scaled El Centro, 5-Story Frame.



a) Left End of Beam A-B.

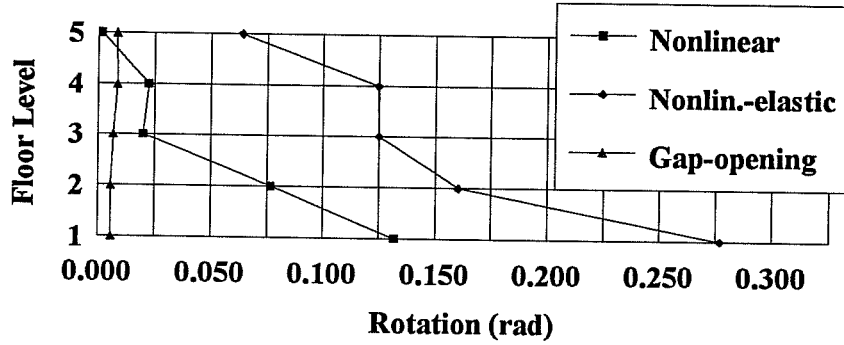


b) Right End of Beam A-B.

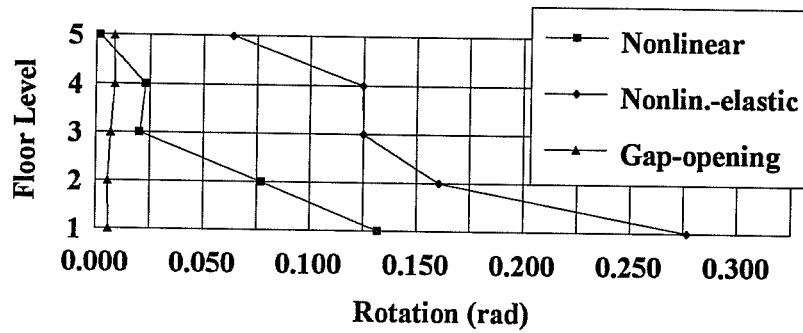


c) Left End of Beam B-C.

Figure 4.25 Accumulated Plastic Rotations, Viña del Mar, 5-Story Frame.

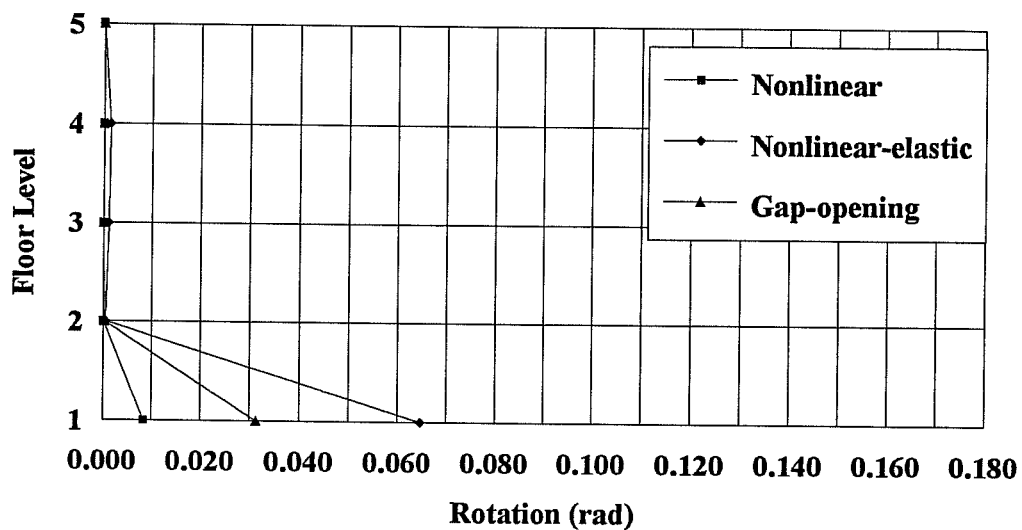


d) Right End of Beam B-C.

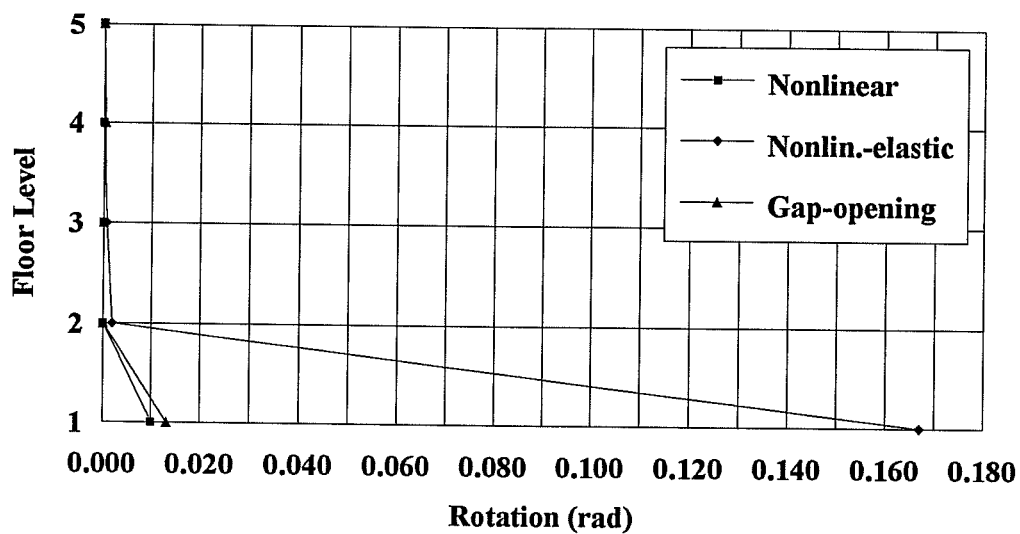


e) Left End of Beam C-D.

Figure 4.25 (cont'd) Accumulated Plastic Rotations, Viña del Mar, 5-Story Frame.



a) Scaled El Centro.



b) Viña del Mar.

Figure 4.26 Accumulated Plastic Rotations in Columns, 5-Story Frame.

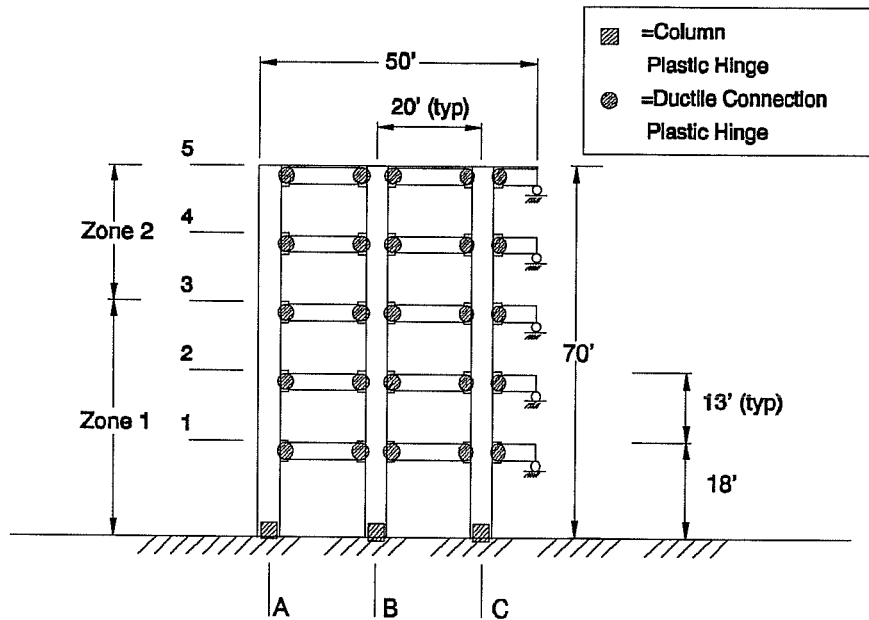
Table 4.5 Maximum Plastic Rotations and Maximum Accumulated Plastic Rotations for Connection Elements, 5-Story Frame.

	Nonlinear Behavior		Nonlinear-elastic Behavior		Gap-opening Behavior	
	Max (rad)	Accum. (rad)	Max (rad)	Accum. (rad)	Max (rad)	Accum. (rad)
El Centro	0.0041	0.0387	0.0074	0.1067	0.0075	0.0073
El Centro (Sc)	0.0044	0.0614	0.0082	0.1087	0.0113	0.0111
Vina del Mar	0.0050	0.1664	0.0112	0.3187	0.0089	0.0088

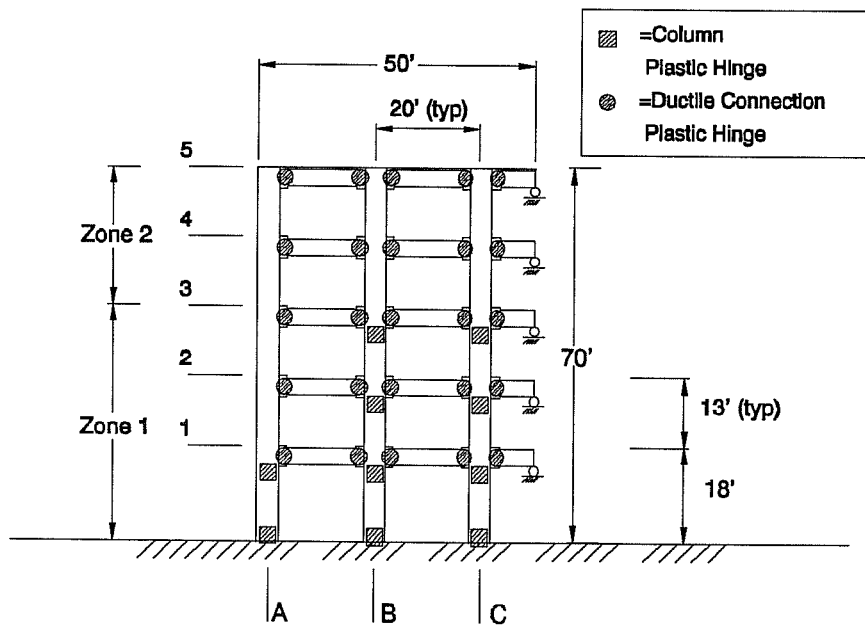
motions. Table 4.5 tabulates the maximum relative rotation and the maximum accumulated plastic rotation which occurred in any connection element. The locations of plastic hinges are shown in Figs. 4.27 through 4.29.

The structure modeled with nonlinear connections performed similar to the 15-story frame; column hinges only formed at the ground level with small accumulated plastic rotations (Fig. 4.26). However one area of concern is the large accumulated plastic rotations experienced in first-level connections. The maximum accumulated plastic rotation in a first-level connection for the Viña del Mar record of 0.1664 radians is nearly seven times the maximum accumulated plastic rotation in the same connections for the 15-story frame (0.0241 radians during scaled El Centro) (Table 4.2). It is likely that the larger accumulated plastic rotations were due in great part to the larger number of inelastic cycles (due to the shorter period) experienced by the 5-story structure. The maximum relative rotations experienced by the nonlinear connections were the smallest of the three hysteretic behaviors considered for all ground motions (Table 4.5). Maximum rotations were very similar to the maximum rotations in the 15-story frame (0.0042 to 0.0067 radians).

The building with gap-opening connections formed more column hinges than the building with nonlinear connections. The column hinges were in similar locations for the scaled El Centro and Viña del Mar base motions (Figs. 4.28c and 4.29c), forming at the strength zone boundary in the B and C column lines. For the El Centro record, most of these column hinges did not form (Fig. 4.27c). Plastic rotations in the columns and especially the connections were relatively small. Note in Figs. 4.23 through 4.25 that the accumulated excursions on the

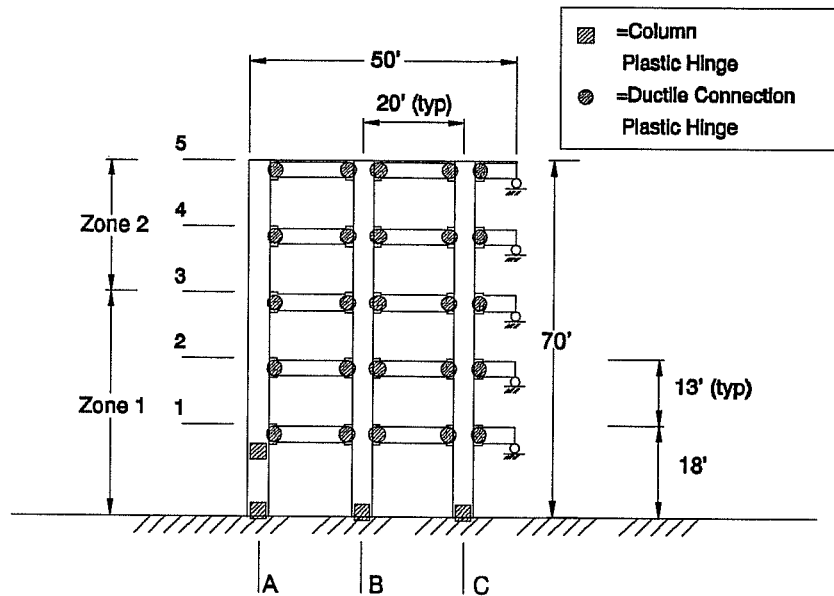


a) Nonlinear Behavior.



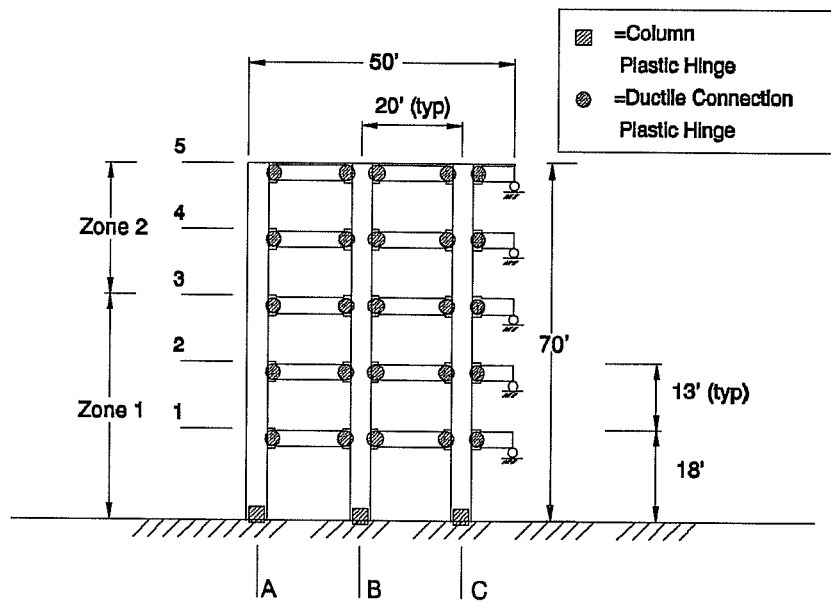
b) Nonlinear-Elastic Behavior.

Figure 4.27 Locations of Plastic Hinges, El Centro, 5-Story Frame.



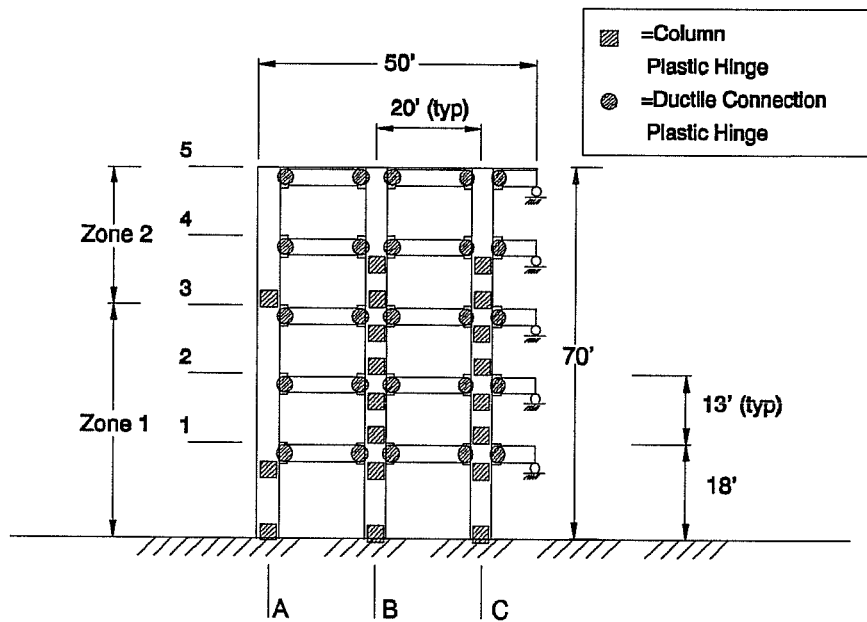
c) Gap-Opening Behavior.

Figure 4.27 (cont'd) Locations of Plastic Hinges, El Centro, 5-Story Frame.

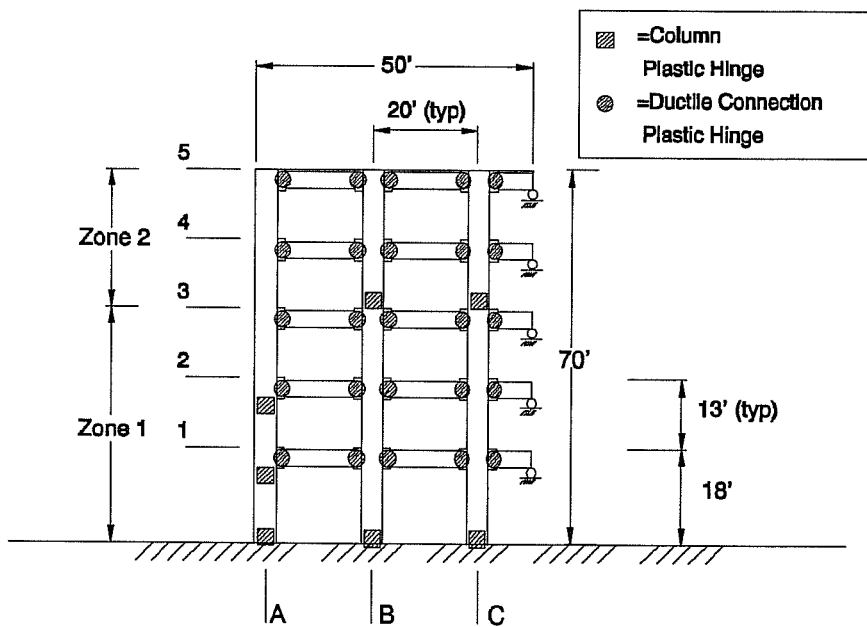


a) Nonlinear Behavior.

Figure 4.28 Locations of Plastic Hinges, Scaled El Centro, 5-Story Frame.

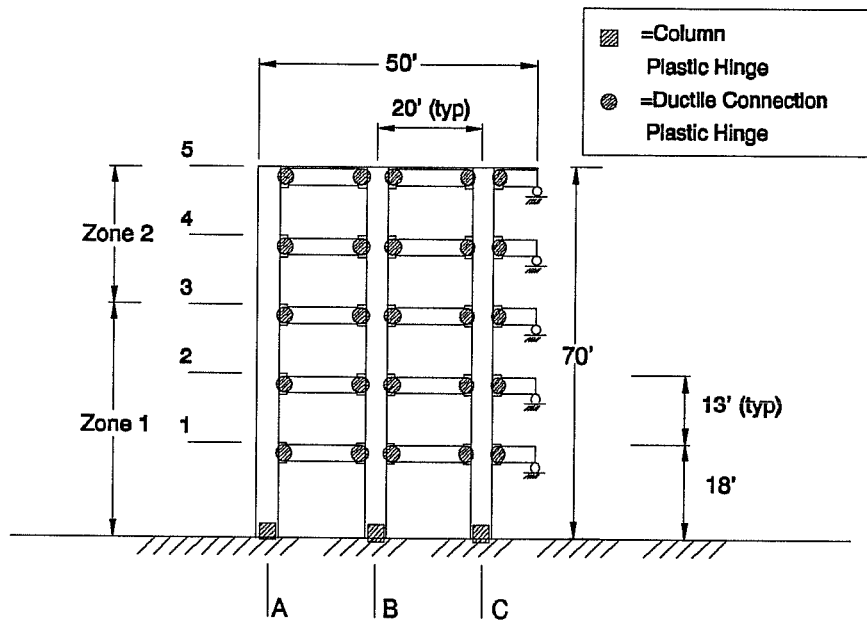


b) Nonlinear-Elastic Behavior.

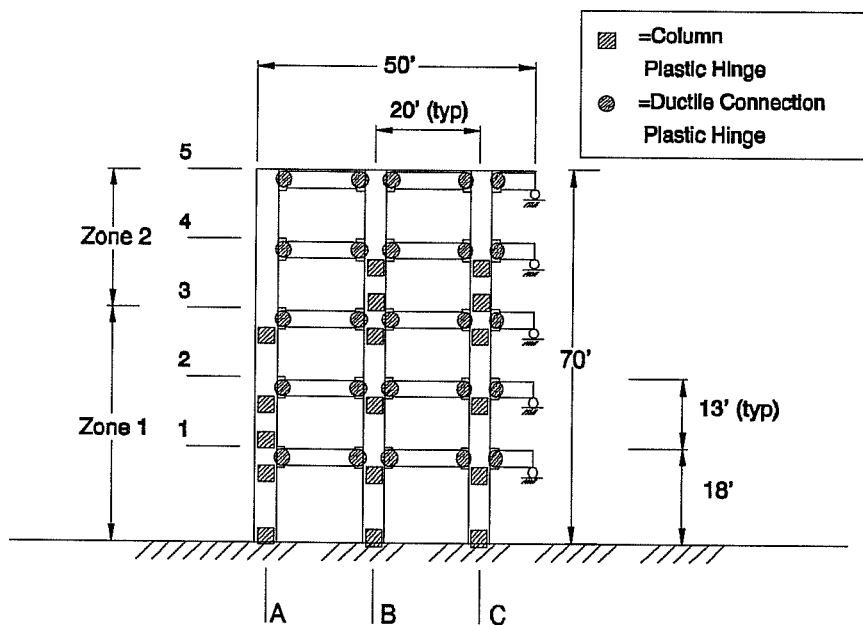


c) Gap-Opening Behavior.

Figure 4.28 (cont'd) Locations of Plastic Hinges,
Scaled El Centro, 5-Story Structure.

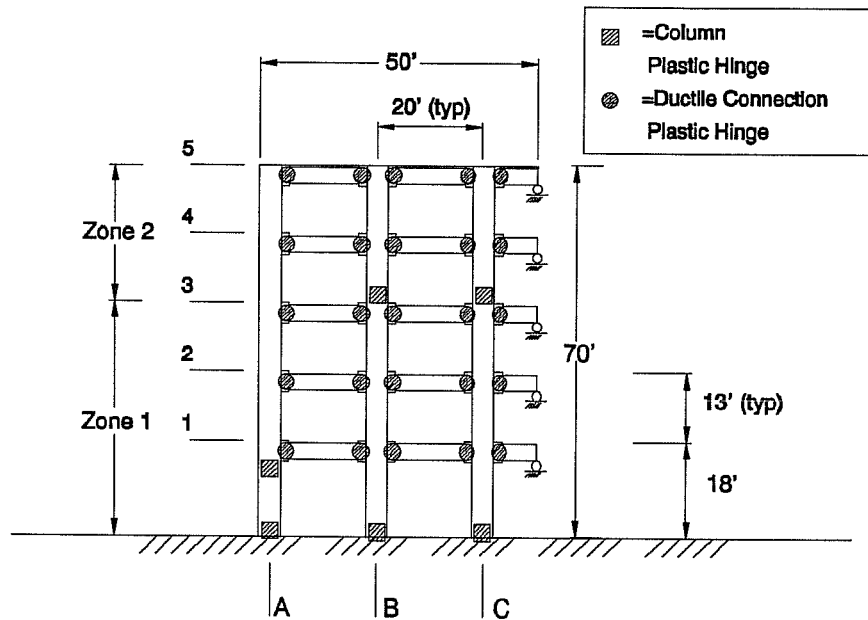


a) Nonlinear Behavior.



b) Nonlinear-Elastic Behavior.

Figure 4.29 Locations of Plastic Hinges, Viña del Mar, 5-Story Frame.



c) Gap-Opening Behavior.

Figure 4.29 (cont'd) Locations of Plastic Hinges, Viña del Mar, 5-Story Frame.

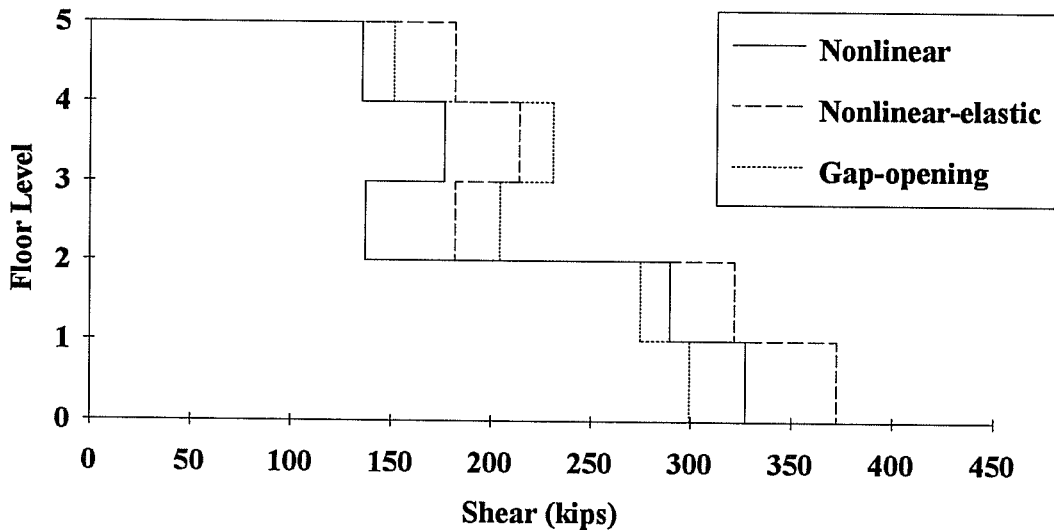
plastic plateau for this type of connection were small and distributed well along the height of the structure (as they were for the 15-story frame), primarily due to the small number of cycles the structure experienced compared to the other two connection cases (Fig. 4.19).

The gap-opening connection deformations listed in Tables 4.3 and 4.5 are very similar for both frames, except for the Viña del Mar earthquake. For this ground motion the connections of the shorter frame had maximum relative rotations and accumulated plastic rotations twice those for the 15-story frame. It is likely that the poorer performance is once again related to the shorter predominant period of the 5-story structure.

The building with nonlinear-elastic connections exhibited substantial inelastic action in the connections and column elements, as for the 15-story structure. The accumulated plastic rotations in the connections and the columns

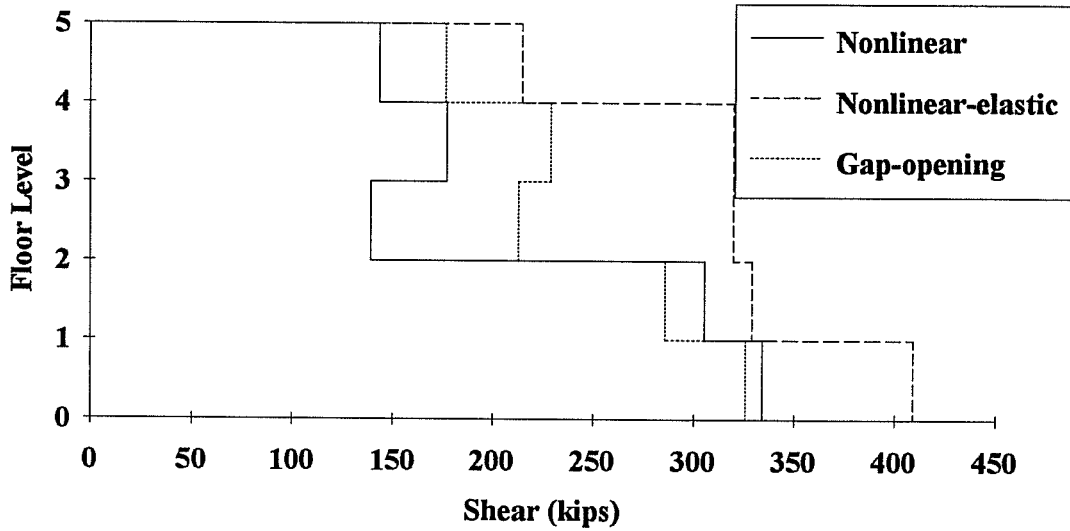
for Viña del Mar were at least double the values observed for the scaled El Centro ground motion (Figs 4.24 through 4.26). Although the deformations in beam connections are of no great concern (See Sec. 4.2.4), the large number of column hinges formed during each of the base motions (Figs. 4.27 through 4.29) may require special detailing provisions.

To reinforce results found in the 15-story frame, Fig. 4.30 demonstrates the higher maximum story shears developed for the structures with nonlinear-elastic and gap-opening connections. In general, the nonlinear-elastic case generated the highest story shear requirements.

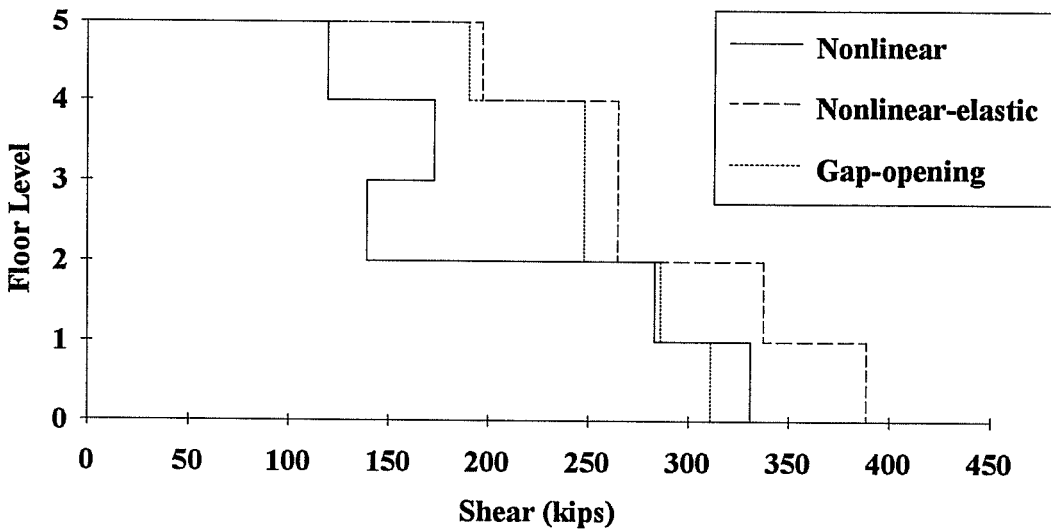


a) El Centro.

Figure 4.30 Story Shear Envelopes, 5-Story Frame.



b) Scaled El Centro.



c) Viña del Mar.

Figure 4.30 (cont'd) Story Shear Envelopes, 5-Story Frame.

5. SUMMARY AND CONCLUSIONS

5.1 Overview

When a new structural system is developed, it is quite difficult, if not impossible, to predict the nonlinear cyclic behavior of connections unless existing details are "borrowed" from a system with known behavior. A group of researchers have been working on the development of a precast frame and wall panel system for use in strong and moderate seismic regions. This coordinated research program, sponsored by the National Science Foundation, has been named the PRESSS program (Precast Seismic Structural Systems). Early in the program a 15-story prototype frame building was developed. Currently, precast ductile beam-column subassemblages are being tested at the University of Texas and the University of Minnesota. In this analytical study, different idealized hysteretic models describing the nonlinear response of the beam-column connections were used to investigate the dynamic response of the prototype structure (and a smaller version of the prototype structure) to earthquake loads to perhaps identify the characteristics of the hysteretic models that result in acceptable behavior, or determine what areas in the design of precast frames may need special consideration.

DRAIN-2DX, an inelastic dynamic analysis program was used to evaluate the overall response of the PRESSS prototype precast reinforced concrete 15-story building and a similar 5-story building (with identical plan and member dimensions, but with dissimilar member capacities). The beam-column connections in the buildings were modeled using three different hysteretic models. The models are described in more detail in Chapter 2, and are referred to in this report by the following names: "nonlinear", "nonlinear-elastic", and "gap-opening" hysteretic models. The basic nonlinear model is intended to provide a baseline behavior representative of monolithic reinforced-concrete frame construction, exhibiting a large energy-absorbing hysteresis. The nonlinear-elastic model could be representative of post-tensioned connections and has the least ability to absorb energy. The gap-opening model is intended to represent opening and closing of

precast joints as the result of yielding and slip of reinforcement and has energy-absorbing capabilities somewhere in between the other two hysteretic models. Each structural configuration was subjected to different earthquake acceleration records: El Centro, 1940, El Centro scaled up to have a maximum 0.5g acceleration, and Viña del Mar, 1985.

5.2 Summary of Results

The 15-story and 5-story structures generally demonstrated the same trends in behavior when changes were made in the connection model or earthquake record. However, because the two buildings had very different natural periods (due to their dissimilar heights) quite different overall responses resulted for the same earthquake.

The distribution of member capacities into zones and the number of story levels in the zones also caused different building responses. The 15-story structure demonstrated more nonlinear activity around the strength discontinuities than did the 5-story structure.

The 5-story and 15-story precast reinforced concrete building responses to changes in hysteretic behavior of the beam-column connections are summarized in the following sections.

5.2.1 Nonlinear Hysteresis (Fig. 2.1a)

Responses of the 15-story and 5-story buildings were very similar when the nonlinear hysteretic connection model was used. Both structures demonstrated smaller responses than exhibited by the buildings incorporating the other connection models, including smaller responses in the following: displacements, building drifts, interstory drifts, and story shears. One undesirable trait for this type of connection model was the residual drift that accumulated in each case.

The dissimilar periods for the 5- and 15-story buildings generally had little effect on the response. Only for the Viña del Mar ground motion was there a noticeable increase in the response of the shorter building. Building drifts for the

two frames were similar, with building drifts ranging between 0.30% and 0.44% for each ground motion.

The strength discontinuities appeared to have only a slight influence on the interstory drifts, displacement, and rotation envelopes. The transformation from the first to second zone above the fifth story in the 15-story structure caused slight jumps in the plots mentioned above. The strength change in the top third of the 15-story structure and the discontinuity of strengths in the 5-story frame appeared to be of no consequence.

Interstory drifts were smallest for this connection model (Figs. 4.6 and 4.21). This observation may have significance in the control of nonstructural damage.

Rotation envelopes were comparable for the two frames (with maximum rotations ranging from 0.0050 to 0.0075 radians for all three base motions) and were the smallest rotations exhibited for all connection models. This was especially noticeable for the 5-story structure (Fig. 4.22), where rotations were typically less than half the rotations produced by the other connection models.

Inelastic behavior was consistent with monolithic reinforced-concrete frame behavior. Building responses followed closely the traditional strong beam-weak column strategy, with hinges forming primarily in all beam connections and in the columns at the foundations. The few upper-story columns that formed plastic hinges (in the 15-story structure with the basic El Centro and Viña del Mar ground motions) had relatively small inelastic rotations (less than 0.0004 radians).

Accumulated plastic rotations in the connections of the 5-story frame were much larger than those generated in the 15-story frame. (Accumulated plastic rotation is defined as the summation of the inelastic rotations in the element during an earthquake analysis.) This was primarily due to the larger number of inelastic response cycles experienced by the 5-story building. For the Viña del Mar ground motion, the accumulated plastic rotations were very large (0.1664 radians) (Table 4.5). This indicates that some connections must be designed with sufficient toughness to handle numerous inelastic cycles of deformation. For the 15-story building the maximum accumulated plastic rotations in the connections

were approximately one-seventh of the maximum for the 5-story building (Table 4.3). Maximum relative rotations for connections in both the 5- and 15-story frames were slight (0.0067 and 0.0050 radians) in comparison to other connection behavior, indicating the connections with nonlinear hysteretic behavior only slightly opened the joint at the beam-column interface (which causes relative rotations between the beam interface and the center of the connection).

5.2.2 Nonlinear-Elastic Hysteresis (Fig. 2.1b)

The structures modeled with connections displaying nonlinear-elastic hysteresis (typical of post-tensioned connections) experienced substantial nonlinear activity in the structural components of the lateral-force-resisting frames. Lateral forces were higher, and as a result more columns yielded than for the nonlinear case.

Building drifts for the 15-story structure were comparable to drifts computed for the structure with nonlinear connections. However, for the 5-story building, building drifts were 1.8 to 3.2 times the building drifts for the 15-story building, with a maximum of 0.98% for the Viña del Mar earthquake motion. Small residual drifts also resulted in the 5-story building.

Higher lateral forces, especially in the top half of the 15-story building resulted in higher internal forces, and increased deformations. The hinging and increased deformations were most pronounced in the regions where strength discontinuities existed.

A very high level of nonlinear activity in the beam connections and columns was produced by this type of connection model (Figs. 4.8 through 4.11 and Figs. 4.23 through 4.26). However, since no significant inelastic material behavior is expected in the beam connections (because they are post-tensioned and unbonded), the large nonlinear rotations in beam connections may have no significance. The same cannot be said for the inelastic deformations calculated for the columns. At the very least, hinging regions in the columns would have to be detailed for ductile behavior. Perhaps a more plausible solution would be to increase design forces in upper stories of the structure to avoid hinging of the

columns. Obviously, the latter solution would have a negative impact on the economy of the system.

5.2.3 Gap-Opening Hysteresis (Fig 2.1c)

This type of connection model mimics opening and closing of cracks or joints and the loss of bond and slippage of reinforcement in precast ductile connections. Because of the severe pinching in the hysteretic model, very long response periods were generated, which resulted in large lateral drifts and limited cycles of deformation when compared with the other two connection cases.

Due to the long response periods, the 5- and 15-story structures responded better when subjected to the Viña del Mar earthquake motion, which did not excite long response periods like the El Centro ground motion (Figs. 4.2 and 4.3). The response of the 5-story frame did not improve as dramatically since its period was not as long as for the 15-story building. The two structures responded most to the El Centro base motions, reaching drifts of 1.03% (for the 5-story structure). Interstory drifts were also relatively high during the scaled El Centro record for both frames (greater than 1.1%).

Response of the gap-opening connections was highly influenced by the strength discontinuities in the buildings. Sharp increases in interstory drifts (Fig. 4.6b) and maximum rotations (Fig. 4.7b) were experienced by the 15-story building during the scaled El Centro motion.

The connection elements had very low accumulated plastic rotations (Figs. 4.8 through 4.10 and 4.23 through 4.25) primarily because of the small number of inelastic deformation cycles the structures experienced. However, the connections did experience large relative rotations (Tables 4.3 and 4.5) as cracks and joints at the beam-column interface opened and closed, indicating the need for connections to possess adequate ductility.

Inelastic activity occurred in upper-story column members, and story shears (and lateral forces) were greater than shears calculated for the nonlinear connection case.

5.3 Conclusions

The primary objective of this study was to examine the responses during strong motion earthquakes of two precast reinforced concrete buildings using three different hysteretic models to represent the behavior of the beam-column connections. The following was concluded from the analyses:

- The buildings with nonlinear connections demonstrated the greatest ability to absorb energy, contain inelastic activity, and limit drifts.
- Only structures with nonlinear connections exhibited strong column-weak beam type of behavior by forming most hinges in the beam-column connections.
- Buildings having nonlinear connections sometimes experienced sizeable permanent deformations (as much as 0.21%).
- Buildings with nonlinear-elastic connections displayed larger deformations in the connections and larger overall drifts. In addition, larger story shears (as much as 2.3 times the nonlinear connection case) and substantial column hinging were also experienced. Similar trends were also experienced for structures with gap-opening connections. Significant column hinging is inconsistent with the typical strong column-weak beam design approach commonly used in proportioning reinforced-concrete frame systems, and strongly suggests that larger design forces are appropriate for frame systems with either nonlinear-elastic or gap-opening beam-column connections.
- Because beam-column connections having nonlinear-elastic hysteretic response are intended to remain elastic during large seismic events, the large connection rotations that were computed in this study suggest that special confinement details may need to be used in these connections to enable the concrete to withstand the large curvatures that may result.
- Frames with gap-opening connections exhibited longer response periods and also displayed higher response modes.
- It is apparent that buildings with nonlinear-elastic and gap-opening connection behavior need to be designed for larger forces, because

greater inelastic activity was concentrated at and above locations where member capacity reductions occurred.

REFERENCES

- 1 Abrams, D. P., "Laboratory Definitions of Behavior for Structural Components and Building Systems," *Earthquake-Resistant Concrete Structures Inelastic Response and Design*, SP 127-4, American Concrete Institute, Detroit, Michigan, 1991, pp. 91-152.
- 2 *Catalog of Earthquake Records*, revised by José A. Pincheira, Phil M. Ferguson Structural Engineering Laboratory, University of Texas, Austin, Texas, June 1992.
- 3 Celebi, M., "Hysteretic Behavior of Reinforced Concrete Beams Under Influence of Shear and Bending," Synopsis, *Fifth Symposium on Earthquake Engineering*, Sarita Prakashan, India, Nov. 9-11, 1974, pp. 375-380.
- 4 Charney, F. A., "Correlation of the Analytical and Experimental Inelastic Response of a 1/5-Scale Seven-Story Reinforced Concrete Frame-Wall Structure," *Earthquake-Resistant Concrete Structures Inelastic Response and Design*, American Concrete Institute, Detroit, Michigan, 1991, pp. 261-361.
- 5 Cheok, G. S. and Lew, H. S., "Performance of 1/3-Scale Model Precast Concrete Beam-Column Connections Subjected to Cyclic Inelastic Load - Report No. 2", *NISTIR 4589*, National Institute of Standards and Technology, Gaithersburg, MD, June, 1991.
- 6 Clough, R. W., Benuska, K. L. and Wilson, E. L., "Inelastic Earthquake Response of Tall Buildings", *Proceedings, Third World Conference on Earthquake Engineering, New Zealand*, Vol. 11, New Zealand National Committee on Earthquake Engineering, 1965.
- 7 Corley, W. G., "Rotational Capacity of Reinforced Concrete Beams," *Journal of the Structural Division*, ASCE, Vol. 92, No. ST5, Oct. 1966, pp. 121-146.
- 8 *Design of Earthquake-Resistant Buildings*, Wakabayashi, M., McGraw-Hill Book Company, New York City, New York, 1986.
- 9 *DRAIN-2DX User's Guide*, University of California, Berkeley, California, July 1992.
- 10 *Dynamics of Structures*, Clough, R. W., and Penzien, J., McGraw-Hill Book Company, New York City, New York, 1975.
- 11 Filippou, F. C., "A Simple Model for Reinforcing Bar Anchorages Under Cyclic Excitations," *Report No. EERC 85-05*, Earthquake Engineering

- Research Center, University of California, Berkeley, California, Mar., 1985.
- 12 Filippou, F. C., and Issa, A., "Nonlinear Analysis of Reinforced Concrete Frames Under Cyclic Load Reversals," *Report No. EERC 88-12*, Earthquake Engineering Research Center, University of California, Berkeley, California, Sept., 1988.
 - 13 Filippou, F. C., Popov, E. P., and Bertero, V. V., "Effects of Bond Deterioration on Hysteretic Behavior of Reinforced Concrete Joints," *Report No. EERC 83-19*, Earthquake Engineering Research Center, University of California, Berkeley, California, Aug., 1983.
 - 14 Filippou, F. C., Popov, E. P., and Bertero, V. V., "Modeling of R/C Joints Under Cyclic Excitations," *Journal of Structural Engineering*, ASCE, Vol. 109, No. 11, Nov., 1983, pp. 2666-2684.
 - 15 Giberson, M. F., "Two Nonlinear Beams with Definitions of Ductility," *Journal of the Structural Division*, ASCE, Vol. 95, No. ST2, Feb., 1969, pp. 137-157.
 - 16 Jirsa, J. O., "Beam-Column Joints: Irrational Solutions to a Rational Problem," *Significant Developments in Engineering Practice and Research*, SP-72, American Concrete Institute, Detroit, Michigan, 1981.
 - 17 Jirsa, J. O., "Behavior of Elements and Subassemblages--R. C. Frames," *Proceedings, Workshop of Earthquake-Resistant Reinforced Concrete Building Construction*, University of California, Berkeley, July, 1977.
 - 18 Kanaan, A. E., and Powell, G. H., "Drain-2D, A General Purpose Computer Program for Dynamic Analysis of Inelastic Plane Structures with User's Guide," *Reports No. EERC 73-6 and 73-22*, Earthquake Engineering Research Center, University of California, Berkeley, California, Apr., 1973, Revised Sept., 1973 and Aug., 1975.
 - 19 Keshavarzian, M., and Schnobrich, W. C., "Analytical Models for the Nonlinear Seismic Analysis of Reinforced Concrete Structures," *Engineering Structures*, Butterworth & Co. Ltd., Vol. 7, Apr., 1985, pp. 131-142.
 - 20 Newmark, N. M. and Hall, W. J., "Earthquake Spectra and Design," *Engineering Monographs on Earthquake Criteria, Structural Design, and Strong Motion Records*, Earthquake Engineering Research Institute, University of Illinois, Urbana-Champaign, Illinois, 1982.

- 21 Pauley, T., "A Critique of the Special Provisions for Seismic Design of the Building Code Requirements for Reinforced Concrete," *ACI Journal, Proceedings* V. 83, No. 2, Mar.-Apr. 1986, pp. 274-283.
- 22 Priestley, M. J. N., "Overview of PRESSS Research Program," *PCI Journal*, Vol. 36, July-Aug., 1991, pp. 50-57.
- 23 Priestly, M. J. N., "Report on the Third U. S. PRESSS Coordinating Meeting," San Diego, California, Edited by Priestley, M. J. N., Report No. PRESSS - 92/02.
- 24 *RCCOLA User's Manual*, Klingner, R. E., University of Texas, Austin, Texas.
- 25 Saatcioglu, M., "Modeling Hysteretic Force-Deformation Relationships for Reinforced Concrete Elements," *Earthquake-Resistant Concrete Structures Inelastic Response and Design*, SP 127-5, American Concrete Institute, Detroit, Michigan, 1991, pp. 153-198.
- 26 Scott, B. D., Park, R., and Priestley, M. J. N., "Stress-Strain Behavior of Concrete Confined by Overlapping Hoops at Low and High Strain Rates," *ACI Journal, Proceedings* V. 79, No. 1, Jan.-Feb., 1982, pp. 13-27.
- 27 *The Seismic Design Handbook*, edited by Naeim, F., Van Nostrand Reinhold, New York City, New York, 1989.
- 28 Sozen, M. A., "Hysteresis in Structural Elements," *Applied Mechanics in Earthquake Engineering*, ASME, Nov., 1974, pp. 63-98.
- 29 Takeda, T., Sozen, M. A., and Nielsen, N. N., "Reinforced Concrete Response to Simulated Earthquakes," *Journal of the Structural Division*, ASCE, Vol. 96, No. ST12, Dec., 1970, pp. 2557-2573.
- 30 *Uniform Building Code*, 1991 edition, International Conference of Building Officials, Whittier, California, 1991.

VITA

Lori Wilson Brewer was born on November 11, 1968 to Richard E. and Margaret M. Wilson. She is the youngest of five children and grew up in St. James, Missouri, a rural community 100 miles west of St. Louis.

In 1987, the year of her high school graduation she was awarded an Air Force Reserve Officer Training Corps scholarship to attend college with tuition and fees paid. She entered the University of Kansas, in Lawrence, Kansas (her parents' alma mater) in the fall of that year. She graduated in the spring of 1992 with a Bachelor of Science in Architectural Engineering and was commissioned as a Second Lieutenant in the Air Force.

In the fall of that year, she entered the University of Texas at Austin to work toward a masters degree in the field of Civil Engineering.

Lori was married to John Anthony Brewer on May 29, 1993, in her hometown of St. James. John is also a Second Lieutenant in the Air Force and is a KC-135 pilot. The couple is moving to Griffiss Air Force Base in upstate New York in October of this year.

Permanent address: 302 West Hardy
St. James, Missouri 65559

This thesis was typed by the author.